

The genetic code, algebra of projection operators and problems of inherited biological ensembles

Sergey V. Petoukhov

Head of Laboratory of Biomechanical System, Mechanical Engineering Research Institute
of the Russian Academy of Sciences, Moscow

spetoukhov@gmail.com, petoukhov@imash.ru, <http://symmetry.hu/isabm/petoukhov.html>,
<http://petoukhov.com/>

Comment: Some materials of this article were presented in the International Workshop on Genomic Signal Processing (Bucharest, Romania, June 27-28, 2011), “Symmetry Festival-2013” (Delft, Netherlands, August 2-7, 2013, <http://symmetry.hu/festival2013.html>), the international conference “Theoretical approaches to bioinformation systems - TABIS 2013” (Belgrad, Serbia, September 17-22, 2013, <http://www.tabis2013.ipb.ac.rs/>)

Summary. This article is devoted to applications of projection operators to simulate phenomenological properties of the molecular-genetic code system. Oblique projection operators are under consideration, which are connected with matrix representations of the genetic coding system in forms of the Rademacher and Hadamard matrices. Evidences are shown that sums of such projectors give abilities for adequate simulations of ensembles of inherited biological phenomena including ensembles of biological cycles, morphogenetic ensembles of phyllotaxis patterns, etc. For such modeling, the author proposes multidimensional vector spaces, whose subspaces are under a selective control (or coding) by means of a set of matrix operators on base of genetic projectors. Development of genetic biomechanics is discussed. The author proposes and describes special systems of multidimensional numbers under names “tensorcomplex numbers”, “tensordouble numbers”, etc. Described results can be used for developing algebraic biology, biotechnical applications and some other fields of science and technology.

Content

1. About the partnership of the genetic code and mathematics
 2. Genetic Rademacher matrices as sums of projectors
 3. Genetic Hadamard matrices as sums of projectors
 4. Inherited biocycles and a selective control of cyclic changes of vectors in a multidimensional space. Problems of genetic biomechanics.
 5. About a direction of rotation of vectors under influence of the cyclic groups of the operators
 6. Hamilton’s quaternions, Cockle’s split-quaternions, their extensions and projector operators
 7. Genetic matrices as sums of Kronecker products of oblique (2×2) -projectors. Extensions of the genetic matrices into $(2^n \times 2^n)$ -matrices
 8. An application of oblique projectors to simulate ensembles of phyllotaxis patterns in living bodies
 9. The symbolic matrices of genetic duplets and triplets
 10. Genetic projectors and evolutionary changes of dialects of the genetic code
 11. About «tensorcomplex» numbers
 12. About «tensordouble» numbers
- Some concluding remarks

1. ABOUT THE PARTNERSHIP OF THE GENETIC CODE AND MATHEMATICS

Science has led to a new understanding of life itself: "*Life is a partnership between genes and mathematics*" [Stewart, 1999]. But what kind of mathematics can be a partner for the genetic coding system? This article shows some evidences that algebra of projectors can be one of main parts of such mathematics. Till now the notion of projection operators (or briefly, projectors) was one of important in many fields of non-biological science: physics including quantum mechanics; mathematics; computer science and informatics including theory of digital codes; chemistry; mathematical logic, etc. On basis of materials of this article, the author thinks that projectors can become one of the main notions and effective mathematical tools in mathematical biology. Moreover they will help not only to a development of algebraic biology and a new understanding of living matter but also to a mutual enrichment of different branches of science.

Projectors are expressed by means of square matrices (<http://mathworld.wolfram.com/ProjectionMatrix.html>, [https://en.wikipedia.org/wiki/Projection_\(linear_algebra\)](https://en.wikipedia.org/wiki/Projection_(linear_algebra))). A necessary and sufficient condition that a matrix P is a projection operator is the fulfillment of the following condition: $P^2 = P$. A set of projectors is separated into two sub-sets:

- orthogonal projectors, which are expressed by symmetric matrices and theory of which is well developed and has a lot of applications;
- oblique projectors, which are expressed by non-symmetric matrices; their theory and its applications are developed much weaker as the author can judge. Namely oblique projectors will be the main objects of attention in this article.

This article is a continuation and an essential development of the author's article about relations between the genetic system and projection operators [Petoukhov, 2010].

In accordance with Mendel's laws of independent inheritance of traits, information from the micro-world of genetic molecules dictates constructions in the macro-world of living organisms under strong noise and interference. This dictation is realized by means of unknown algorithms of multi-channel noise-immunity coding. For example, in human organism, his skin color, eye color and hair color are inherited genetically independently of each other. It is possible if appropriate kinds of information are conducted via independent informational channels and if a general "phase space" of living organism contains sub-spaces with a possibility of a selective control or a selective coding of processes in them. So, any living organism is an algorithmic machine of multi-channel noise-immunity coding with ability to a selective control and coding of different sub-spaces of its phase space (a model approach to phase spaces with a selective control of their sub-spaces is presented in this article). This machine works in conditions of ontogenetic development of the organism when a multi-dimensionality of its phase space is increased step by step.

To understand such genetic machine, it is appropriate to use the theory of noise-immunity coding and transmission of digital information, taking into account the discrete nature of the genetic code. In this theory, mathematical matrices have the basic importance. The use of matrix representations and analysis in the study of phenomenological features of molecular-genetic ensembles has led to the development of a special scientific direction under a name "Matrix Genetics" [Petoukhov, 2008; Petoukhov, He, 2009]. Namely researches of the "matrix genetics" gave results that are

represented in this article.

Concerning the theme of projectors in inherited biological phenomena, one can note that our genetically inherited visual system works on the principle of projection of external objects at the retina. This projection is modeled using projection operators. The author believes that the value of projectors for bioinformatics is not limited to this single fact of biological significance of projection operators, but that the whole system of genetic and sensory informatics is based on their active use. This ubiquitous use of projection operators reflects and ensures (in some degree) the unity of any organism and interrelations of its parts.

The set of projection operators, which are associated with the matrix representation of the genetic code, provides new opportunities for modeling ensembles of inherited cycles; ensembles of phyllotaxis structures; a numeric specificity of reproduction of genetic information in acts of mitosis and meiosis of biological cells, etc. In the frame of the "projector conception" arisen here in genetic informatics, some features of evolutionary transformations of variants (or dialects) of the genetic code are clarified.

The main mathematical objects of the article are four matrices R_4 , R_8 , H_4 and H_8 shown on Figure 1. Why these numeric matrices are chosen from infinite set of matrices? The reason is that they are connected with phenomenology of the genetic code system in matrix forms of its representation as it was shown in works [Petoukhov, 2008b, 2011a,b, 2012a,b] and as it will be additionally demonstrated in the end of this article. The matrices R_4 and R_8 are conditionally termed "Rademacher matrices" because each of their columns represents one of known Rademacher functions. The matrices H_4 and H_8 belong to a great set of Hadamard matrices, which are widely used for noise-immunity coding in technologies of signals processing and which are connected with complete orthogonal systems of Walsh functions.

$$\begin{aligned}
 R_4 &= \begin{bmatrix} 1 & 1 & 1 & -1 \\ -1 & 1 & -1 & -1 \\ 1 & -1 & 1 & 1 \\ -1 & -1 & -1 & 1 \end{bmatrix} ; \quad R_8 = \begin{bmatrix} 1 & 1 & 1 & 1 & 1 & 1 & -1 & -1 \\ 1 & 1 & 1 & 1 & 1 & 1 & -1 & -1 \\ -1 & -1 & 1 & 1 & -1 & -1 & -1 & -1 \\ -1 & -1 & 1 & 1 & -1 & -1 & -1 & -1 \\ 1 & 1 & -1 & -1 & 1 & 1 & 1 & 1 \\ 1 & 1 & -1 & -1 & 1 & 1 & 1 & 1 \\ -1 & -1 & -1 & -1 & -1 & -1 & 1 & 1 \\ -1 & -1 & -1 & -1 & -1 & -1 & 1 & 1 \end{bmatrix} \\
 H_4 &= \begin{bmatrix} 1 & 1 & -1 & 1 \\ -1 & 1 & 1 & 1 \\ 1 & -1 & 1 & 1 \\ -1 & -1 & -1 & 1 \end{bmatrix} ; \quad H_8 = \begin{bmatrix} 1 & -1 & 1 & -1 & -1 & 1 & 1 & -1 \\ 1 & 1 & 1 & 1 & -1 & -1 & 1 & 1 \\ -1 & 1 & 1 & -1 & 1 & -1 & 1 & -1 \\ -1 & -1 & 1 & 1 & 1 & 1 & 1 & 1 \\ 1 & -1 & -1 & 1 & 1 & -1 & 1 & -1 \\ 1 & 1 & -1 & -1 & 1 & 1 & 1 & 1 \\ -1 & 1 & -1 & 1 & -1 & 1 & 1 & -1 \\ -1 & -1 & -1 & -1 & -1 & -1 & 1 & 1 \end{bmatrix}
 \end{aligned}$$

Figure 1: numeric matrices H_4 , H_8 , R_4 and R_8 which are connected with phenomenology of the genetic coding system [Petoukhov, 2011, 2012a,b]

Every of these matrices can be decomposed into sum of sparse matrices, each of which contains only one non-zero column. Such decomposition can be conditionally termed a «column decomposition». Every of such matrices can be also decomposed into a sum of sparse matrices, each of which contains only one non-zero row. Such decomposition can be conditionally termed a «row decomposition».

2. GENETIC RADEMACHER MATRICES AS SUMS OF PROJECTORS

Let us begin with the column decomposition $R_4=c_0+c_1+c_2+c_3$ and the row decomposition $R_4=r_0+r_1+r_2+r_3$ of the Rademacher (4*4)-matrix R_4 (Figure 2).

$$R_4 = c_0+c_1+c_2+c_3 = \begin{vmatrix} 1 & 0 & 0 & 0 \\ -1 & 0 & 0 & 0 \\ 1 & 0 & 0 & 0 \\ -1 & 0 & 0 & 0 \end{vmatrix} + \begin{vmatrix} 0 & 1 & 0 & 0 \\ 0 & 1 & 0 & 0 \\ 0 & -1 & 0 & 0 \\ 0 & -1 & 0 & 0 \end{vmatrix} + \begin{vmatrix} 0 & 0 & 1 & 0 \\ 0 & 0 & -1 & 0 \\ 0 & 0 & 1 & 0 \\ 0 & 0 & -1 & 0 \end{vmatrix} + \begin{vmatrix} 0 & 0 & 0 & -1 \\ 0 & 0 & 0 & -1 \\ 0 & 0 & 0 & 1 \\ 0 & 0 & 0 & 1 \end{vmatrix}$$

$$R_4 = r_0+r_1+r_2+r_3 = \begin{vmatrix} 1 & 1 & 1 & -1 \\ 0 & 0 & 0 & 0 \\ 0 & 0 & 0 & 0 \\ 0 & 0 & 0 & 0 \end{vmatrix} + \begin{vmatrix} 0 & 0 & 0 & 0 \\ -1 & 1 & -1 & -1 \\ 0 & 0 & 0 & 0 \\ 0 & 0 & 0 & 0 \end{vmatrix} + \begin{vmatrix} 0 & 0 & 0 & 0 \\ 0 & 0 & 0 & 0 \\ 1 & -1 & 1 & 1 \\ 0 & 0 & 0 & 0 \end{vmatrix} + \begin{vmatrix} 0 & 0 & 0 & 0 \\ 0 & 0 & 0 & 0 \\ 0 & 0 & 0 & 0 \\ -1 & -1 & -1 & 1 \end{vmatrix}$$

Figure 2. The «column decomposition» (upper layer) and the «row decomposition» (bottom layer) of the Rademacher matrix R_4 from Figure 1

Each of these sparse matrices c_0, c_1, c_2, c_3 and r_0, r_1, r_2, r_3 is a projection operator because it satisfies the criterion of projectors $P^2=P$ (for example, $c_0^2=c_0$, etc). Every of these projectors is an oblique (non-ortogonal) projector because it is expressed by means of a non-symmetrical matrix. Every of sets (c_0, c_1, c_2, c_3) and (r_0, r_1, r_2, r_3) consists of non-commutative projectors. We will conditionally name projectors c_0, c_1, c_2, c_3 as «column projectors» and projectors r_0, r_1, r_2, r_3 as «row projectors».

Let us examine all possible variants of sums of pairs of the different column projectors c_0, c_1, c_2 and c_3 : $(c_0+c_1), (c_0+c_2), (c_0+c_3), (c_1+c_2), (c_1+c_3), (c_2+c_3)$. The result of this examination is the following: matrices (c_0+c_1) and (c_2+c_3) with a weight coefficient $2^{-0.5}$ lead to cyclic groups with their period 8 in cases of their exponentiation: $(2^{-0.5}*(c_0+c_1))^n, (2^{-0.5}*(c_2+c_3))^n$, where $n = 1, 2, 3, \dots$ (Figure 3).

$$(2^{-0.5}*(c_0+c_1))^1 = \begin{vmatrix} 2^{-0.5} & 2^{-0.5} & 0 & 0 \\ -2^{-0.5} & 2^{-0.5} & 0 & 0 \\ 2^{-0.5} & -2^{-0.5} & 0 & 0 \\ -2^{-0.5} & -2^{-0.5} & 0 & 0 \end{vmatrix} ; \quad (2^{-0.5}*(c_2+c_3))^1 = \begin{vmatrix} 0 & 0 & 2^{-0.5} & -2^{-0.5} \\ 0 & 0 & -2^{-0.5} & -2^{-0.5} \\ 0 & 0 & 2^{-0.5} & 2^{-0.5} \\ 0 & 0 & -2^{-0.5} & 2^{-0.5} \end{vmatrix}$$

$$(2^{-0.5}*(c_0+c_1))^2 = \begin{vmatrix} 0 & 1 & 0 & 0 \\ -1 & 0 & 0 & 0 \\ 1 & 0 & 0 & 0 \\ 0 & -1 & 0 & 0 \end{vmatrix} ; \quad (2^{-0.5}*(c_2+c_3))^2 = \begin{vmatrix} 0 & 0 & 1 & 0 \\ 0 & 0 & 0 & -1 \\ 0 & 0 & 0 & 1 \\ 0 & 0 & -1 & 0 \end{vmatrix}$$

$$\begin{aligned}
(2^{-0.5*(c_0+c_1)})^3 &= \begin{vmatrix} -2^{-0.5} & 2^{-0.5} & 0 & 0 \\ -2^{-0.5} & -2^{-0.5} & 0 & 0 \\ 2^{-0.5} & 2^{-0.5} & 0 & 0 \\ 2^{-0.5} & -2^{-0.5} & 0 & 0 \end{vmatrix} ; & (2^{-0.5*(c_2+c_3)})^3 &= \begin{vmatrix} 0 & 0 & 2^{-0.5} & 2^{-0.5} \\ 0 & 0 & 2^{-0.5} & -2^{-0.5} \\ 0 & 0 & -2^{-0.5} & 2^{-0.5} \\ 0 & 0 & -2^{-0.5} & -2^{-0.5} \end{vmatrix} \\
(2^{-0.5*(c_0+c_1)})^4 &= \begin{vmatrix} -1 & 0 & 0 & 0 \\ 0 & -1 & 0 & 0 \\ 0 & 1 & 0 & 0 \\ 1 & 0 & 0 & 0 \end{vmatrix} ; & (2^{-0.5*(c_2+c_3)})^4 &= \begin{vmatrix} 0 & 0 & 0 & 1 \\ 0 & 0 & 1 & 0 \\ 0 & 0 & -1 & 0 \\ 0 & 0 & 0 & -1 \end{vmatrix} \\
(2^{-0.5*(c_0+c_1)})^5 &= \begin{vmatrix} -2^{-0.5} & -2^{-0.5} & 0 & 0 \\ 2^{-0.5} & -2^{-0.5} & 0 & 0 \\ -2^{-0.5} & 2^{-0.5} & 0 & 0 \\ 2^{-0.5} & 2^{-0.5} & 0 & 0 \end{vmatrix} ; & (2^{-0.5*(c_2+c_3)})^5 &= \begin{vmatrix} 0 & 0 & -2^{-0.5} & 2^{-0.5} \\ 0 & 0 & 2^{-0.5} & 2^{-0.5} \\ 0 & 0 & -2^{-0.5} & -2^{-0.5} \\ 0 & 0 & 2^{-0.5} & -2^{-0.5} \end{vmatrix} \\
(2^{-0.5*(c_0+c_1)})^6 &= \begin{vmatrix} 0 & -1 & 0 & 0 \\ 1 & 0 & 0 & 0 \\ -1 & 0 & 0 & 0 \\ 0 & 1 & 0 & 0 \end{vmatrix} ; & (2^{-0.5*(c_2+c_3)})^6 &= \begin{vmatrix} 0 & 0 & -1 & 0 \\ 0 & 0 & 0 & 1 \\ 0 & 0 & 0 & -1 \\ 0 & 0 & 1 & 0 \end{vmatrix} \\
(2^{-0.5*(c_0+c_1)})^7 &= \begin{vmatrix} 2^{-0.5} & -2^{-0.5} & 0 & 0 \\ 2^{-0.5} & 2^{-0.5} & 0 & 0 \\ -2^{-0.5} & -2^{-0.5} & 0 & 0 \\ -2^{-0.5} & 2^{-0.5} & 0 & 0 \end{vmatrix} ; & (2^{-0.5*(c_2+c_3)})^7 &= \begin{vmatrix} 0 & 0 & -2^{-0.5} & -2^{-0.5} \\ 0 & 0 & -2^{-0.5} & 2^{-0.5} \\ 0 & 0 & 2^{-0.5} & -2^{-0.5} \\ 0 & 0 & 2^{-0.5} & 2^{-0.5} \end{vmatrix} \\
(2^{-0.5*(c_0+c_1)})^8 &= \begin{vmatrix} 1 & 0 & 0 & 0 \\ 0 & 1 & 0 & 0 \\ 0 & -1 & 0 & 0 \\ -1 & 0 & 0 & 0 \end{vmatrix} ; & (2^{-0.5*(c_2+c_3)})^8 &= \begin{vmatrix} 0 & 0 & 0 & -1 \\ 0 & 0 & -1 & 0 \\ 0 & 0 & 1 & 0 \\ 0 & 0 & 0 & 1 \end{vmatrix} \\
(2^{-0.5*(c_0+c_1)})^9 &= \begin{vmatrix} 2^{-0.5} & 2^{-0.5} & 0 & 0 \\ -2^{-0.5} & 2^{-0.5} & 0 & 0 \\ 2^{-0.5} & -2^{-0.5} & 0 & 0 \\ -2^{-0.5} & -2^{-0.5} & 0 & 0 \end{vmatrix} ; & (2^{-0.5*(c_2+c_3)})^9 &= \begin{vmatrix} 0 & 0 & 2^{-0.5} & -2^{-0.5} \\ 0 & 0 & -2^{-0.5} & -2^{-0.5} \\ 0 & 0 & 2^{-0.5} & 2^{-0.5} \\ 0 & 0 & -2^{-0.5} & 2^{-0.5} \end{vmatrix}
\end{aligned}$$

Figure 3. The illustration of cyclic groups of operators on the basis of sums of projection operators (c_0+c_1) and (c_2+c_3) from Figure 2 in cases of their exponentiation.

These two sums of column projectors (c_0+c_1) and (c_2+c_3) are marked by green colour in the left table on Figure 4, where every of cells represents a sum of those projectors, which denote its column and row.

Two other examined sums of column projectors (c_0+c_2) and (c_1+c_3) is doubled when squaring: $(c_0+c_2)^n = 2^{n-1}*(c_0+c_2)$, $(c_1+c_3)^n = 2^{n-1}*(c_1+c_3)$, where $n = 1, 2, 3, \dots$ (these sums are marked by red colours in the left table on Figure 4) . This doubling reminds dichotomic dividing of biological cells in a result of mitosis when doubling of genetic information occurs.

The last examined sums of the column projectors (c_0+c_3) and (c_1+c_2) possess the following feature. Matrices of their second power is quadrupled in a result of exponentiation in integer powers: $((c_0+c_3)^2)^n = 4^{n-1}*(c_0+c_3)^2$, $((c_1+c_2)^2)^n = 4^{n-1}*(c_1+c_2)^2$, where $n = 1, 2, 3, \dots$

(this feature can be used to simulate a genetic phenomenon of tetra-reproduction of gametes and genetic information in a course of meiosis). The cells with these sums (c_0+c_3) and (c_1+c_2) are marked by yellow colour in the left table on Figure 4.

If we examine the row projectors r_0, r_1, r_2 and r_3 from Figure 2, we receive the same tabular structure with a small change: red and yellow cells are swapped (Figure 4, right). Matrices $2^{-0.5}*(r_0+r_1)$ and $2^{-0.5}*(r_2+r_3)$ are bases for cyclic groups with a period 8 in relation to their exponentiation (green cells in the right table on Figure 4). Matrices (r_0+r_2) and (r_1+r_3) is doubled when squaring: $(r_0+r_2)^n = 2^{n-1}*(r_0+r_2)$, $(r_1+r_3)^n = 2^{n-1}*(r_1+r_3)$, where $n = 1, 2, 3, \dots$ (red cells in the right table on Figure 4). Matrices (r_0+r_3) and (r_1+r_2) possess the «quadruplet» property: $((r_0+r_3)^2)^n = 4^{n-1}*(r_0+r_3)^2$, $((r_1+r_2)^2)^n = 4^{n-1}*(r_1+r_2)^2$, where $n = 1, 2, 3, \dots$ (yellow cells in the right table on Figure 4). The cells on the main diagonal correspond to sum of two projectors themselves: $(c_i+c_i)^n = 2^n*c_i$, $(r_i+r_i)^n = 2^n*r_i$, where $i = 0, 1, 2, 3$.

	C₀	C₁	C₂	C₃
C₀	-	C₀+C₁	C₀+C₂	C₀+C₃
C₁	C₁+C₀	-	C₁+C₂	C₁+C₃
C₂	C₂+C₀	C₂+C₁	-	C₂+C₃
C₃	C₃+C₀	C₃+C₁	C₃+C₂	-

	r₀	r₁	r₂	r₃
r₀	-	r₀+r₁	r₀+r₂	r₀+r₃
r₁	r₁+r₀	-	r₁+r₂	r₁+r₃
r₂	r₂+r₀	r₂+r₁	-	r₂+r₃
r₃	r₃+r₀	r₃+r₁	r₃+r₂	-

Figure 4. Tables of some features of sums of pairs of different «column projectors» c_0, c_1, c_2, c_3 and of «row projectors» r_0, r_1, r_2, r_3 (from the Rademacher matrix R_4 on Figure 2) in relation to their exponentiation. Explanations in text.

One can mention that the structure of this symmetric table is unexpectedly coincided with the structure of the typical (4*4)-matrix of dyadic shifts, which is known in theory of signal processing and which is related with some phenomenologic properties of molecular-genetic systems [Ahmed, Rao, 1975; Petoukhov, 2008, 2012a; Petoukhov, He, 2009].

It should be noted that cyclic features of (4*4)-matrices $2^{-0.5}*(c_0+c_1)$, $2^{-0.5}*(c_2+c_3)$, $2^{-0.5}*(r_0+r_1)$ and $2^{-0.5}*(r_2+r_3)$ in cases of their exponentiation exist due to their connections with matrix representations of 2-parametric complex numbers in 4-dimensional space; these connections are shown by means of a new decomposition of each of these matrices into sum of new sparse matrices e_0 and e_1 (Figures 5, 6, two upper levels, where the multiplication table for e_0 and e_1 in the right column is identical to the multiplication table of complex numbers). The dichotomic features of (4*4)-matrices (c_0+c_2) , (c_1+c_3) , (r_0+r_3) , (r_1+r_2) and tetra-reproduction features of (4*4)-matrices $((c_0+c_3)^2)^n = 4^{n-1}*(c_0+c_3)^2$, $((c_1+c_2)^2)^n = 4^{n-1}*(c_1+c_2)^2$, $((r_0+r_2)^2)^n = 4^{n-1}*(r_0+r_2)^2$, $((r_1+r_3)^2)^n = 4^{n-1}*(r_1+r_3)^2$ exist due to their connections with matrix representations of 2-parametric split-complex numbers in 4-dimensional space (Figures 5, 6, four bottom levels, where the multiplication table for e_0 and e_1 in the right column is identical to the multiplication table of split-complex numbers). Synonyms of split-complex numbers are Lorentz numbers, hyperbolic numbers, double numbers, perplex numbers, etc. - http://en.wikipedia.org/wiki/Split-complex_number). Split-complex numbers are a two-dimensional commutative algebra over the real numbers. Additional details about such (4*4)-matrix representations of complex numbers and split-complex numbers see in [Petoukhov, 2012b].

$c_0+c_1=$	$\begin{bmatrix} 1 & 1 & 0 & 0 \\ -1 & 1 & 0 & 0 \\ 1 & -1 & 0 & 0 \\ -1 & -1 & 0 & 0 \end{bmatrix}$	$= e_0+e_1=$	$\begin{bmatrix} 1 & 0 & 0 & 0 \\ 0 & 1 & 0 & 0 \\ 0 & -1 & 0 & 0 \\ -1 & 0 & 0 & 0 \end{bmatrix}$	+	$\begin{bmatrix} 0 & 1 & 0 & 0 \\ -1 & 0 & 0 & 0 \\ 1 & 0 & 0 & 0 \\ 0 & -1 & 0 & 0 \end{bmatrix}$;	$\begin{bmatrix} & e_0 & e_1 \\ e_0 & e_0 & e_1 \\ e_1 & e_1 & -e_0 \end{bmatrix}$
$c_2+c_3=$	$\begin{bmatrix} 0 & 0 & 1 & -1 \\ 0 & 0 & -1 & -1 \\ 0 & 0 & 1 & 1 \\ 0 & 0 & -1 & 1 \end{bmatrix}$	$= e_0+e_1=$	$\begin{bmatrix} 0 & 0 & 0 & -1 \\ 0 & 0 & -1 & 0 \\ 0 & 0 & 1 & 0 \\ 0 & 0 & 0 & 1 \end{bmatrix}$	+	$\begin{bmatrix} 0 & 0 & 1 & 0 \\ 0 & 0 & 0 & -1 \\ 0 & 0 & 0 & 1 \\ 0 & 0 & -1 & 0 \end{bmatrix}$;	$\begin{bmatrix} & e_0 & e_1 \\ e_0 & e_0 & e_1 \\ e_1 & e_1 & -e_0 \end{bmatrix}$
$c_0+c_2=$	$\begin{bmatrix} 1 & 0 & 1 & 0 \\ -1 & 0 & -1 & 0 \\ 1 & 0 & 1 & 0 \\ -1 & 0 & -1 & 0 \end{bmatrix}$	$= e_0+e_1=$	$\begin{bmatrix} 1 & 0 & 0 & 0 \\ -1 & 0 & 0 & 0 \\ 0 & 0 & 1 & 0 \\ 0 & 0 & -1 & 0 \end{bmatrix}$	+	$\begin{bmatrix} 0 & 0 & 1 & 0 \\ 0 & 0 & -1 & 0 \\ 1 & 0 & 0 & 0 \\ -1 & 0 & 0 & 0 \end{bmatrix}$;	$\begin{bmatrix} & e_0 & e_1 \\ e_0 & e_0 & e_1 \\ e_1 & e_1 & e_0 \end{bmatrix}$
$c_1+c_3=$	$\begin{bmatrix} 0 & 1 & 0 & -1 \\ 0 & 1 & 0 & -1 \\ 0 & -1 & 0 & 1 \\ 0 & -1 & 0 & 1 \end{bmatrix}$	$= e_0+e_1=$	$\begin{bmatrix} 0 & 1 & 0 & 0 \\ 0 & 1 & 0 & 0 \\ 0 & 0 & 0 & 1 \\ 0 & 0 & 0 & 1 \end{bmatrix}$	+	$\begin{bmatrix} 0 & 0 & 0 & -1 \\ 0 & 0 & 0 & -1 \\ 0 & -1 & 0 & 0 \\ 0 & -1 & 0 & 0 \end{bmatrix}$;	$\begin{bmatrix} & e_0 & e_1 \\ e_0 & e_0 & e_1 \\ e_1 & e_1 & e_0 \end{bmatrix}$
$0.5*(c_0+c_3)^2=$	$\begin{bmatrix} 1 & 0 & 0 & -1 \\ 0 & 0 & 0 & 0 \\ 0 & 0 & 0 & 0 \\ -1 & 0 & 0 & 1 \end{bmatrix}$	$= e_0+e_1=$	$\begin{bmatrix} 1 & 0 & 0 & 0 \\ 0 & 0 & 0 & 0 \\ 0 & 0 & 0 & 0 \\ 0 & 0 & 0 & 1 \end{bmatrix}$	+	$\begin{bmatrix} 0 & 0 & 0 & -1 \\ 0 & 0 & 0 & 0 \\ 0 & 0 & 0 & 0 \\ -1 & 0 & 0 & 0 \end{bmatrix}$;	$\begin{bmatrix} & e_0 & e_1 \\ e_0 & e_0 & e_1 \\ e_1 & e_1 & e_0 \end{bmatrix}$
$0.5*(c_1+c_2)^2=$	$\begin{bmatrix} 0 & 0 & 0 & 0 \\ 0 & 1 & -1 & 0 \\ 0 & -1 & 1 & 0 \\ 0 & 0 & 0 & 0 \end{bmatrix}$	$= e_0+e_1=$	$\begin{bmatrix} 0 & 0 & 0 & 0 \\ 0 & 1 & 0 & 0 \\ 0 & 0 & 1 & 0 \\ 0 & 0 & 0 & 0 \end{bmatrix}$	+	$\begin{bmatrix} 0 & 0 & 0 & 0 \\ 0 & 0 & -1 & 0 \\ 0 & -1 & 0 & 0 \\ 0 & 0 & 0 & 0 \end{bmatrix}$;	$\begin{bmatrix} & e_0 & e_1 \\ e_0 & e_0 & e_1 \\ e_1 & e_1 & e_0 \end{bmatrix}$

Figure 5. The table represents special decompositions of (4*4)-matrices (c_0+c_1) , (c_2+c_3) , (c_0+c_2) , (c_1+c_3) , $0.5*(c_0+c_3)^2$ and $0.5*(c_1+c_2)^2$ into sum of two matrices e_0+e_1 . The table shows direct relations of these matrices with matrix representations of 2-parametric complex numbers and split-complex numbers. Here c_0 , c_1 , c_2 and c_3 are column projectors from Figure 2. For each set of matrices e_0 and e_1 at every tabular level, the right column of this table contains its multiplication table: for two upper levels it is a known multiplication table of complex numbers; for other four levels it is a known multiplication table of split-complex numbers.

$r_0+r_1=$	$\begin{bmatrix} 1 & 1 & 1 & -1 \\ -1 & 1 & -1 & -1 \\ 0 & 0 & 0 & 0 \\ 0 & 0 & 0 & 0 \end{bmatrix}$	$= e_0+e_1=$	$\begin{bmatrix} 1 & 0 & 1 & 0 \\ 0 & 1 & 0 & -1 \\ 0 & 0 & 0 & 0 \\ 0 & 0 & 0 & 0 \end{bmatrix}$	+	$\begin{bmatrix} 0 & 1 & 0 & -1 \\ -1 & 0 & -1 & 0 \\ 0 & 0 & 0 & 0 \\ 0 & 0 & 0 & 0 \end{bmatrix}$;	$\begin{bmatrix} & e_0 & e_1 \\ e_0 & e_0 & e_1 \\ e_1 & e_1 & -e_0 \end{bmatrix}$
------------	--	--------------	---	---	---	---	--

$r_2+r_3 =$	$\begin{bmatrix} 0 & 0 & 0 & 0 \\ 0 & 0 & 0 & 0 \\ 1 & -1 & 1 & 1 \\ -1 & -1 & -1 & 1 \end{bmatrix}$	$= e_0+e_1=$	$\begin{bmatrix} 0 & 0 & 0 & 0 \\ 0 & 0 & 0 & 0 \\ 1 & 0 & 1 & 0 \\ 0 & -1 & 0 & 1 \end{bmatrix}$	$+$	$\begin{bmatrix} 0 & 0 & 0 & 0 \\ 0 & 0 & 0 & 0 \\ 0 & -1 & 0 & 1 \\ -1 & 0 & -1 & 0 \end{bmatrix}$	$;$ $\begin{bmatrix} & e_0 & e_1 \\ e_0 & e_0 & e_1 \\ e_1 & e_1 & -e_0 \end{bmatrix}$
$0.5*(r_0+r_2)^2=$	$\begin{bmatrix} 1 & 0 & 1 & 0 \\ 0 & 0 & 0 & 0 \\ 1 & 0 & 1 & 0 \\ 0 & 0 & 0 & 0 \end{bmatrix}$	$= e_0+e_1=$	$\begin{bmatrix} 1 & 0 & 0 & 0 \\ 0 & 0 & 0 & 0 \\ 0 & 0 & 1 & 0 \\ 0 & 0 & 0 & 0 \end{bmatrix}$	$+$	$\begin{bmatrix} 0 & 0 & 1 & 0 \\ 0 & 0 & 0 & 0 \\ 1 & 0 & 0 & 0 \\ 0 & 0 & 0 & 0 \end{bmatrix}$	$;$ $\begin{bmatrix} & e_0 & e_1 \\ e_0 & e_0 & e_1 \\ e_1 & e_1 & e_0 \end{bmatrix}$
$0.5*(r_1+r_3)^2=$	$\begin{bmatrix} 0 & 0 & 0 & 0 \\ 0 & 1 & 0 & -1 \\ 0 & 0 & 0 & 0 \\ 0 & -1 & 0 & 1 \end{bmatrix}$	$= e_0+e_1=$	$\begin{bmatrix} 0 & 0 & 0 & 0 \\ 0 & 1 & 0 & 0 \\ 0 & 0 & 0 & 0 \\ 0 & 0 & 0 & 1 \end{bmatrix}$	$+$	$\begin{bmatrix} 0 & 0 & 0 & 0 \\ 0 & 0 & 0 & -1 \\ 0 & 0 & 0 & 0 \\ 0 & -1 & 0 & 0 \end{bmatrix}$	$;$ $\begin{bmatrix} & e_0 & e_1 \\ e_0 & e_0 & e_1 \\ e_1 & e_1 & e_0 \end{bmatrix}$
$r_0+r_3 =$	$\begin{bmatrix} 1 & 1 & 1 & -1 \\ 0 & 0 & 0 & 0 \\ 0 & 0 & 0 & 0 \\ -1 & -1 & -1 & 1 \end{bmatrix}$	$= e_0+e_1=$	$\begin{bmatrix} 1 & 1 & 0 & 0 \\ 0 & 0 & 0 & 0 \\ 0 & 0 & 0 & 0 \\ 0 & 0 & -1 & 1 \end{bmatrix}$	$+$	$\begin{bmatrix} 0 & 0 & 1 & -1 \\ 0 & 0 & 0 & 0 \\ 0 & 0 & 0 & 0 \\ -1 & -1 & 0 & 0 \end{bmatrix}$	$;$ $\begin{bmatrix} & e_0 & e_1 \\ e_0 & e_0 & e_1 \\ e_1 & e_1 & e_0 \end{bmatrix}$
$r_1+r_2 =$	$\begin{bmatrix} 0 & 0 & 0 & 0 \\ -1 & 1 & -1 & -1 \\ 1 & -1 & 1 & 1 \\ 0 & 0 & 0 & 0 \end{bmatrix}$	$= e_0+e_1=$	$\begin{bmatrix} 0 & 0 & 0 & 0 \\ -1 & 1 & 0 & 0 \\ 0 & 0 & 1 & 1 \\ 0 & 0 & 0 & 0 \end{bmatrix}$	$+$	$\begin{bmatrix} 0 & 0 & 0 & 0 \\ 0 & 0 & -1 & -1 \\ 1 & -1 & 0 & 0 \\ 0 & 0 & 0 & 0 \end{bmatrix}$	$;$ $\begin{bmatrix} & e_0 & e_1 \\ e_0 & e_0 & e_1 \\ e_1 & e_1 & e_0 \end{bmatrix}$

Figure 6. The table represents special decompositions of $(4*4)$ -matrices (r_0+r_1) , (r_2+r_3) , $0.5*(r_0+r_2)^2$, $0.5*(r_1+r_3)^2$, (r_0+r_3) and (r_1+r_2) into sum of two matrices e_0+e_1 . The table shows direct relations of these matrices with matrix representations of 2-parametric complex numbers and split-complex numbers. Here r_0 , r_1 , r_2 and r_3 are row projectors from Figure 2. For each set of matrices e_0 and e_1 at every tabular level, the right column of this table contains its multiplication table: for two upper levels it is a known multiplication table of complex numbers; for other four levels it is a known multiplication table of split-complex numbers.

Now let us turn to the Rademacher $(8*8)$ -matrix R_8 (Figure 1) to analyze its column decomposition $R_8 = s_0+s_1+s_2+s_3+s_4+s_5+s_6 +s_7$ (Figure 7) and its row decomposition $R_8 = v_0+v_1+v_2+v_3+v_4+v_5+v_6+v_7$ (Figure 8).

$$R_8 = s_0+s_1+s_2+s_3+s_4+s_5+s_6+s_7 = \begin{bmatrix} 1 & 0 & 0 & 0 & 0 & 0 & 0 & 0 \\ 1 & 0 & 0 & 0 & 0 & 0 & 0 & 0 \\ -1 & 0 & 0 & 0 & 0 & 0 & 0 & 0 \\ -1 & 0 & 0 & 0 & 0 & 0 & 0 & 0 \\ 1 & 0 & 0 & 0 & 0 & 0 & 0 & 0 \\ 1 & 0 & 0 & 0 & 0 & 0 & 0 & 0 \\ -1 & 0 & 0 & 0 & 0 & 0 & 0 & 0 \\ -1 & 0 & 0 & 0 & 0 & 0 & 0 & 0 \end{bmatrix} + \begin{bmatrix} 0 & 1 & 0 & 0 & 0 & 0 & 0 & 0 \\ 0 & 1 & 0 & 0 & 0 & 0 & 0 & 0 \\ 0 & -1 & 0 & 0 & 0 & 0 & 0 & 0 \\ 0 & -1 & 0 & 0 & 0 & 0 & 0 & 0 \\ 0 & 1 & 0 & 0 & 0 & 0 & 0 & 0 \\ 0 & 1 & 0 & 0 & 0 & 0 & 0 & 0 \\ 0 & -1 & 0 & 0 & 0 & 0 & 0 & 0 \\ 0 & -1 & 0 & 0 & 0 & 0 & 0 & 0 \end{bmatrix} +$$

$$\begin{vmatrix} 0 & 0 & 0 & 0 & 0 & 0 & 0 & 0 \\ 0 & 0 & 0 & 0 & 0 & 0 & 0 & 0 \\ 0 & 0 & 0 & 0 & 0 & 0 & 0 & 0 \\ 0 & 0 & 0 & 0 & 0 & 0 & 0 & 0 \\ 0 & 0 & 0 & 0 & 0 & 0 & 0 & 0 \\ 1 & 1 & -1 & -1 & 1 & 1 & 1 & 1 \\ 0 & 0 & 0 & 0 & 0 & 0 & 0 & 0 \\ 0 & 0 & 0 & 0 & 0 & 0 & 0 & 0 \end{vmatrix} + \begin{vmatrix} 0 & 0 & 0 & 0 & 0 & 0 & 0 & 0 \\ 0 & 0 & 0 & 0 & 0 & 0 & 0 & 0 \\ 0 & 0 & 0 & 0 & 0 & 0 & 0 & 0 \\ 0 & 0 & 0 & 0 & 0 & 0 & 0 & 0 \\ 0 & 0 & 0 & 0 & 0 & 0 & 0 & 0 \\ 0 & 0 & 0 & 0 & 0 & 0 & 0 & 0 \\ -1 & -1 & -1 & -1 & -1 & -1 & 1 & 1 \\ 0 & 0 & 0 & 0 & 0 & 0 & 0 & 0 \end{vmatrix} + \begin{vmatrix} 0 & 0 & 0 & 0 & 0 & 0 & 0 & 0 \\ 0 & 0 & 0 & 0 & 0 & 0 & 0 & 0 \\ 0 & 0 & 0 & 0 & 0 & 0 & 0 & 0 \\ 0 & 0 & 0 & 0 & 0 & 0 & 0 & 0 \\ 0 & 0 & 0 & 0 & 0 & 0 & 0 & 0 \\ 0 & 0 & 0 & 0 & 0 & 0 & 0 & 0 \\ 0 & 0 & 0 & 0 & 0 & 0 & 0 & 0 \\ -1 & -1 & -1 & -1 & -1 & -1 & 1 & 1 \end{vmatrix}$$

Figure 8. The «row decomposition» $R_8 = v_0 + v_1 + v_2 + v_3 + v_4 + v_5 + v_6 + v_7$ of the Rademacher (8*8)-matrix R_8 (Figure 1) where every of matrices $v_0, v_1, v_2, v_3, v_4, v_5, v_6, v_7$ is a projection operator

By analogy with the described case of the projection (4*4)-operators c_0, c_1, c_2, c_3 and r_0, r_1, r_2, r_3 (Figures 3-6), one can analyse features of sums of pairs of the column projection (8*8)-operators $s_0, s_1, s_2, s_3, s_4, s_5, s_6, s_7$ (Figure 7) and of the row projection (8*8)-operators $v_0, v_1, v_2, v_3, v_4, v_5, v_6, v_7$ in relation to their exponentiation. In other words, one can analyze features of matrices $(s_0 + s_1)^n, (s_0 + s_3)^n, \dots$ and $(v_0 + v_1)^n, (v_0 + v_2)^n, \dots$ where $n = 1, 2, 3, \dots$. Such analysis leads to resulting tables on Figure 9.

	s_0	s_1	s_2	s_3	s_4	s_5	s_6	s_7
s_0	-							
s_1		-						
s_2			-					
s_3				-				
s_4					-			
s_5						-		
s_6							-	
s_7								-

	v_0	v_1	v_2	v_3	v_4	v_5	v_6	v_7
v_0	-							
v_1		-						
v_2			-					
v_3				-				
v_4					-			
v_5						-		
v_6							-	
v_7								-

Figure 9. Tables of some features of sums of pairs of different column projectors s_0, s_1, \dots, s_7 (from Figure 7) and of row projectors v_0, v_1, \dots, v_7 (from the Rademacher matrix R_8 on Figure 8) in relation to their exponentiation. Explanations in text.

Every of cells in these tables on Figure 9 represents a sum of those projectors which denote its column and row by analogy with Figure 4. Again we have three types of such sums which are marked by green, red and yellow and which possess the similar properties in comparison with the cases on Figure 4.

In each of tables on Figure 9, green cells correspond to those matrices, exponentiations of which generate 8 cyclic groups. The left table contains 16 green cells that correspond to the following cyclic groups with a period 8: $(2^{-0.5} \cdot (s_0 + s_2))^n$, $(2^{-0.5} \cdot (s_0 + s_3))^n$, $(2^{-0.5} \cdot (s_1 + s_2))^n$, $(2^{-0.5} \cdot (s_1 + s_3))^n$, $(2^{-0.5} \cdot (s_4 + s_6))^n$, $(2^{-0.5} \cdot (s_4 + s_7))^n$, $(2^{-0.5} \cdot (s_5 + s_6))^n$, $(2^{-0.5} \cdot (s_5 + s_7))^n$. The right table contains 16 green cells with the same

tabular location that correspond to the following cyclic groups with a period 8:
 $(2^{-0.5*(v_0+v_2)})^n$, $(2^{-0.5*(v_0+v_3)})^n$, $(2^{-0.5*(v_1+v_2)})^n$, $(2^{-0.5*(v_1+v_3)})^n$, $(2^{-0.5*(v_4+v_6)})^n$,
 $(2^{-0.5*(v_4+v_7)})^n$, $(2^{-0.5*(v_5+v_6)})^n$, $(2^{-0.5*(v_5+v_7)})^n$.

Red cells in tables on Figure 9 contain those matrices which possess a doubling property in relation to their exponentiation. The left table contains 24 red cells, matrices of which satisfy the following feature: $(s_0+s_1)^n = 2^{n-1}*(s_0+s_1)$, $(s_0+s_4)^n = 2^{n-1}*(s_0+s_4)$, etc. The right table also contains 24 red cells with the same feature but with another tabular location: $(v_0+v_1)^n = 2^{n-1}*(v_0+v_1)$, $(v_0+v_4)^n = 2^{n-1}*(v_0+v_4)$, etc.

16 yellow cells in each of tables on Figure 9 contain those matrices, which have «quadruplet property»: $((s_0+s_6)^2)^n = 4^{n-1}*(s_0+s_6)^2$, $((v_0+v_4)^2)^n = 4^{n-1}*(v_0+v_4)^2$, etc. The cells on the main diagonal correspond to sum of two projectors themselves: $(s_i+s_i)^n = 2^n*s_i$, $(v_i+v_i)^n = 2^n*v_i$, where $i = 0, 1, 2, \dots, 7$.

3. GENETIC HADAMARD MATRICES AS SUMS OF PROJECTORS

The genetic Hadamard matrix H_4 from Figure 1 can be also decomposed into sum of 4 sparse matrices $H_4 = h_0+h_1+h_2+h_3$ where each of sparse matrices contains only one non-zero column (in a case of the «column decomposition») or only one non-zero row (in a case of the «row decomposition») (Figure 10).

$$H_4 = h_0+h_1+h_2+h_3 = \begin{vmatrix} 1 & 0 & 0 & 0 \\ -1 & 0 & 0 & 0 \\ 1 & 0 & 0 & 0 \\ -1 & 0 & 0 & 0 \end{vmatrix} + \begin{vmatrix} 0 & 1 & 0 & 0 \\ 0 & 1 & 0 & 0 \\ 0 & -1 & 0 & 0 \\ 0 & -1 & 0 & 0 \end{vmatrix} + \begin{vmatrix} 0 & 0 & -1 & 0 \\ 0 & 0 & 1 & 0 \\ 0 & 0 & 1 & 0 \\ 0 & 0 & -1 & 0 \end{vmatrix} + \begin{vmatrix} 0 & 0 & 0 & 1 \\ 0 & 0 & 0 & 1 \\ 0 & 0 & 0 & 1 \\ 0 & 0 & 0 & 1 \end{vmatrix}$$

$$H_4 = g_0+g_1+g_2+g_3 = \begin{vmatrix} 1 & 1 & -1 & 1 \\ 0 & 0 & 0 & 0 \\ 0 & 0 & 0 & 0 \\ 0 & 0 & 0 & 0 \end{vmatrix} + \begin{vmatrix} 0 & 0 & 0 & 0 \\ -1 & 1 & 1 & 1 \\ 0 & 0 & 0 & 0 \\ 0 & 0 & 0 & 0 \end{vmatrix} + \begin{vmatrix} 0 & 0 & 0 & 0 \\ 0 & 0 & 0 & 0 \\ 1 & -1 & 1 & 1 \\ 0 & 0 & 0 & 0 \end{vmatrix} + \begin{vmatrix} 0 & 0 & 0 & 0 \\ 0 & 0 & 0 & 0 \\ 0 & 0 & 0 & 0 \\ -1 & -1 & -1 & 1 \end{vmatrix}$$

Figure 10. The «column decomposition» (upper layer) and the «row decomposition» (bottom layer) of the Hadamard matrix H_4 from Figure 1

Each of these sparse matrices h_0, h_1, h_2, h_3 and g_0, g_1, g_2, g_3 on Figure 10 is a projector. We will conditionally name projectors h_0, h_1, h_2, h_3 again as «column projectors» and projectors g_0, g_1, g_2, g_3 as «row projectors».

By analogy with the previous section about the Rademacher matrix R_4 , one can analyse features of sums of pairs of these column projectors and row projectors in relation to their exponentiation. In other words, one can analyze features of matrices $(h_0+h_1)^n$, $(h_0+h_2)^n, \dots$ and $(g_0+g_1)^n, (g_0+g_2)^n, \dots$ where $n = 1, 2, 3, \dots$. Such analysis leads to resulting tables on Figure 11.

	h_0	h_1	h_2	h_3
h_0	-			
h_1		-		
h_2			-	
h_3				-

	g_0	g_1	g_2	g_3
g_0	-			
g_1		-		
g_2			-	
g_3				-

Figure 11. Tables of some features of sums of pairs of the different «column projectors» h_0, h_1, h_2, h_3 (in the left table) and of the «row projectors» g_0, g_1, g_2, g_3 (from the Hadamard matrix H_4 on Figure 10) in relation to their exponentiation. Explanations in text.

Both tables on Figure 11 are identical in their mosaics. Every of their cells correspond to a sum of those column projectors (or row projectors), which denote its column and row. 12 green cells correspond to matrices, exponentiations of which lead to cyclic groups with a period 8: $(2^{-0.5}*(h_0+h_1))^n, (2^{-0.5}*(h_0+h_2))^n, \dots, (2^{-0.5}*(g_0+g_1))^n, (2^{-0.5}*(g_0+g_2))^n, \dots$, where $n = 1, 2, 3, \dots$. The cells on the main diagonal correspond to sum of two projectors themselves: $(h_i+h_i)^n = 2^n*h_i, (g_i+g_i)^n = 2^n*g_i$, where $i = 0, 1, 2, 3$.

Cyclic properties of these (4*4)-matrix operators exist due to a connection of these operators with complex numbers. Figures 12 and 13 show existence of a special decomposition of every of these (4*4)-matrices into such set of two sparse matrices e_0 and e_1 , which is closed relative to multiplication and which defines their multiplication table that coincides with the known multiplication table of complex numbers.

$$\begin{aligned}
 h_0+h_1 &= \begin{vmatrix} 1 & 1 & 0 & 0 \\ -1 & 1 & 0 & 0 \\ 1 & -1 & 0 & 0 \\ -1 & -1 & 0 & 0 \end{vmatrix} = e_0+e_1 = \begin{vmatrix} 1 & 0 & 0 & 0 \\ 0 & 1 & 0 & 0 \\ 0 & -1 & 0 & 0 \\ -1 & 0 & 0 & 0 \end{vmatrix} + \begin{vmatrix} 0 & 1 & 0 & 0 \\ -1 & 0 & 0 & 0 \\ 1 & 0 & 0 & 0 \\ 0 & -1 & 0 & 0 \end{vmatrix} ; \begin{array}{|c|c|} \hline & e_0 \quad e_1 \\ \hline e_0 & e_0 \quad e_1 \\ \hline e_1 & e_1 \quad -e_0 \\ \hline \end{array} \\
 h_0+h_2 &= \begin{vmatrix} 1 & 0 & -1 & 0 \\ -1 & 0 & 1 & 0 \\ 1 & 0 & 1 & 0 \\ -1 & 0 & -1 & 0 \end{vmatrix} = e_0+e_1 = \begin{vmatrix} 1 & 0 & 0 & 0 \\ -1 & 0 & 0 & 0 \\ 0 & 0 & 1 & 0 \\ 0 & 0 & -1 & 0 \end{vmatrix} + \begin{vmatrix} 0 & 0 & -1 & 0 \\ 0 & 0 & 1 & 0 \\ 1 & 0 & 0 & 0 \\ -1 & 0 & 0 & 0 \end{vmatrix} ; \begin{array}{|c|c|} \hline & e_0 \quad e_1 \\ \hline e_0 & e_0 \quad e_1 \\ \hline e_1 & e_1 \quad -e_0 \\ \hline \end{array} \\
 h_0+h_3 &= \begin{vmatrix} 1 & 0 & 0 & 1 \\ -1 & 0 & 0 & 1 \\ 1 & 0 & 0 & 1 \\ -1 & 0 & 0 & 1 \end{vmatrix} = e_0+e_1 = \begin{vmatrix} 1 & 0 & 0 & 0 \\ 0 & 0 & 0 & 1 \\ 1 & 0 & 0 & 0 \\ 0 & 0 & 0 & 1 \end{vmatrix} + \begin{vmatrix} 0 & 0 & 0 & 1 \\ -1 & 0 & 0 & 0 \\ 0 & 0 & 0 & 1 \\ -1 & 0 & 0 & 0 \end{vmatrix} ; \begin{array}{|c|c|} \hline & e_0 \quad e_1 \\ \hline e_0 & e_0 \quad e_1 \\ \hline e_1 & e_1 \quad -e_0 \\ \hline \end{array} \\
 h_1+h_2 &= \begin{vmatrix} 0 & 1 & -1 & 0 \\ 0 & 1 & 1 & 0 \\ 0 & -1 & 1 & 0 \\ 0 & -1 & -1 & 0 \end{vmatrix} = e_0+e_1 = \begin{vmatrix} 0 & 0 & -1 & 0 \\ 0 & 1 & 0 & 0 \\ 0 & 0 & 1 & 0 \\ 0 & -1 & 0 & 0 \end{vmatrix} + \begin{vmatrix} 0 & 1 & 0 & 0 \\ 0 & 0 & 1 & 0 \\ 0 & -1 & 0 & 0 \\ 0 & 0 & -1 & 0 \end{vmatrix} ; \begin{array}{|c|c|} \hline & e_0 \quad e_1 \\ \hline e_0 & e_0 \quad e_1 \\ \hline e_1 & e_1 \quad -e_0 \\ \hline \end{array} \\
 h_1+h_3 &= \begin{vmatrix} 0 & 1 & 0 & 1 \\ 0 & 1 & 0 & 1 \\ 0 & -1 & 0 & 1 \\ 0 & -1 & 0 & 1 \end{vmatrix} = e_0+e_1 = \begin{vmatrix} 0 & 1 & 0 & 0 \\ 0 & 1 & 0 & 0 \\ 0 & 0 & 0 & 1 \\ 0 & 0 & 0 & 1 \end{vmatrix} + \begin{vmatrix} 0 & 0 & 0 & 1 \\ 0 & 0 & 0 & 1 \\ 0 & -1 & 0 & 0 \\ 0 & -1 & 0 & 0 \end{vmatrix} ; \begin{array}{|c|c|} \hline & e_0 \quad e_1 \\ \hline e_0 & e_0 \quad e_1 \\ \hline e_1 & e_1 \quad -e_0 \\ \hline \end{array}
 \end{aligned}$$

$$h_2+h_3 = \begin{vmatrix} 0 & 0 & -1 & 1 \\ 0 & 0 & 1 & 1 \\ 0 & 0 & 1 & 1 \\ 0 & 0 & -1 & 1 \end{vmatrix} = e_0+e_1 = \begin{vmatrix} 0 & 0 & 0 & 1 \\ 0 & 0 & 1 & 0 \\ 0 & 0 & 1 & 0 \\ 0 & 0 & 0 & 1 \end{vmatrix} + \begin{vmatrix} 0 & 0 & -1 & 0 \\ 0 & 0 & 0 & 1 \\ 0 & 0 & 0 & 1 \\ 0 & 0 & -1 & 0 \end{vmatrix} ; \begin{array}{|c|c|c|} \hline & e_0 & e_1 \\ \hline e_0 & e_0 & e_1 \\ \hline e_1 & e_1 & -e_0 \\ \hline \end{array}$$

Figure 12. The table represents special decompositions of (4*4)-matrices (h_0+h_1) , (h_0+h_2) , (h_0+h_3) , (h_1+h_2) , (h_1+h_3) , (h_2+h_3) into sum of two matrices e_0+e_1 . The table shows direct relations of these matrices with matrix representations of 2-parametric complex numbers. Here h_0 , h_1 , h_2 and h_3 are column projectors of the Hadamard matrix H_4 from Figure 10. For each set of matrices e_0 and e_1 at every tabular level, the right column of the table contains its multiplication table, which coincides with the multiplication table of complex numbers.

$$g_0+g_1 = \begin{vmatrix} 1 & 1 & -1 & 1 \\ -1 & 1 & 1 & 1 \\ 0 & 0 & 0 & 0 \\ 0 & 0 & 0 & 0 \end{vmatrix} = e_0+e_1 = \begin{vmatrix} 1 & 0 & -1 & 0 \\ 0 & 1 & 0 & 1 \\ 0 & 0 & 0 & 0 \\ 0 & 0 & 0 & 0 \end{vmatrix} + \begin{vmatrix} 0 & 1 & 0 & 1 \\ -1 & 0 & 1 & 0 \\ 0 & 0 & 0 & 0 \\ 0 & 0 & 0 & 0 \end{vmatrix} ; \begin{array}{|c|c|c|} \hline & e_0 & e_1 \\ \hline e_0 & e_0 & e_1 \\ \hline e_1 & e_1 & -e_0 \\ \hline \end{array}$$

$$g_0+g_2 = \begin{vmatrix} 1 & 1 & -1 & 1 \\ 0 & 0 & 0 & 0 \\ 1 & -1 & 1 & 1 \\ 0 & 0 & 0 & 0 \end{vmatrix} = e_0+e_1 = \begin{vmatrix} 1 & 0 & 0 & 1 \\ 0 & 0 & 0 & 0 \\ 0 & -1 & 1 & 0 \\ 0 & 0 & 0 & 0 \end{vmatrix} + \begin{vmatrix} 0 & 1 & -1 & 0 \\ 0 & 0 & 0 & 0 \\ 1 & 0 & 0 & 1 \\ 0 & 0 & 0 & 0 \end{vmatrix} ; \begin{array}{|c|c|c|} \hline & e_0 & e_1 \\ \hline e_0 & e_0 & e_1 \\ \hline e_1 & e_1 & -e_0 \\ \hline \end{array}$$

$$g_0+g_3 = \begin{vmatrix} 1 & 1 & -1 & 1 \\ 0 & 0 & 0 & 0 \\ 0 & 0 & 0 & 0 \\ -1 & -1 & -1 & 1 \end{vmatrix} = e_0+e_1 = \begin{vmatrix} 1 & 1 & 0 & 0 \\ 0 & 0 & 0 & 0 \\ 0 & 0 & 0 & 0 \\ 0 & 0 & -1 & 1 \end{vmatrix} + \begin{vmatrix} 0 & 0 & -1 & 1 \\ 0 & 0 & 0 & 0 \\ 0 & 0 & 0 & 0 \\ -1 & -1 & 0 & 0 \end{vmatrix} ; \begin{array}{|c|c|c|} \hline & e_0 & e_1 \\ \hline e_0 & e_0 & e_1 \\ \hline e_1 & e_1 & -e_0 \\ \hline \end{array}$$

$$g_1+g_2 = \begin{vmatrix} 0 & 0 & 0 & 0 \\ -1 & 1 & 1 & 1 \\ 1 & -1 & 1 & 1 \\ 0 & 0 & 0 & 0 \end{vmatrix} = e_0+e_1 = \begin{vmatrix} 0 & 0 & 0 & 0 \\ -1 & 1 & 0 & 0 \\ 0 & 0 & 1 & 1 \\ 0 & 0 & 0 & 0 \end{vmatrix} + \begin{vmatrix} 0 & 0 & 0 & 0 \\ 0 & 0 & 1 & 1 \\ 1 & -1 & 0 & 0 \\ 0 & 0 & 0 & 0 \end{vmatrix} ; \begin{array}{|c|c|c|} \hline & e_0 & e_1 \\ \hline e_0 & e_0 & e_1 \\ \hline e_1 & e_1 & -e_0 \\ \hline \end{array}$$

$$g_1+g_3 = \begin{vmatrix} 0 & 0 & 0 & 0 \\ -1 & 1 & 1 & 1 \\ 0 & 0 & 0 & 0 \\ -1 & -1 & -1 & 1 \end{vmatrix} = e_0+e_1 = \begin{vmatrix} 0 & 0 & 0 & 0 \\ 0 & 1 & 1 & 0 \\ 0 & 0 & 0 & 0 \\ -1 & 0 & 0 & 1 \end{vmatrix} + \begin{vmatrix} 0 & 0 & 0 & 0 \\ -1 & 0 & 0 & 1 \\ 0 & 0 & 0 & 0 \\ 0 & -1 & -1 & 0 \end{vmatrix} ; \begin{array}{|c|c|c|} \hline & e_0 & e_1 \\ \hline e_0 & e_0 & e_1 \\ \hline e_1 & e_1 & -e_0 \\ \hline \end{array}$$

$$g_2+g_3 = \begin{vmatrix} 0 & 0 & 0 & 0 \\ 0 & 0 & 0 & 0 \\ 1 & -1 & 1 & 1 \\ -1 & -1 & -1 & 1 \end{vmatrix} = e_0+e_1 = \begin{vmatrix} 0 & 0 & 0 & 0 \\ 0 & 0 & 0 & 0 \\ 1 & 0 & 1 & 0 \\ 0 & -1 & 0 & 1 \end{vmatrix} + \begin{vmatrix} 0 & 0 & 0 & 0 \\ 0 & 0 & 0 & 0 \\ 0 & -1 & 0 & 1 \\ -1 & 0 & -1 & 0 \end{vmatrix} ; \begin{array}{|c|c|c|} \hline & e_0 & e_1 \\ \hline e_0 & e_0 & e_1 \\ \hline e_1 & e_1 & -e_0 \\ \hline \end{array}$$

Figure 13. The table represents special decompositions of (4*4)-matrices (g_0+g_1) , (g_0+g_2) , (g_0+g_3) , (g_1+g_2) , (g_1+g_3) , (g_2+g_3) into sum of two matrices e_0+e_1 . The table shows direct relations of these matrices with matrix representations of 2-parametric complex numbers. Here g_0 , g_1 , g_2 and g_3 are row projectors from Figure 10. For each set of matrices e_0 and e_1 at every tabular level, the right column of the table contains its multiplication table, which coincides with the multiplication table of complex numbers.

Now let us turn to the genetic Hadamard matrix H_8 from Figure 1. It can be also decomposed into sum of 8 sparse matrices $H_8=u_0+u_1+u_2+u_3+u_4+u_5+u_6+u_7$ where each of sparse matrices contains only one non-zero column (in a case of the «column decomposition») or only one non-zero row (in a case of the «row decomposition») (Figure 14).

$$\begin{aligned}
 H_8 = u_0 + u_1 + u_2 + u_3 + u_4 + u_5 + u_6 + u_7 = & \begin{bmatrix} 1 & 0 & 0 & 0 & 0 & 0 & 0 & 0 \\ 1 & 0 & 0 & 0 & 0 & 0 & 0 & 0 \\ -1 & 0 & 0 & 0 & 0 & 0 & 0 & 0 \\ -1 & 0 & 0 & 0 & 0 & 0 & 0 & 0 \\ 1 & 0 & 0 & 0 & 0 & 0 & 0 & 0 \\ 1 & 0 & 0 & 0 & 0 & 0 & 0 & 0 \\ -1 & 0 & 0 & 0 & 0 & 0 & 0 & 0 \\ -1 & 0 & 0 & 0 & 0 & 0 & 0 & 0 \end{bmatrix} + \begin{bmatrix} 0 & -1 & 0 & 0 & 0 & 0 & 0 & 0 \\ 0 & 1 & 0 & 0 & 0 & 0 & 0 & 0 \\ 0 & 1 & 0 & 0 & 0 & 0 & 0 & 0 \\ 0 & -1 & 0 & 0 & 0 & 0 & 0 & 0 \\ 0 & -1 & 0 & 0 & 0 & 0 & 0 & 0 \\ 0 & 1 & 0 & 0 & 0 & 0 & 0 & 0 \\ 0 & 1 & 0 & 0 & 0 & 0 & 0 & 0 \\ 0 & -1 & 0 & 0 & 0 & 0 & 0 & 0 \end{bmatrix} + \\
 & \begin{bmatrix} 0 & 0 & 1 & 0 & 0 & 0 & 0 & 0 \\ 0 & 0 & 1 & 0 & 0 & 0 & 0 & 0 \\ 0 & 0 & 1 & 0 & 0 & 0 & 0 & 0 \\ 0 & 0 & 1 & 0 & 0 & 0 & 0 & 0 \\ 0 & 0 & -1 & 0 & 0 & 0 & 0 & 0 \\ 0 & 0 & -1 & 0 & 0 & 0 & 0 & 0 \\ 0 & 0 & -1 & 0 & 0 & 0 & 0 & 0 \\ 0 & 0 & -1 & 0 & 0 & 0 & 0 & 0 \end{bmatrix} + \begin{bmatrix} 0 & 0 & 0 & -1 & 0 & 0 & 0 & 0 \\ 0 & 0 & 0 & 1 & 0 & 0 & 0 & 0 \\ 0 & 0 & 0 & -1 & 0 & 0 & 0 & 0 \\ 0 & 0 & 0 & 1 & 0 & 0 & 0 & 0 \\ 0 & 0 & 0 & 1 & 0 & 0 & 0 & 0 \\ 0 & 0 & 0 & -1 & 0 & 0 & 0 & 0 \\ 0 & 0 & 0 & 1 & 0 & 0 & 0 & 0 \\ 0 & 0 & 0 & -1 & 0 & 0 & 0 & 0 \end{bmatrix} + \\
 & \begin{bmatrix} 0 & 0 & 0 & 0 & -1 & 0 & 0 & 0 \\ 0 & 0 & 0 & 0 & -1 & 0 & 0 & 0 \\ 0 & 0 & 0 & 0 & 1 & 0 & 0 & 0 \\ 0 & 0 & 0 & 0 & 1 & 0 & 0 & 0 \\ 0 & 0 & 0 & 0 & 1 & 0 & 0 & 0 \\ 0 & 0 & 0 & 0 & -1 & 0 & 0 & 0 \\ 0 & 0 & 0 & 0 & -1 & 0 & 0 & 0 \\ 0 & 0 & 0 & 0 & -1 & 0 & 0 & 0 \end{bmatrix} + \\
 & \begin{bmatrix} 0 & 0 & 0 & 0 & 0 & 1 & 0 & 0 \\ 0 & 0 & 0 & 0 & 0 & -1 & 0 & 0 \\ 0 & 0 & 0 & 0 & 0 & -1 & 0 & 0 \\ 0 & 0 & 0 & 0 & 0 & 1 & 0 & 0 \\ 0 & 0 & 0 & 0 & 0 & -1 & 0 & 0 \\ 0 & 0 & 0 & 0 & 0 & 1 & 0 & 0 \\ 0 & 0 & 0 & 0 & 0 & 1 & 0 & 0 \\ 0 & 0 & 0 & 0 & 0 & -1 & 0 & 0 \end{bmatrix} + \begin{bmatrix} 0 & 0 & 0 & 0 & 0 & 0 & 1 & 0 \\ 0 & 0 & 0 & 0 & 0 & 0 & 1 & 0 \\ 0 & 0 & 0 & 0 & 0 & 0 & 1 & 0 \\ 0 & 0 & 0 & 0 & 0 & 0 & 1 & 0 \\ 0 & 0 & 0 & 0 & 0 & 0 & 1 & 0 \\ 0 & 0 & 0 & 0 & 0 & 0 & 1 & 0 \\ 0 & 0 & 0 & 0 & 0 & 0 & 1 & 0 \\ 0 & 0 & 0 & 0 & 0 & 0 & 1 & 0 \end{bmatrix} + \begin{bmatrix} 0 & 0 & 0 & 0 & 0 & 0 & 0 & -1 \\ 0 & 0 & 0 & 0 & 0 & 0 & 0 & 1 \\ 0 & 0 & 0 & 0 & 0 & 0 & 0 & -1 \\ 0 & 0 & 0 & 0 & 0 & 0 & 0 & 1 \\ 0 & 0 & 0 & 0 & 0 & 0 & 0 & -1 \\ 0 & 0 & 0 & 0 & 0 & 0 & 0 & 1 \\ 0 & 0 & 0 & 0 & 0 & 0 & 0 & -1 \\ 0 & 0 & 0 & 0 & 0 & 0 & 0 & 1 \end{bmatrix}
 \end{aligned}$$

Figure 14. The «column decomposition» $H_8=u_0+u_1+u_2+u_3+u_4+u_5+u_6+u_7$ of the Hadamard (8*8)-matrix H_8 (Figure 1) where every of sparse matrices u_0 , u_1 , u_2 , u_3 , u_4 , u_5 , u_6 , u_7 is a projection operator

$$\begin{aligned}
& \mathbf{H}_8 = \mathbf{d}_0 + \mathbf{d}_1 + \mathbf{d}_2 + \mathbf{d}_3 + \mathbf{d}_4 + \mathbf{d}_5 + \mathbf{d}_6 + \mathbf{d}_7 = \\
& \begin{vmatrix} 1 & -1 & 1 & -1 & -1 & 1 & 1 & -1 \\ 0 & 0 & 0 & 0 & 0 & 0 & 0 & 0 \\ 0 & 0 & 0 & 0 & 0 & 0 & 0 & 0 \\ 0 & 0 & 0 & 0 & 0 & 0 & 0 & 0 \\ 0 & 0 & 0 & 0 & 0 & 0 & 0 & 0 \\ 0 & 0 & 0 & 0 & 0 & 0 & 0 & 0 \\ 0 & 0 & 0 & 0 & 0 & 0 & 0 & 0 \\ 0 & 0 & 0 & 0 & 0 & 0 & 0 & 0 \end{vmatrix} + \begin{vmatrix} 0 & 0 & 0 & 0 & 0 & 0 & 0 & 0 \\ 1 & 1 & 1 & 1 & -1 & -1 & 1 & 1 \\ 0 & 0 & 0 & 0 & 0 & 0 & 0 & 0 \\ 0 & 0 & 0 & 0 & 0 & 0 & 0 & 0 \\ 0 & 0 & 0 & 0 & 0 & 0 & 0 & 0 \\ 0 & 0 & 0 & 0 & 0 & 0 & 0 & 0 \\ 0 & 0 & 0 & 0 & 0 & 0 & 0 & 0 \\ 0 & 0 & 0 & 0 & 0 & 0 & 0 & 0 \end{vmatrix} \\
& + \begin{vmatrix} 0 & 0 & 0 & 0 & 0 & 0 & 0 & 0 \\ 0 & 0 & 0 & 0 & 0 & 0 & 0 & 0 \\ -1 & 1 & 1 & -1 & 1 & -1 & 1 & -1 \\ 0 & 0 & 0 & 0 & 0 & 0 & 0 & 0 \\ 0 & 0 & 0 & 0 & 0 & 0 & 0 & 0 \\ 0 & 0 & 0 & 0 & 0 & 0 & 0 & 0 \\ 0 & 0 & 0 & 0 & 0 & 0 & 0 & 0 \\ 0 & 0 & 0 & 0 & 0 & 0 & 0 & 0 \end{vmatrix} + \begin{vmatrix} 0 & 0 & 0 & 0 & 0 & 0 & 0 & 0 \\ 0 & 0 & 0 & 0 & 0 & 0 & 0 & 0 \\ 0 & 0 & 0 & 0 & 0 & 0 & 0 & 0 \\ -1 & -1 & 1 & 1 & 1 & 1 & 1 & 1 \\ 0 & 0 & 0 & 0 & 0 & 0 & 0 & 0 \\ 0 & 0 & 0 & 0 & 0 & 0 & 0 & 0 \\ 0 & 0 & 0 & 0 & 0 & 0 & 0 & 0 \\ 0 & 0 & 0 & 0 & 0 & 0 & 0 & 0 \end{vmatrix} + \begin{vmatrix} 0 & 0 & 0 & 0 & 0 & 0 & 0 & 0 \\ 0 & 0 & 0 & 0 & 0 & 0 & 0 & 0 \\ 0 & 0 & 0 & 0 & 0 & 0 & 0 & 0 \\ 0 & 0 & 0 & 0 & 0 & 0 & 0 & 0 \\ 1 & -1 & -1 & 1 & 1 & -1 & 1 & -1 \\ 0 & 0 & 0 & 0 & 0 & 0 & 0 & 0 \\ 0 & 0 & 0 & 0 & 0 & 0 & 0 & 0 \\ 0 & 0 & 0 & 0 & 0 & 0 & 0 & 0 \end{vmatrix} \\
& + \begin{vmatrix} 0 & 0 & 0 & 0 & 0 & 0 & 0 & 0 \\ 0 & 0 & 0 & 0 & 0 & 0 & 0 & 0 \\ 0 & 0 & 0 & 0 & 0 & 0 & 0 & 0 \\ 0 & 0 & 0 & 0 & 0 & 0 & 0 & 0 \\ 0 & 0 & 0 & 0 & 0 & 0 & 0 & 0 \\ 1 & 1 & -1 & -1 & 1 & 1 & 1 & 1 \\ 0 & 0 & 0 & 0 & 0 & 0 & 0 & 0 \\ 0 & 0 & 0 & 0 & 0 & 0 & 0 & 0 \end{vmatrix} + \begin{vmatrix} 0 & 0 & 0 & 0 & 0 & 0 & 0 & 0 \\ 0 & 0 & 0 & 0 & 0 & 0 & 0 & 0 \\ 0 & 0 & 0 & 0 & 0 & 0 & 0 & 0 \\ 0 & 0 & 0 & 0 & 0 & 0 & 0 & 0 \\ 0 & 0 & 0 & 0 & 0 & 0 & 0 & 0 \\ 0 & 0 & 0 & 0 & 0 & 0 & 0 & 0 \\ -1 & 1 & -1 & 1 & -1 & 1 & 1 & -1 \\ 0 & 0 & 0 & 0 & 0 & 0 & 0 & 0 \end{vmatrix} + \begin{vmatrix} 0 & 0 & 0 & 0 & 0 & 0 & 0 & 0 \\ 0 & 0 & 0 & 0 & 0 & 0 & 0 & 0 \\ 0 & 0 & 0 & 0 & 0 & 0 & 0 & 0 \\ 0 & 0 & 0 & 0 & 0 & 0 & 0 & 0 \\ 0 & 0 & 0 & 0 & 0 & 0 & 0 & 0 \\ 0 & 0 & 0 & 0 & 0 & 0 & 0 & 0 \\ 0 & 0 & 0 & 0 & 0 & 0 & 0 & 0 \\ -1 & -1 & -1 & -1 & -1 & -1 & 1 & 1 \end{vmatrix}
\end{aligned}$$

Figure 15. The «row decomposition» $\mathbf{H}_8 = \mathbf{d}_0 + \mathbf{d}_1 + \mathbf{d}_2 + \mathbf{d}_3 + \mathbf{d}_4 + \mathbf{d}_5 + \mathbf{d}_6 + \mathbf{d}_7$ of the Hadamard (8*8)-matrix \mathbf{H}_8 (Figure 1) where every of sparse matrices $\mathbf{d}_0, \mathbf{d}_1, \mathbf{d}_2, \mathbf{d}_3, \mathbf{d}_4, \mathbf{d}_5, \mathbf{d}_6, \mathbf{d}_7$ is a projection operator

Every of these sparse matrices $\mathbf{u}_0, \mathbf{u}_1, \mathbf{u}_2, \mathbf{u}_3, \mathbf{u}_4, \mathbf{u}_5, \mathbf{u}_6, \mathbf{u}_7$ and $\mathbf{d}_0, \mathbf{d}_1, \mathbf{d}_2, \mathbf{d}_3, \mathbf{d}_4, \mathbf{d}_5, \mathbf{d}_6, \mathbf{d}_7$ on Figures 14, 15 is a projector. We will conditionally name projectors $\mathbf{u}_0, \mathbf{u}_1, \mathbf{u}_2, \mathbf{u}_3, \mathbf{u}_4, \mathbf{u}_5, \mathbf{u}_6, \mathbf{u}_7$ again as «column projectors» and projectors $\mathbf{d}_0, \mathbf{d}_1, \mathbf{d}_2, \mathbf{d}_3, \mathbf{d}_4, \mathbf{d}_5, \mathbf{d}_6, \mathbf{d}_7$ as «row projectors».

By analogy with the previous sections, one can analyse features of sums of pairs of these column projectors and row projectors in relation to their exponentiation. In other words, one can analyze features of matrices $(\mathbf{u}_0 + \mathbf{u}_1)^n, (\mathbf{u}_0 + \mathbf{u}_3)^n, \dots$ and $(\mathbf{d}_0 + \mathbf{d}_1)^n, (\mathbf{d}_0 + \mathbf{d}_2)^n, \dots$ where $n = 1, 2, 3, \dots$. Such analysis leads to resulting tables on Figure 16.

	\mathbf{u}_0	\mathbf{u}_1	\mathbf{u}_2	\mathbf{u}_3	\mathbf{u}_4	\mathbf{u}_5	\mathbf{u}_6	\mathbf{u}_7
\mathbf{u}_0	-							
\mathbf{u}_1		-						
\mathbf{u}_2			-					
\mathbf{u}_3				-				
\mathbf{u}_4					-			
\mathbf{u}_5						-		
\mathbf{u}_6							-	
\mathbf{u}_7								-

	\mathbf{d}_0	\mathbf{d}_1	\mathbf{d}_2	\mathbf{d}_3	\mathbf{d}_4	\mathbf{d}_5	\mathbf{d}_6	\mathbf{d}_7
\mathbf{d}_0	-							
\mathbf{d}_1		-						
\mathbf{d}_2			-					
\mathbf{d}_3				-				
\mathbf{d}_4					-			
\mathbf{d}_5						-		
\mathbf{d}_6							-	
\mathbf{d}_7								-

Figure 16. Tables of some features of sums of pairs of the different column projectors u_0, u_1, \dots, u_7 (from Figure 14) and of the row projectors d_0, d_1, \dots, d_7 (from Figure 15) in relation to their exponentiation. This is the case of the Hadamard matrix H_8 from Figure 1. Explanations in text.

Both tables on Figure 16 have the identical mosaic with 32 green cells and 24 yellow cells. The green cells in these tables correspond to those matrices, exponentiations of which generate cyclic groups with a period 8:

- $(2^{-0.5*(u_0+u_1)})^n, (2^{-0.5*(u_0+u_2)})^n, (2^{-0.5*(u_0+u_4)})^n, (2^{-0.5*(u_0+u_6)})^n,$
 $(2^{-0.5*(u_1+u_3)})^n, (2^{-0.5*(u_1+u_5)})^n, (2^{-0.5*(u_1+u_7)})^n, (2^{-0.5*(u_2+u_3)})^n,$
 $(2^{-0.5*(u_2+u_4)})^n, (2^{-0.5*(u_2+u_6)})^n, (2^{-0.5*(u_3+u_5)})^n, (2^{-0.5*(u_3+u_7)})^n,$
 $(2^{-0.5*(u_4+u_5)})^n, (2^{-0.5*(u_4+u_6)})^n, (2^{-0.5*(u_5+u_7)})^n, (2^{-0.5*(u_6+u_7)})^n$ (in the left table);
- $(2^{-0.5*(d_0+d_1)})^n, (2^{-0.5*(d_0+d_2)})^n, (2^{-0.5*(d_0+d_4)})^n, (2^{-0.5*(d_0+d_6)})^n,$
 $(2^{-0.5*(d_1+d_3)})^n, (2^{-0.5*(d_1+d_5)})^n, (2^{-0.5*(d_1+d_7)})^n, (2^{-0.5*(d_2+d_3)})^n,$
 $(2^{-0.5*(d_2+d_4)})^n, (2^{-0.5*(d_2+d_6)})^n, (2^{-0.5*(d_3+d_5)})^n, (2^{-0.5*(d_3+d_7)})^n,$
 $(2^{-0.5*(d_4+d_5)})^n, (2^{-0.5*(d_4+d_6)})^n, (2^{-0.5*(d_5+d_7)})^n, (2^{-0.5*(d_6+d_7)})^n$ (in the right table).

Cyclic properties of these $(8*8)$ -matrix operators exist due to a connection of these operators with complex numbers. Figure 17 shows some examples of decompositions of the $(8*8)$ -matrices from green cells on Figure 16 into corresponding sets of two sparse matrices, each of which is closed in relation to multiplication and each of which defines the multiplication table of complex numbers (see some additional details about representations of complex numbers by means of (2^n*2^n) -matrices in [Petoukhov, 2012b]). It should be noted here that our study in the field of matrix genetics has revealed methods of extension of these $(8*8)$ -genetic matrices R_4, R_8, H_4, H_8 (Figure 1) into (2^n*2^n) -matrices which are also sums of "column projectors" and "row projectors" and which give by analogy as much cyclic groups as needed to model big ensembles of cyclic processes.

$$\begin{array}{l}
 \mathbf{u}_0 + \mathbf{u}_4 = \begin{bmatrix} 1 & 0 & 0 & 0 & -1 & 0 & 0 & 0 \\ 1 & 0 & 0 & 0 & -1 & 0 & 0 & 0 \\ -1 & 0 & 0 & 0 & 1 & 0 & 0 & 0 \\ -1 & 0 & 0 & 0 & 1 & 0 & 0 & 0 \\ 1 & 0 & 0 & 0 & 1 & 0 & 0 & 0 \\ 1 & 0 & 0 & 0 & 1 & 0 & 0 & 0 \\ -1 & 0 & 0 & 0 & -1 & 0 & 0 & 0 \\ -1 & 0 & 0 & 0 & -1 & 0 & 0 & 0 \end{bmatrix} = \begin{bmatrix} 1 & 0 & 0 & 0 & 0 & 0 & 0 & 0 \\ 1 & 0 & 0 & 0 & 0 & 0 & 0 & 0 \\ -1 & 0 & 0 & 0 & 0 & 0 & 0 & 0 \\ -1 & 0 & 0 & 0 & 0 & 0 & 0 & 0 \\ 0 & 0 & 0 & 0 & 1 & 0 & 0 & 0 \\ 0 & 0 & 0 & 0 & 1 & 0 & 0 & 0 \\ 0 & 0 & 0 & 0 & -1 & 0 & 0 & 0 \\ 0 & 0 & 0 & 0 & -1 & 0 & 0 & 0 \end{bmatrix} + \begin{bmatrix} 0 & 0 & 0 & 0 & -1 & 0 & 0 & 0 \\ 0 & 0 & 0 & 0 & -1 & 0 & 0 & 0 \\ 0 & 0 & 0 & 0 & 1 & 0 & 0 & 0 \\ 0 & 0 & 0 & 0 & 1 & 0 & 0 & 0 \\ 1 & 0 & 0 & 0 & 0 & 0 & 0 & 0 \\ 1 & 0 & 0 & 0 & 0 & 0 & 0 & 0 \\ -1 & 0 & 0 & 0 & 0 & 0 & 0 & 0 \\ -1 & 0 & 0 & 0 & 0 & 0 & 0 & 0 \end{bmatrix} = \mathbf{e}_0 + \mathbf{e}_4; \\
 \\
 \mathbf{u}_1 + \mathbf{u}_5 = \begin{bmatrix} 0 & -1 & 0 & 0 & 0 & 1 & 0 & 0 \\ 0 & 1 & 0 & 0 & 0 & -1 & 0 & 0 \\ 0 & 1 & 0 & 0 & 0 & -1 & 0 & 0 \\ 0 & -1 & 0 & 0 & 0 & 1 & 0 & 0 \\ 0 & -1 & 0 & 0 & 0 & -1 & 0 & 0 \\ 0 & 1 & 0 & 0 & 0 & 1 & 0 & 0 \\ 0 & 1 & 0 & 0 & 0 & 1 & 0 & 0 \\ 0 & -1 & 0 & 0 & 0 & -1 & 0 & 0 \end{bmatrix} = \begin{bmatrix} 0 & -1 & 0 & 0 & 0 & 0 & 0 & 0 \\ 0 & 1 & 0 & 0 & 0 & 0 & 0 & 0 \\ 0 & 1 & 0 & 0 & 0 & 0 & 0 & 0 \\ 0 & -1 & 0 & 0 & 0 & 0 & 0 & 0 \\ 0 & 0 & 0 & 0 & -1 & 0 & 0 & 0 \\ 0 & 0 & 0 & 0 & 1 & 0 & 0 & 0 \\ 0 & 0 & 0 & 0 & 1 & 0 & 0 & 0 \\ 0 & 0 & 0 & 0 & -1 & 0 & 0 & 0 \end{bmatrix} + \begin{bmatrix} 0 & 0 & 0 & 0 & 0 & 1 & 0 & 0 \\ 0 & 0 & 0 & 0 & 0 & -1 & 0 & 0 \\ 0 & 0 & 0 & 0 & 0 & -1 & 0 & 0 \\ 0 & 0 & 0 & 0 & 0 & 1 & 0 & 0 \\ 0 & -1 & 0 & 0 & 0 & 0 & 0 & 0 \\ 0 & 1 & 0 & 0 & 0 & 0 & 0 & 0 \\ 0 & 1 & 0 & 0 & 0 & 0 & 0 & 0 \\ 0 & -1 & 0 & 0 & 0 & 0 & 0 & 0 \end{bmatrix} = \mathbf{e}_1 + \mathbf{e}_5; \\
 \end{array}$$

	\mathbf{e}_0	\mathbf{e}_4
\mathbf{e}_0	\mathbf{e}_0	\mathbf{e}_4
\mathbf{e}_4	\mathbf{e}_4	$-\mathbf{e}_0$

	\mathbf{e}_1	\mathbf{e}_5
\mathbf{e}_1	\mathbf{e}_1	\mathbf{e}_5
\mathbf{e}_5	\mathbf{e}_5	$-\mathbf{e}_1$

$$\begin{aligned}
u_2 + u_6 &= \begin{bmatrix} 00 & 100010 \\ 00 & 100010 \\ 00 & 100010 \\ 00 & 100010 \\ 00 & -100010 \\ 00 & -100010 \\ 00 & -100010 \\ 00 & -100010 \end{bmatrix} = \begin{bmatrix} 00 & 100000 \\ 00 & 100000 \\ 00 & 100000 \\ 00 & 100000 \\ 00000010 \\ 00000010 \\ 00000010 \\ 00000010 \end{bmatrix} = \begin{bmatrix} 00 & 000010 \\ 00 & 000010 \\ 00 & 000010 \\ 00 & 000010 \\ 00 & -100000 \\ 00 & -100000 \\ 00 & -100000 \\ 00 & -100000 \end{bmatrix} = e_2 + e_6; \\
&\quad \begin{array}{|c|c|} \hline & e_2 \quad e_6 \\ \hline e_2 & e_2 \quad e_6 \\ \hline e_6 & e_6 \quad -e_2 \\ \hline \end{array} \\
\\
u_3 + u_7 &= \begin{bmatrix} 000 & -1000 & -1 \\ 000 & 1000 & 1 \\ 000 & -1000 & -1 \\ 000 & 1000 & 1 \\ 000 & 1000 & -1 \\ 000 & -1000 & 1 \\ 000 & 1000 & -1 \\ 000 & -1000 & 1 \end{bmatrix} = \begin{bmatrix} 000 & -10000 \\ 000 & 10000 \\ 000 & -10000 \\ 000 & 10000 \\ 000 & 0000 & -1 \\ 000 & 0000 & 1 \\ 000 & 0000 & -1 \\ 000 & 0000 & 1 \end{bmatrix} + \begin{bmatrix} 0000000 & -1 \\ 000 & 0000 & 1 \\ 0000000 & -1 \\ 000 & 0000 & 1 \\ 000 & 10000 \\ 000 & -10000 \\ 000 & 10000 \\ 000 & -10000 \end{bmatrix} = e_3 + e_7; \\
&\quad \begin{array}{|c|c|} \hline & e_3 \quad e_7 \\ \hline e_3 & e_3 \quad e_7 \\ \hline e_7 & e_7 \quad -e_3 \\ \hline \end{array}
\end{aligned}$$

Figure 17. The decomposition of the (8*8)-matrices u_0+u_4 , u_1+u_5 , u_2+u_6 , u_3+u_7 , which are examples of (8*8)-matrices from green cells on Figure 16, into corresponding sets of two sparse matrices e_0 and e_4 , e_1 and e_5 , e_2 and e_6 , e_3 and e_7 , each of which is closed in relation to multiplication and each of which defines the multiplication table of complex numbers (on the right)

Figure 17 testifies that the Hadamard (8*8)-matrix $H_8 = (u_0+u_4)+(u_1+u_5)+(u_2+u_6)+(u_3+u_7)$ (Fig. 1) is a sum of 4 complex numbers in 8-dimensional space.

Yellow cells in tables on Figure 16 correspond to matrices with the following property: $((u_i+u_j)^2)^n = 2^{n-1}*(u_i+u_j)$ and $((d_i+d_j)^2)^n = 2^{n-1}*(d_i+d_j)$ where $i \neq j$, $i, j = 0, 1, 2, \dots, 7$, $n = 1, 2, 3, \dots$. Cells on the main diagonal correspond to matrices $(u_i+u_i)^n = 2^n u_i$.

4. INHERITED BIOCYCLES AND A SELECTIVE CONTROL OF CYCLIC CHANGES OF VECTORS IN A MULTIDIMENSIONAL SPACE. PROBLEMS OF GENETIC BIOMECHANICS

Any living organism is an object with a huge ensemble of inherited cyclic processes, which form a hierarchy at different levels. Even every protein is involved in a cycle of the "birth and death," because after a certain time it breaks down into its constituent amino acids and they are then collected into a new protein. According to chronomedicine and biorhythmology, various diseases of the body are associated with disturbances (dys-synchronization) in these cooperative ensembles of biocycles. All inherited physiological subsystems of the body should be agreed with the structural organization of genetic coding for their coding and transmission to descendants; in other words, they bear the stamp of its features. We develop a "genetic biomechanics", which studies deep coherence between inherited physiological systems and molecular-genetic structures.

Our discovery of the described cyclic groups (on basis of genetic projectors), which are connected with phenomenological properties of molecular-genetic systems in their matrix forms of representation, gives a mathematical approach to simulate ensembles of cyclic processes. In this approach an idea of multi-dimensional vector space is used to simulate inherited biological phenomena including cooperative ensembles of cyclic processes.

Multidimensional vectors of this bioinformation space can be changed under influence of those matrix operators on the basis of genetic projectors that were described in previous section. Due to special properties of these operators a useful possibility exists to provide a selective control (or a selective coding) of cyclic changes (and some other changes) of separate coordinates of multidimensional vectors in this space.

Let us explain this by one example. Let us take, for instance, the cyclic group of operators $Y^n = (2^{-0.5}*(s_0+s_2))^n$ (see Figures 7 and 9, on the left) and an arbitrary 8-dimensional vector $X=[x_0, x_1, x_2, x_3, x_4, x_5, x_6, x_7]$. Then let us analyze an expression $X*Y^n = [x_0, x_1, x_2, x_3, x_4, x_5, x_6, x_7]*(2^{-0.5}*(s_0+s_2))^n = Z_n$ that leads to a new vector $Z_n=[z_0, z_1, z_2, z_3, z_4, z_5, z_6, z_7]$ (here $n = 1, 2, 3, \dots$). Figure 18 shows a cyclic transformation of coordinates of vectors Z_n ; vectors $X*Y^1$ and $X*Y^9$ are identical because the period of this cyclic group $Y^n = (2^{-0.5}*(s_0+s_2))^n$ is equal to 8.

$X*Y^1 = Z_1 =$	$2^{-0.5}*[(x_0+x_1-x_2-x_3+x_4+x_5-x_6-x_7), 0, (x_0+x_1+x_2+x_3-x_4-x_5-x_6-x_7), 0, 0, 0, 0, 0]$
$X*Y^2 = Z_2 =$	$[(x_4-x_3-x_2+x_5), 0, (x_0+x_1-x_6-x_7), 0, 0, 0, 0, 0]$
$X*Y^3 = Z_3 =$	$2^{-0.5}*[(x_4-x_1-x_2-x_3-x_0+x_5+x_6+x_7), 0, (x_0+x_1-x_2-x_3+x_4+x_5-x_6-x_7), 0, 0, 0, 0, 0]$
$X*Y^4 = Z_4 =$	$[(x_6-x_1-x_0+x_7), 0, (x_4-x_3-x_2+x_5), 0, 0, 0, 0, 0]$
$X*Y^5 = Z_5 =$	$2^{-0.5}*[(x_2-x_1-x_0+x_3-x_4-x_5+x_6+x_7), 0, (x_4-x_1-x_2-x_3-x_0+x_5+x_6+x_7), 0, 0, 0, 0, 0]$
$X*Y^6 = Z_6 =$	$[(x_2+x_3-x_4-x_5), 0, (x_6-x_1-x_0+x_7), 0, 0, 0, 0, 0]$
$X*Y^7 = Z_7 =$	$2^{-0.5}*[(x_0+x_1+x_2+x_3-x_4-x_5-x_6-x_7), 0, (x_2-x_1-x_0+x_3-x_4-x_5+x_6+x_7), 0, 0, 0, 0, 0]$
$X*Y^8 = Z_8 =$	$[(x_0+x_1-x_6-x_7), 0, (x_2+x_3-x_4-x_5), 0, 0, 0, 0, 0]$
$X*Y^9 = Z_9 =$	$2^{-0.5}*[(x_0+x_1-x_2-x_3+x_4+x_5-x_6-x_7), 0, (x_0+x_1+x_2+x_3-x_4-x_5-x_6-x_7), 0, 0, 0, 0, 0]$

Figure 18. The illustration of a selective control (or selective coding) of cyclic changes of coordinates of a vector $X*Y^n = Z_n$ where Y^n is the cyclic group with its period 8.

One can see from Figure 18 that only coordinates z_0 and z_2 have cyclic changes in this set of new vectors Z_n , all other coordinates are equal to zero. In other words, all cycles are realized on a 2-dimensional plane (z_0, z_2) inside the 8-dimensional space. If one uses another cyclic group of operators, for example, $(2^{-0.5}*(s_1+s_3))^n$ (s_1 and s_2 are from Figure 7) then the same initial vector $X=[x_0, x_1, x_2, x_3, x_4, x_5, x_6, x_7]$ will be transformed into a cyclic set of vectors in another 2-dimensional plane (z_1, z_3) of the same 8-dimensional space. One should conclude that, in this model approach, the same initial information in a form of a multidimensional vector X could generate a few cyclic processes in different planes of appropriate multidimensional space by means of using cyclic operators of the described type. In other words, we have here a multi-purpose using of vector information due to such operators (for instance, this informational vector can represent a fragment of a nucleotide sequence that can be used to organize many cyclic processes in different planes or subspaces of a phase space of genetic phenomena).

In the proposed model approach, one more benefit is that different cyclic processes of such cooperative ensemble can be easy coordinated and synchronized including an

assignment of their relative phase shifts, starting times and different tempos of their cycles.

One technical remark is needed here. If we use a cyclic operator on the basis of the “column projectors”, then a vector X should be multiplied by the matrix on the right in accordance with the sample: $[x_0, x_1, x_2, x_3, x_4, x_5, x_6, x_7] \cdot (2^{-0.5 \cdot (s_0 + s_2)})^n$. But if we use a cyclic operator on the basis of the “row projectors” (for instance, v_0 and v_2 from Figure 8) then a vector X should be multiplied by the matrix on the left in accordance with the following sample: $(2^{-0.5 \cdot (v_0 + v_2)})^n \cdot [x_0; x_1; x_2; x_3; x_4; x_5; x_6; x_7]$.

Below we will describe extensions of the genetic (4^*) -matrices R_4 and H_4 (Figure 1) into $2^n \times 2^n$ -matrices every of which consists of 2^n “column projectors” (or 2^n “row projectors”); summation of projectors from this expanded set leads to new cyclic groups, etc. by analogy with the described cases (see Figures 4, 9, 11, 16). It gives a great number of cyclic groups of operators with similar properties of the selective control (or selective coding) of cyclic changes of coordinates of 2^n -dimensional vectors. These numerous cyclic groups are useful to simulate big cooperative ensembles of cyclic processes, for instance, an ensemble of cyclic motions of legs, hands and separate muscles during different gaits (walking, running, etc.) simultaneously with heartbeats, breathing cycles, metabolic cycles, etc. Such models and their practical applications are created in the author's laboratory. The problem of inherited ensembles biological cycles are closely linked to the fundamental problems of the biological clock and time, aging, etc. Taking into account results, which were obtained in “matrix genetics”, the author puts forward “a biological concept of projectors”, which interprets the living body as a colony of projection operators.

It should be noted that in a case of a cyclic group of vector transformations with a period 8 (for example, in the case of the cyclic group $(2^{-0.5 \cdot (s_0 + s_2)})^n$) that has only 8 discrete stages inside one cycle, one can enlarge a quantity of stages in “ k ” times by changing of the power in a form n/k : the cyclic group $(2^{-0.5 \cdot (s_0 + s_2)})^{n/k}$ has $k \cdot n$ stages inside one cycle (here “ n ” and “ k ” - integer positive numbers). The more value of “ k ”, the less discretization of the cycle and the more smooth (uninterrupted) type of this cyclic process.

It can be added that many gaits (which are based on cyclic movements of the limbs and the corresponding muscle actuators) have genetically inherited character. So, newborn turtles and crocodiles, when they hatched from eggs, crawl with quite coordinated movements to water without any training from anybody; a newborn foal, after a bit time, begins to walk and run; centipedes crawl by means of coordinated movements of a great number of their legs (this number sometimes reaches up to 750) on the basis of inherited algorithms of control of legs. One should emphasize that, in the previous history, gaits and locomotion algorithms were studied in biomechanics of movements without any connection with the structures of genetic coding and with inheritance of unified control algorithms. The projection operations are associated with many kinds of movements and planned actions of our body to achieve the goal by the shortest path: for example, sending a billiard ball in the goal, we use a projection operation; directing a finger to the button of computer or piano, we make a projection action, etc. In other words, the concept of projection operators can be additionally used to simulate a broad class of such biomechanical actions.

Subject of genetically inherited ability of coordinating movements of body parts is connected with fundamental problems of congenital knowledge about surrounding space and of physiological foundations of geometry. Various researches have long put forward ideas about the importance of kinematic organization of body and its movements in the genesis of spatial representations of the individual. For example, H. Poincare has put these ideas into

the foundation of his teachings about the physiological foundations of geometry and about the origin of spatial representations in individuum.

According to Poincare, the concept of space and geometry arises from an individual on the basis of kinematic organization of his body with using characterizations of positions and movements of body parts relative to each other, ie in the kinematic organization of the body is something that precedes the concept of space [Poincare, 1913]. Evolutionary development of the whole apparatus of kinematic activity of our body has provided a coherence of this apparatus with realities of the physical world. Because of this, each newborn organism receives adequate spatial representations not only through personal contact during ontogeny with the objects of the surrounding world, but also at the expense of achievements of previous generations enshrined in the apparatus of body movements in the phylogenesis. According to Poincare, for organism, which is absolutely immobile, spatial and geometric concepts are excluded. *«To localize an object simply means to represent to oneself the movements that would be necessary to reach it. I will explain myself. It is not a question of representing the movements themselves in space, but solely of representing to oneself the muscular sensations which accompany these movements and which do not presuppose the preexistence of the notion of space.* [Poincare, 1913, p. 247]. *«I have just said that it is to our own body that we naturally refer exterior objects; that we carry about everywhere with us a system of axes to which we refer all the points of space and that this system of axes seems to be invariably bound to our body. It should be noticed that rigorously we could not speak of axes invariably bound to the body unless the different parts of this body were themselves invariably bound to one another. As this is not the case, we ought, before referring exterior objects to these fictitious axes, to suppose our body brought back to the initial attitude»* [Poincare, 1913, p. 247]. *«We should therefore not have been able to construct space if we had not had an instrument to measure it; well, this instrument to which we relate everything, which we use instinctively, it is our own body. It is in relation to our body that we place exterior objects, and the only spatial relations of these objects that we can represent are their relations to our body. It is our body which serves us, so to speak, as system of axes of coordinates»* [Poincare, 1913, p. 418]. In times of Poincare science did not know about the genetic code, but from the modern point of view these thoughts by Poincare testify in favor the importance of the structural organization of the genetic system for physiological foundations of geometry and innate notions of space, which are connected with inherited apparatus and algorithms of body movements. And they are in tune with the results of matrix genetics, which are presented in our paper.

Modern physiology makes a significant addition to the teachings of the Poincare about an innate relationship of body and spatial representations, claiming an existence of a priori notions about our body shell. This statement is due to the study of the so-called phantom sensations in disabled: a special sense of the presence of natural parts of the body, which are absent in reality. It was found [Vetter, Weinstein, 1967; Weinstein, Sersen, 1961] that phantom sensations occur not only in cases of disabled with amputees, but also in people with congenital absence of limbs. Hence, the notion of the individual scheme of our body is not conditioned by our experiences, but has an innate character.

Additional materials relating to innate spatial representations, including the concept of B. Russell [Russell, 1956] about an innate character of ideas of projective geometry for each

person, as well as an overview of works E. Schroedinger and other researchers about the geometry of spaces of visual perception, can be found in the book [Petoukhov, 1981].

We note here that although the concept of space is the primary concept for most physical theories, one can develop a meaningful theory in theoretical physics, in which it serves as only one of secondary notions, which are deduced from primary bases of a numeric system of a discrete character. We mean the "binary geometrophysics" [Vladimirov, 2008], ideas of which generate some associations with the ability of animal organisms (initially endowed with discrete molecular genetic information) to receive spatial representations and to create spatial movements on the basis of this primary information of discrete character.

5. ABOUT A DIRECTION OF ROTATION OF VECTORS UNDER INFLUENCE OF THE CYCLIC GROUPS OF THE OPERATORS

In configurations and functions of biological objects frequently one direction of rotation is preferable (it concerns the famous problem of biological dissymmetry). Taking this into account, it is interesting what one can say about directions of rotation of 4-dimensional and 8-dimensional vectors under influence of the cyclic groups described in previous sections. Figure 19 gives answer and shows directions of cyclic rotation of vectors $[x_0, x_1, x_2, x_3] \cdot (2^{-0.5} \cdot (c_i + c_j))^n$, $(2^{-0.5} \cdot (r_i + r_j))^n \cdot [x_0, x_1, x_2, x_4]$, $[x_0, x_1, x_2, x_3, x_4, x_5, x_6, x_7] \cdot (2^{-0.5} \cdot (s_i + s_j))^n$, $(2^{-0.5} \cdot (v_i + v_j))^n \cdot [x_0, x_1, x_2, x_3, x_4, x_5, x_6, x_7]$ under enlarging "n" ($i \neq j$); all these cyclic operators correspond to green cells in tables on Figure 19, they are based on summation of pairs of the projectors of the Rademacher matrices R_4 and R_8 from Figure 1).

	c ₀	c ₁	c ₂	c ₃
c ₀		↻		
c ₁	↻	-		
c ₂			-	↻
c ₃			↻	-

	r ₀	r ₁	r ₂	r ₃
r ₀	-	↻		
r ₁	↻	-		
r ₂			-	↻
r ₃			↻	-

	s ₀	s ₁	s ₂	s ₃	s ₄	s ₅	s ₆	s ₇
s ₀	-		↻	↻				
s ₁		-	↻	↻				
s ₂	↻	↻	-					
s ₃	↻	↻		-				
s ₄					-		↻	↻
s ₅						-	↻	↻
s ₆					↻	↻	-	
s ₇					↻	↻		-

	v ₀	v ₁	v ₂	v ₃	v ₄	v ₅	v ₆	v ₇
v ₀	-		↻	↻				
v ₁		-	↻	↻				
v ₂	↻	↻	-					
v ₃	↻	↻		-				
v ₄					-		↻	↻
v ₅						-	↻	↻
v ₆					↻	↻	-	
v ₇					↻	↻		-

Figure 19. In addition to Figures 4 and 9, the tables show directions of rotations of 4-dimensional and 8-dimensional vectors under influence of the cyclic groups of operators, which correspond to green cells and which are based on summation of pairs of the "column projectors" (on the left, see Figures 2, 4, 7, 9) and of the "row projectors" (on the right, see Figures 2, 4, 8, 9) of the Rademacher matrices R_4 and R_8 (Figure 1). The symbol ↻ means counter-clockwise rotation, the symbol ↻ means clockwise rotation.

Figure 20 shows directions of cyclic rotation of vectors $[x_0, x_1, x_2, x_3] \cdot (2^{-0.5} \cdot (h_i + h_j))^n$,

$(2^{-0.5}*(g_i+g_j))^n[x_0, x_1, x_2, x_4]$, $[x_0, x_1, x_2, x_3, x_4, x_5, x_6, x_7]*(2^{-0.5}*(u_i+u_j))^n$, $(2^{-0.5}*(d_i+d_j))^n*[x_0, x_1, x_2, x_3, x_4, x_5, x_6, x_7]$ under enlarging “n” ($i \neq j$; all these operators correspond to green cells in tables on Figure 19, they are based on summation of pairs of projectors of the Rademacher matrices R_4 and R_8 from Figure 1).).

	h ₀	h ₁	h ₂	h ₃
h ₀	-	↻	↻	↻
h ₁	↻	-	↻	↻
h ₂	↻	↻	-	↻
h ₃	↻	↻	↻	-

	g ₀	g ₁	g ₂	g ₃
g ₀	-	↻	↻	↻
g ₁	↻	-	↻	↻
g ₂	↻	↻	-	↻
g ₃	↻	↻	↻	-

	u ₀	u ₁	u ₂	u ₃	u ₄	u ₅	u ₆	u ₇
u ₀	-	↻	↻		↻		↻	
u ₁	↻	-		↻		↻		↻
u ₂	↻		-	↻			↻	
u ₃		↻	↻	-		↻		↻
u ₄	↻		↻		-	↻		
u ₅		↻		↻	↻	-		↻
u ₆	↻		↻		↻		-	↻
u ₇		↻		↻		↻	↻	-

	d ₀	d ₁	d ₂	d ₃	d ₄	d ₅	d ₆	d ₇
d ₀	-	↻	↻		↻		↻	
d ₁	↻	-		↻		↻		↻
d ₂	↻		-	↻			↻	
d ₃		↻	↻	-		↻		↻
d ₄	↻		↻		-	↻		
d ₅		↻		↻	↻	-		↻
d ₆	↻		↻		↻		-	↻
d ₇		↻		↻		↻	↻	-

Figure 20. In addition to Figures 11 and 16, the tables show directions of rotations of 4-dimensional and 8-dimensional vectors under influence of the cyclic groups of operators, which correspond to green cells and which are based on summation of pairs of the “column projectors” (on the left, see Figures 10, 11, 14, 16) and of the “row projectors” (on the right, see Figures 10, 11, 15, 16) of the Hadamard matrices H_4 and H_8 (Figure 1). The symbol ↻ means counter-clockwise rotation, the symbol ↻ means clockwise rotation.

Each of tables on Figures 19 and 20 contains completely different (asymmetrical) number of rotations in the clockwise and counterclockwise. These facts give evidences in favor of an idea that living matter at its basic level of genetic information has certain informational reasons to provide dissymmetry of inherited biological structures and processes. Taking this into account, the author thinks about a possibility of informational reasons for biological dis-symmetry. Here one can remind for a comparison that usually scientists look for reasons of biological dis-symmetry in physical or chemical sciences but not in informatic science.

6. HAMILTON'S QUATERNIONS, COCKLE'S SPLIT-QUATERNIONS, THEIR EXTENSIONS AND PROJECTION OPERATORS

In previous sections we described cases of summation of pairs of the oblique projectors. Now let us consider cases of summation of 4 of these projectors and cases of summation of 8 of these projectors.

The matrix H_4 (Figure 1) is sum of the four “column projectors” or the four “row projector” (Figure 10). But H_4 has also another decomposition in a form of four sparse matrices H_{40} , H_{41} , H_{42} and H_{43} (Figure 21). This set is closed in relation to multiplication and it defines their multiplication table (Figure 21, bottom level) that is identical to the known

multiplication table of quaternions by Hamilton. From this point of view, the matrix H_4 is the quaternion by Hamilton with unit coordinates. (Such type of decompositions is termed a dyadic-shift decomposition because it corresponds to structures of matrices of dyadic shifts, well known in technology of signals processing [Ahmed, Rao, 1975]).

$$H_4 = H_{40} + H_{41} + H_{42} + H_{43} =$$

1	0	0	0
0	1	0	0
0	0	1	0
0	0	0	1

$$+$$

0	1	0	0
-	0	0	0
0	0	0	1
0	0	-	0

$$+$$

0	0	-	0
0	0	0	1
1	0	0	0
0	-	0	0

$$+$$

0	0	0	1
0	0	1	0
0	-	0	0
-	0	0	0

	1	H_{41}	H_{42}	H_{43}
1	1	H_{41}	H_{42}	H_{43}
H_{41}	H_{41}	- 1	H_{43}	- H_{42}
H_{42}	H_{42}	- H_{43}	- 1	H_{41}
H_{43}	H_{43}	H_{42}	- H_{41}	- 1

Figure 21. The dyadic-shift decomposition of the (4*4)-matrix H_4 (from Figure 1) gives the set of 4 sparse matrices H_{40} , H_{41} , H_{42} and H_{43} , which corresponds to the multiplication table of quaternions by Hamilton (bottom row). The matrix H_{40} is identity matrix

Here one can mention that Hamilton quaternions are closely related to the Pauli matrices, the theory of the electromagnetic field (Maxwell wrote his equation on the language of quaternions Hamilton), the special theory of relativity, the theory of spins, quantum theory of chemical valency, etc. In the twentieth century thousands of works were devoted to quaternions in physics [http://arxiv.org/abs/math-ph/0511092]. Now Hamilton quaternions are manifested in the genetic code system. Our scientific direction - "matrix genetics" - has led to the discovery of an important bridge among physics, biology and computer science for their mutual enrichment. In our studies, we have received a new example of the effectiveness of mathematics: abstract mathematical structures, which have been derived by mathematicians at the tip of the pen 160 years ago, are embodied long ago in the information basis of living matter - the system of genetic coding. The mathematical structures, which are discovered by mathematicians in a result of painful reflections (like Hamilton, who has wasted 10 years of continuous thought to reveal his quaternions), are already represented in the genetic coding system.

Let us turn now to the (8*8)-matrix H_8 (Figure 1) that can be represented as sum of two matrices $HL_8 = u_0 + u_2 + u_4 + u_6$ and $HR_8 = u_1 + u_3 + u_5 + u_7$ (Figure 22). Here u_0, u_1, \dots, u_7 are the «column projectors» from Figure 14.

$$H_8 = HL_8 + HR_8 =$$

1	0	1	0	-1	0	1	0
1	0	1	0	-1	0	1	0
-1	0	1	0	1	0	1	0
-1	0	1	0	1	0	1	0
1	0	-1	0	1	0	1	0
1	0	-1	0	1	0	1	0
-1	0	-1	0	-1	0	1	0
-1	0	-1	0	-1	0	1	0

$$+$$

0	-1	0	-1	0	1	0	-1
0	1	0	1	0	-1	0	1
0	1	0	-1	0	-1	0	-1
0	-1	0	1	0	1	0	1
0	-1	0	1	0	-1	0	-1
0	1	0	-1	0	1	0	1
0	1	0	1	0	1	0	-1
0	-1	0	-1	0	-1	0	1

Figure 22. The representation of the Hadamard matrix H_8 (from Figure 1) as sum of two sparse matrices HL_8 and HR_8

Figure 23 shows a decomposition of the matrix HL_8 (from Figure 22) as a sum of 4 matrices: $HL_8 = HL_{80} + HL_{81} + HL_{82} + HL_{83}$. The set of matrices HL_{80} , HL_{81} , HL_{82} and HL_{83} is closed in relation to multiplication and it defines the multiplication table that is identical to the multiplication table of quaternions by Hamilton. General expression for quaternions in this case can be written as $Q_L = a_0*HL_{80} + a_1*HL_{81} + a_2*HL_{82} + a_3*HL_{83}$, where a_0, a_1, a_2, a_3 are real numbers. From this point of view, the $(8*8)$ -genomatrix HL_8 is the 4-parametric quaternion by Hamilton with unit coordinates.

$$HL_8 = HL_{80} + HL_{81} + HL_{82} + HL_{83} =$$

$\begin{pmatrix} 1 & 0 & 1 & 0 & -1 & 0 & 1 & 0 \\ 1 & 0 & 1 & 0 & -1 & 0 & 1 & 0 \\ -1 & 0 & 1 & 0 & 1 & 0 & 1 & 0 \\ -1 & 0 & 1 & 0 & 1 & 0 & 1 & 0 \\ 1 & 0 & -1 & 0 & 1 & 0 & 1 & 0 \\ 1 & 0 & -1 & 0 & 1 & 0 & 1 & 0 \\ -1 & 0 & -1 & 0 & -1 & 0 & 1 & 0 \\ -1 & 0 & -1 & 0 & -1 & 0 & 1 & 0 \end{pmatrix}$	=	$\begin{pmatrix} 1 & 0 & 0 & 0 & 0 & 0 & 0 & 0 \\ 1 & 0 & 0 & 0 & 0 & 0 & 0 & 0 \\ 0 & 0 & 1 & 0 & 0 & 0 & 0 & 0 \\ 0 & 0 & 1 & 0 & 0 & 0 & 0 & 0 \\ 0 & 0 & 0 & 0 & 1 & 0 & 0 & 0 \\ 0 & 0 & 0 & 0 & 1 & 0 & 0 & 0 \\ 0 & 0 & 0 & 0 & 0 & 0 & 1 & 0 \\ 0 & 0 & 0 & 0 & 0 & 0 & 1 & 0 \end{pmatrix}$	+	$\begin{pmatrix} 0 & 0 & 1 & 0 & 0 & 0 & 0 & 0 \\ 0 & 0 & 1 & 0 & 0 & 0 & 0 & 0 \\ -1 & 0 & 0 & 0 & 0 & 0 & 0 & 0 \\ -1 & 0 & 0 & 0 & 0 & 0 & 0 & 0 \\ 0 & 0 & 0 & 0 & 0 & 0 & 1 & 0 \\ 0 & 0 & 0 & 0 & 0 & 0 & 1 & 0 \\ 0 & 0 & 0 & -1 & 0 & 0 & 0 & 0 \\ 0 & 0 & 0 & -1 & 0 & 0 & 0 & 0 \end{pmatrix}$
+				
+				

	HL ₈₀	HL ₈₁	HL ₈₂	HL ₈₃
HL ₈₀	HL ₈₀	HL ₈₁	HL ₈₂	HL ₈₃
HL ₈₁	HL ₈₁	- HL ₈₀	HL ₈₃	- HL ₈₂
HL ₈₂	HL ₈₂	- HL ₈₃	- HL ₈₀	HL ₈₁
HL ₈₃	HL ₈₃	HL ₈₂	- HL ₈₁	- HL ₈₀

Figure 23. Upper rows: the decomposition of the matrix HL_8 (from Figure 22) as sum of 4 matrices: $HL_8 = HL_{80} + HL_{81} + HL_{82} + HL_{83}$. Bottom row: the multiplication table of these 4 matrices HL_{80} , HL_{81} , HL_{82} and HL_{83} , which is identical to the multiplication table of quaternions by Hamilton. The matrix HL_{80} represents the real unit for this matrix set

The similar situation holds true for the matrix HR_8 (from Figure 22). Figure 24 shows a decomposition of the matrix HR_8 as a sum of 4 matrices: $HR_8 = HR_{80} + HR_{81} + HR_{82} + HR_{83}$. The set of matrices HR_{80} , HR_{81} , HR_{82} and HR_{83} is closed in relation to multiplication and it defines the multiplication table that is identical to the same multiplication table of quaternions by Hamilton. General expression of quaternions in this case can be written as $Q_R = a_0*HR_{80} + a_1*HR_{81} + a_2*HR_{82} + a_3*HR_{83}$, where a_0, a_1, a_2, a_3 are real numbers. From this point of view, the $(8*8)$ -genomatrix HR_8 is the quaternion by Hamilton with unit coordinates.

$$HR_8 = HR_{80} + HR_{81} + HR_{82} + HR_{83} =$$

$$\begin{array}{c}
\begin{array}{|c|} \hline \begin{array}{cccccc} 0 & -1 & 0 & -1 & 0 & -1 \\ 0 & 1 & 0 & 1 & 0 & 1 \\ 0 & 1 & 0 & -1 & 0 & -1 \\ 0 & -1 & 0 & 1 & 0 & 1 \\ 0 & -1 & 0 & 1 & 0 & -1 \\ 0 & 1 & 0 & -1 & 0 & 1 \\ 0 & 1 & 0 & 1 & 0 & -1 \\ 0 & -1 & 0 & -1 & 0 & 1 \end{array} \\ \hline \end{array} \\
= \\
\begin{array}{c}
\begin{array}{|c|} \hline \begin{array}{cccccc} 0 & -1 & 0 & 0 & 0 & 0 \\ 0 & 1 & 0 & 0 & 0 & 0 \\ 0 & 0 & -1 & 0 & 0 & 0 \\ 0 & 0 & 1 & 0 & 0 & 0 \\ 0 & 0 & 0 & -1 & 0 & 0 \\ 0 & 0 & 0 & 0 & 1 & 0 \\ 0 & 0 & 0 & 0 & 0 & -1 \\ 0 & 0 & 0 & 0 & 0 & 1 \end{array} \\ \hline \end{array} \\
+ \\
\begin{array}{|c|} \hline \begin{array}{cccccc} 0 & 0 & -1 & 0 & 0 & 0 \\ 0 & 0 & 1 & 0 & 0 & 0 \\ 0 & 1 & 0 & 0 & 0 & 0 \\ 0 & -1 & 0 & 0 & 0 & 0 \\ 0 & 0 & 0 & 0 & 0 & -1 \\ 0 & 0 & 0 & 0 & 0 & 1 \\ 0 & 0 & 0 & 0 & 1 & 0 \\ 0 & 0 & 0 & 0 & -1 & 0 \end{array} \\ \hline \end{array} \\
+ \\
\begin{array}{c}
\begin{array}{|c|} \hline \begin{array}{cccccc} 0 & 0 & 0 & 0 & 1 & 0 \\ 0 & 0 & 0 & 0 & -1 & 0 \\ 0 & 0 & 0 & 0 & 0 & -1 \\ 0 & 0 & 0 & 0 & 0 & 1 \\ 0 & -1 & 0 & 0 & 0 & 0 \\ 0 & 1 & 0 & 0 & 0 & 0 \\ 0 & 0 & 0 & 1 & 0 & 0 \\ 0 & 0 & 0 & -1 & 0 & 0 \end{array} \\ \hline \end{array} \\
+ \\
\begin{array}{|c|} \hline \begin{array}{cccccc} 0 & 0 & 0 & 0 & 0 & -1 \\ 0 & 0 & 0 & 0 & 0 & 1 \\ 0 & 0 & 0 & -1 & 0 & 0 \\ 0 & 0 & 0 & 1 & 0 & 0 \\ 0 & 0 & 1 & 0 & 0 & 0 \\ 0 & 0 & -1 & 0 & 0 & 0 \\ 0 & 1 & 0 & 0 & 0 & 0 \\ 0 & -1 & 0 & 0 & 0 & 0 \end{array} \\ \hline \end{array}
\end{array}$$

	HR ₈₀	HR ₈₁	HR ₈₂	HR ₈₃
HR ₈₀	HR ₈₀	HR ₈₁	HR ₈₂	HR ₈₃
HR ₈₁	HR ₈₁	- HR ₈₀	HR ₈₃	- HR ₈₂
HR ₈₂	HR ₈₂	- HR ₈₃	- HR ₈₀	HR ₈₁
HR ₈₃	HR ₈₃	HR ₈₂	- HR ₈₁	- HR ₈₀

Figure 24. upper rows: the decomposition of the matrix HR_8 (from Figure 22) as sum of 4 matrices: $H_{8R} = H_{08R} + H_{18R} + H_{28R} + H_{38R}$. Bottom row: the multiplication table of these 4 matrices HR_{80} , HR_{81} , HR_{82} and HR_{83} , which is identical to the multiplication table of quaternions by Hamilton. HR_{80} represents the real unit for this matrix set

The initial (8*8)-matrix H_8 (Figure 1) can be also decomposed in another way on the base of dyadic-shift decomposition. Figure 25 shows such dyadic-shift decomposition $H_8 = H_{80} + H_{81} + H_{82} + H_{83} + H_{84} + H_{85} + H_{86} + H_{87}$, when 8 sparse matrices H_{80} , H_{81} , H_{82} , H_{83} , H_{84} , H_{85} , H_{86} , H_{87} arise (H_{80} is identity matrix). The set H_{80} , H_{81} , H_{82} , H_{83} , H_{84} , H_{85} , H_{86} , H_{87} is closed in relation to multiplication and it defines the multiplication table on Figure 25. This multiplication table is identical to the multiplication table of 8-dimensional hypercomplex numbers that are termed as biquaternions by Hamilton (or Hamiltons' quaternions over the field of complex numbers). General expression for biquaternions in this case can be written as $Q_8 = a_0 * H_{80} + a_1 * H_{81} + a_2 * H_{82} + a_3 * H_{83} + a_4 * H_{84} + a_5 * H_{85} + a_6 * H_{86} + a_7 * H_{87}$, where a_0 , a_1 , a_2 , a_3 , a_4 , a_5 , a_6 , a_7 are real numbers. From this point of view, the (8*8)-genomatrix H_8 is Hamilton's biquaternion with unit coordinates.

[illegible]

	1	H ₈₁	H ₈₂	H ₈₃	H ₈₄	H ₈₅	H ₈₆	H ₈₇
1	1	H ₈₁	H ₈₂	H ₈₃	H ₈₄	H ₈₅	H ₈₆	H ₈₇
H ₈₁	H ₈₁	-1	H ₈₃	- H ₈₂	H ₈₅	- H ₈₄	H ₈₇	- H ₈₆
H ₈₂	H ₈₂	H ₈₃	-1	- H ₈₁	- H ₈₆	- H ₈₇	H ₈₄	H ₈₅
H ₈₃	H ₈₃	- H ₈₂	- H ₈₁	1	- H ₈₇	H ₈₆	H ₈₅	- H ₈₄
H ₈₄	H ₈₄	H ₈₅	H ₈₆	H ₈₇	-1	- H ₈₁	- H ₈₂	- H ₈₃
H ₈₅	H ₈₅	- H ₈₄	H ₈₇	- H ₈₆	- H ₈₁	1	- H ₈₃	H ₈₂
H ₈₆	H ₈₆	H ₈₇	- H ₈₄	- H ₈₅	H ₈₂	H ₈₃	-1	- H ₈₁
H ₈₇	H ₈₇	- H ₈₆	- H ₈₅	H ₈₄	H ₈₃	- H ₈₂	- H ₈₁	1

One can analyze the Rademacher genomatrices R_4 and R_8 (From Figure 1) by a similar way [Petoukhov, 2012b]). In particular, in this case the following results arise:

- The Rademacher (4*4)-matrix R_4 represents split-quaternion by J.Cockle with unit coordinates (<http://en.wikipedia.org/wiki/Split-quaternion>) in the case of its dyadic-shift decomposition;
- The Rademacher (8*8)-matrix R_8 represents bisplit-quaternion by J.Cockle with unit coordinates in the case of its dyadic-shift decomposition;
- If the Rademacher (4*4)-matrix R_4 is represented as sum of two sparse matrices $R_4 = (c_0+c_2) + (c_1+c_3)$ (here c_0, c_1, c_2, c_3 are the column projectors from Figure 2), then the matrix R_4 is sum of two split-complex numbers with unit coordinates because each of summands (c_0+c_2) and (c_1+c_3) is split-complex number with unit coordinates. A similar is true for the case of the “row projectors” r_0, r_1, r_2, r_3 from Figure 2.

Now let us pay a special attention to the Rademacher (8×8) -matrix R_8 as a sum of the following two sparse matrices RL_8 and RR_8 , the first of which is a sum of 4 projectors with even indexes s_0, s_2, s_4, s_6 and the second of which is a sum of 4 projectors with odd indexes s_1, s_3, s_5, s_7 : $R_8 = (s_0 + s_2 + s_4 + s_6) + (s_1 + s_3 + s_5 + s_7) = RL_8 + RR_8$ (here s_0, s_1, \dots, s_7 are the column projectors from Figure 7). Below this decomposition will be useful for analysis of a

correspondence between 64 triplets and 20 amino acids with stop-codons.

$$R_8 = RL_8 + RR_8 = \begin{bmatrix} 1 & 0 & 1 & 0 & 1 & 0 & -1 & 0 \\ 1 & 0 & 1 & 0 & 1 & 0 & -1 & 0 \\ -1 & 0 & 1 & 0 & -1 & 0 & -1 & 0 \\ -1 & 0 & 1 & 0 & -1 & 0 & -1 & 0 \\ 1 & 0 & -1 & 0 & 1 & 0 & 1 & 0 \\ 1 & 0 & -1 & 0 & 1 & 0 & 1 & 0 \\ -1 & 0 & -1 & 0 & -1 & 0 & 1 & 0 \\ -1 & 0 & -1 & 0 & -1 & 0 & 1 & 0 \end{bmatrix} + \begin{bmatrix} 0 & 1 & 0 & 1 & 0 & 1 & 0 & -1 \\ 0 & 1 & 0 & 1 & 0 & 1 & 0 & -1 \\ 0 & -1 & 0 & 1 & 0 & -1 & 0 & -1 \\ 0 & -1 & 0 & 1 & 0 & -1 & 0 & -1 \\ 0 & 1 & 0 & -1 & 0 & 1 & 0 & 1 \\ 0 & 1 & 0 & -1 & 0 & 1 & 0 & 1 \\ 0 & -1 & 0 & -1 & 0 & -1 & 0 & 1 \\ 0 & -1 & 0 & -1 & 0 & -1 & 0 & 1 \end{bmatrix}$$

Figure 26. The decomposition of the Rademacher (8*8)-genomatrix R_8 from Figure 1 in the form $R_8 = RL_8 + RR_8$

Each of these sparse matrices RL_8 and RR_8 can be decomposed into a set of 4 sparse matrices: $RL_8 = RL_{80} + RL_{81} + RL_{82} + RL_{83}$ and $RR_8 = RR_{80} + RR_{81} + RR_{82} + RR_{83}$ (Figures 27 and 28). The first set of matrices RL_{80} , RL_{81} , RL_{82} , RL_{83} is closed relative to multiplication and it defines a known multiplication table of split-quaternions by J. Cockle (<http://en.wikipedia.org/wiki/Split-quaternion>) on Figure 27. The second set of matrices RR_{80} , RR_{81} , RR_{82} , RR_{83} is also closed relative to multiplication and it defines the same multiplication table of split-quaternions by J. Cockle (Figure 28). Consequently, each of matrices RL_8 and RR_8 is split-quaternion by Cockle with unit coordinates.

$$RL_8 = RL_{80} + RL_{81} + RL_{82} + RL_{83} = \begin{bmatrix} 1 & 0 & 0 & 0 & 0 & 0 & 0 & 0 \\ 1 & 0 & 0 & 0 & 0 & 0 & 0 & 0 \\ 0 & 0 & 1 & 0 & 0 & 0 & 0 & 0 \\ 0 & 0 & 1 & 0 & 0 & 0 & 0 & 0 \\ 0 & 0 & 0 & 0 & 1 & 0 & 0 & 0 \\ 0 & 0 & 0 & 0 & 1 & 0 & 0 & 0 \\ 0 & 0 & 0 & 0 & 0 & 0 & 1 & 0 \\ 0 & 0 & 0 & 0 & 0 & 0 & 1 & 0 \end{bmatrix} + \begin{bmatrix} 0 & 0 & 1 & 0 & 0 & 0 & 0 & 0 \\ 0 & 0 & 1 & 0 & 0 & 0 & 0 & 0 \\ -1 & 0 & 0 & 0 & 0 & 0 & 0 & 0 \\ -1 & 0 & 0 & 0 & 0 & 0 & 0 & 0 \\ 0 & 0 & 0 & 0 & 0 & 0 & 0 & 1 \\ 0 & 0 & 0 & 0 & 0 & 0 & 0 & 1 \\ 0 & 0 & 0 & 0 & -1 & 0 & 0 & 0 \\ 0 & 0 & 0 & 0 & -1 & 0 & 0 & 0 \end{bmatrix} +$$

$$+ \begin{bmatrix} 0 & 0 & 0 & 0 & 1 & 0 & 0 & 0 \\ 0 & 0 & 0 & 0 & 1 & 0 & 0 & 0 \\ 0 & 0 & 0 & 0 & 0 & 0 & -1 & 0 \\ 0 & 0 & 0 & 0 & 0 & 0 & -1 & 0 \\ 1 & 0 & 0 & 0 & 0 & 0 & 0 & 0 \\ 1 & 0 & 0 & 0 & 0 & 0 & 0 & 0 \\ 0 & 0 & -1 & 0 & 0 & 0 & 0 & 0 \\ 0 & 0 & -1 & 0 & 0 & 0 & 0 & 0 \end{bmatrix} + \begin{bmatrix} 0 & 0 & 0 & 0 & 0 & 0 & -1 & 0 \\ 0 & 0 & 0 & 0 & 0 & 0 & -1 & 0 \\ 0 & 0 & 0 & 0 & -1 & 0 & 0 & 0 \\ 0 & 0 & 0 & 0 & -1 & 0 & 0 & 0 \\ 0 & 0 & -1 & 0 & 0 & 0 & 0 & 0 \\ 0 & 0 & -1 & 0 & 0 & 0 & 0 & 0 \\ -1 & 0 & 0 & 0 & 0 & 0 & 0 & 0 \\ -1 & 0 & 0 & 0 & 0 & 0 & 0 & 0 \end{bmatrix} ;$$

	RL_{80}	RL_{81}	RL_{82}	RL_{83}
RL_{80}	RL_{80}	RL_{81}	RL_{82}	RL_{83}
RL_{81}	RL_{81}	$-RL_{80}$	RL_{83}	$-RL_{82}$
RL_{82}	RL_{82}	$-RL_{83}$	RL_{80}	$-RL_{81}$
RL_{83}	RL_{83}	RL_{82}	RL_{81}	RL_{80}

Figure 27. The decomposition of the matrix RL_8 from Figure 26 into the set of 4 matrices RL_{80} , RL_{81} , RL_{82} , RL_{83} , which defines the known multiplication table of split-quaternions by J. Cockle (<http://en.wikipedia.org/wiki/Split-quaternion>)

$$RR_8 = RR_{80} + RR_{81} + RR_{82} + RR_{83} = \begin{bmatrix} 0 & 1 & 0 & 0 & 0 & 0 & 0 & 0 \\ 0 & 1 & 0 & 0 & 0 & 0 & 0 & 0 \\ 0 & 0 & 0 & 1 & 0 & 0 & 0 & 0 \\ 0 & 0 & 0 & 1 & 0 & 0 & 0 & 0 \\ 0 & 0 & 0 & 0 & 0 & 1 & 0 & 0 \\ 0 & 0 & 0 & 0 & 0 & 1 & 0 & 0 \\ 0 & 0 & 0 & 0 & 0 & 0 & 1 & 0 \\ 0 & 0 & 0 & 0 & 0 & 0 & 0 & 1 \end{bmatrix} + \begin{bmatrix} 0 & 0 & 0 & 1 & 0 & 0 & 0 & 0 \\ 0 & 0 & 0 & 1 & 0 & 0 & 0 & 0 \\ 0 & -1 & 0 & 0 & 0 & 0 & 0 & 0 \\ 0 & -1 & 0 & 0 & 0 & 0 & 0 & 0 \\ 0 & 0 & 0 & 0 & 0 & 0 & 0 & 1 \\ 0 & 0 & 0 & 0 & 0 & 0 & 0 & 1 \\ 0 & 0 & 0 & 0 & 0 & 0 & 0 & 1 \\ 0 & 0 & 0 & 0 & 0 & 0 & 0 & 1 \end{bmatrix} +$$

$$\begin{array}{c}
\begin{array}{|c|} \hline \begin{array}{cccccccc} 0 & 0 & 0 & 0 & 0 & 1 & 0 & 0 \\ 0 & 0 & 0 & 0 & 0 & 0 & 0 & 1 \\ 0 & 0 & 0 & 0 & 0 & 0 & 0 & 1 \end{array} \\ \hline \end{array} \\
+ \begin{array}{|c|} \hline \begin{array}{cccccccc} 0 & 0 & 0 & 0 & 0 & 1 & 0 & 0 \\ 0 & 0 & 0 & 0 & 0 & 1 & 0 & 0 \\ 0 & 0 & 0 & 0 & 0 & 0 & 0 & -1 \\ 0 & 0 & 0 & 0 & 0 & 0 & 0 & -1 \\ 0 & 1 & 0 & 0 & 0 & 0 & 0 & 0 \\ 0 & 1 & 0 & 0 & 0 & 0 & 0 & 0 \\ 0 & 0 & 0 & -1 & 0 & 0 & 0 & 0 \\ 0 & 0 & 0 & -1 & 0 & 0 & 0 & 0 \end{array} \\ \hline \end{array} \\
+ \begin{array}{|c|} \hline \begin{array}{cccccccc} 0 & 0 & 0 & 0 & 0 & 0 & 0 & -1 \\ 0 & 0 & 0 & 0 & 0 & 0 & 0 & -1 \\ 0 & 0 & 0 & 0 & 0 & -1 & 0 & 0 \\ 0 & 0 & 0 & 0 & -1 & 0 & 0 & 0 \\ 0 & 0 & 0 & -1 & 0 & 0 & 0 & 0 \\ 0 & 0 & 0 & -1 & 0 & 0 & 0 & 0 \\ 0 & -1 & 0 & 0 & 0 & 0 & 0 & 0 \\ 0 & -1 & 0 & 0 & 0 & 0 & 0 & 0 \end{array} \\ \hline \end{array} \\
; \begin{array}{|c|} \hline \begin{array}{|c|} \hline \begin{array}{cccc} \text{RR}_{80} & \text{RR}_{81} & \text{RR}_{82} & \text{RR}_{83} \end{array} \\ \hline \end{array} \\
\begin{array}{|c|} \hline \begin{array}{cccc} \text{RR}_{80} & \text{RR}_{80} & \text{RR}_{81} & \text{RR}_{83} \\ \text{RR}_{81} & \text{RR}_{81} & -\text{RR}_{80} & \text{RR}_{83} \\ \text{RR}_{82} & \text{RR}_{82} & -\text{RR}_{83} & \text{RR}_{80} \\ \text{RR}_{83} & \text{RR}_{83} & \text{RR}_{82} & \text{RR}_{81} \end{array} \\ \hline \end{array} \\
\hline \end{array}
\end{array}$$

Figure 28. The decomposition of the matrix RR_8 from Figure 26 into the set of 4 matrices RR_{80} , RR_{81} , RR_{82} , RR_{83} , which defines the same multiplication table of split-quaternions by J. Cockle (<http://en.wikipedia.org/wiki/Split-quaternion>)

But each of the same (8*8)-matrices RL_8 and RR_8 (Figure 26)) can be decomposed in another way, which leads to its representation in a form of sum of two split-complex numbers: $\text{RL}_8 = (s_0 + s_4) + (s_2 + s_6)$ and $\text{RR}_8 = (s_1 + s_5) + (s_3 + s_7)$, where s_0, s_1, \dots, s_7 are column projectors from the decomposition of R_8 on Figure 7. Figure 29 shows that each of sums $(s_0 + s_4)$, $(s_2 + s_6)$, $(s_1 + s_5)$, $(s_3 + s_7)$ in these decompositions for RL_8 and RR_8 is a (8*8)-matrix representation of split-complex number, whose coordinates are equal to 1. It means also that the whole (8*8)-matrix R_8 is sum of 4 split-complex numbers, whose coordinates are equal to 1, in an 8-dimensional space. These decompositions are useful for analyzing the degeneration of the genetic code in next Sections.

$$\begin{array}{l}
s_0 + s_4 = \begin{array}{|c|} \hline \begin{array}{cccc} 1 & 0 & 0 & 0 \\ 1 & 0 & 0 & 0 \\ -1 & 0 & 0 & 0 \\ -1 & 0 & 0 & 0 \end{array} \\ \hline \end{array} = \begin{array}{|c|} \hline \begin{array}{cccc} 1 & 0 & 0 & 0 \\ 1 & 0 & 0 & 0 \\ -1 & 0 & 0 & 0 \\ -1 & 0 & 0 & 0 \end{array} \\ \hline \end{array} + \begin{array}{|c|} \hline \begin{array}{cccc} 0 & 0 & 0 & 0 \\ 0 & 0 & 0 & 0 \\ 0 & 0 & 0 & 0 \\ 0 & 0 & 0 & 0 \end{array} \\ \hline \end{array} = e_0 + e_4; \quad \begin{array}{|c|} \hline \begin{array}{|c|} \hline \begin{array}{cc} e_0 & e_4 \\ e_0 & e_0 \\ e_4 & e_4 \end{array} \\ \hline \end{array} \\
\hline \end{array}$$

$$\begin{array}{l}
s_2 + s_6 = \begin{array}{|c|} \hline \begin{array}{cccc} 0 & 0 & 1 & 0 \\ 0 & 0 & 1 & 0 \\ 0 & 0 & 1 & 0 \\ 0 & 0 & 1 & 0 \end{array} \\ \hline \end{array} = \begin{array}{|c|} \hline \begin{array}{cccc} 0 & 0 & 1 & 0 \\ 0 & 0 & 1 & 0 \\ 0 & 0 & 1 & 0 \\ 0 & 0 & 1 & 0 \end{array} \\ \hline \end{array} + \begin{array}{|c|} \hline \begin{array}{cccc} 0 & 0 & 0 & 0 \\ 0 & 0 & 0 & 0 \\ 0 & 0 & 0 & 0 \\ 0 & 0 & 0 & 0 \end{array} \\ \hline \end{array} = e_2 + e_6; \quad \begin{array}{|c|} \hline \begin{array}{|c|} \hline \begin{array}{cc} e_2 & e_6 \\ e_2 & e_2 \\ e_6 & e_6 \end{array} \\ \hline \end{array} \\
\hline \end{array}$$

$$\begin{array}{l}
s_1 + s_5 = \begin{array}{|c|} \hline \begin{array}{cccc} 0 & 1 & 0 & 0 \\ 0 & 1 & 0 & 0 \\ 0 & -1 & 0 & 0 \\ 0 & -1 & 0 & 0 \end{array} \\ \hline \end{array} = \begin{array}{|c|} \hline \begin{array}{cccc} 0 & 1 & 0 & 0 \\ 0 & 1 & 0 & 0 \\ 0 & -1 & 0 & 0 \\ 0 & -1 & 0 & 0 \end{array} \\ \hline \end{array} + \begin{array}{|c|} \hline \begin{array}{cccc} 0 & 0 & 0 & 0 \\ 0 & 0 & 0 & 0 \\ 0 & 0 & 0 & 0 \\ 0 & 0 & 0 & 0 \end{array} \\ \hline \end{array} = e_1 + e_5; \quad \begin{array}{|c|} \hline \begin{array}{|c|} \hline \begin{array}{cc} e_1 & e_5 \\ e_1 & e_1 \\ e_5 & e_5 \end{array} \\ \hline \end{array} \\
\hline \end{array}$$

$$s_3+s_7 = \begin{bmatrix} 0 & 0 & 0 & 1 & 0 & 0 & 0 & -1 \\ 0 & 0 & 0 & 1 & 0 & 0 & 0 & -1 \\ 0 & 0 & 0 & 1 & 0 & 0 & 0 & -1 \\ 0 & 0 & 0 & 1 & 0 & 0 & 0 & -1 \\ 0 & 0 & 0 & -1 & 0 & 0 & 0 & 1 \\ 0 & 0 & 0 & -1 & 0 & 0 & 0 & 1 \\ 0 & 0 & 0 & -1 & 0 & 0 & 0 & 1 \\ 0 & 0 & 0 & -1 & 0 & 0 & 0 & 1 \end{bmatrix} = \begin{bmatrix} 0 & 0 & 0 & 1 & 0 & 0 & 0 & 0 \\ 0 & 0 & 0 & 1 & 0 & 0 & 0 & 0 \\ 0 & 0 & 0 & 1 & 0 & 0 & 0 & 0 \\ 0 & 0 & 0 & 1 & 0 & 0 & 0 & 0 \\ 0 & 0 & 0 & 0 & 0 & 0 & 0 & 1 \\ 0 & 0 & 0 & 0 & 0 & 0 & 0 & 1 \\ 0 & 0 & 0 & 0 & 0 & 0 & 0 & 1 \\ 0 & 0 & 0 & 0 & 0 & 0 & 0 & 1 \end{bmatrix} + \begin{bmatrix} 0 & 0 & 0 & 0 & 0 & 0 & 0 & -1 \\ 0 & 0 & 0 & 0 & 0 & 0 & 0 & -1 \\ 0 & 0 & 0 & 0 & 0 & 0 & 0 & -1 \\ 0 & 0 & 0 & 0 & 0 & 0 & 0 & -1 \\ 0 & 0 & 0 & -1 & 0 & 0 & 0 & 0 \\ 0 & 0 & 0 & -1 & 0 & 0 & 0 & 0 \\ 0 & 0 & 0 & -1 & 0 & 0 & 0 & 0 \\ 0 & 0 & 0 & -1 & 0 & 0 & 0 & 0 \end{bmatrix} = e_3 + e_7;$$

	e_3	e_7
e_3	e_3	e_7
e_7	e_7	e_3

Figure 29. Decompositions of sums of projectors (s_0+s_4), (s_2+s_6), (s_1+s_5), (s_3+s_7), which show that each of these sums is an (8*8)-matrix representation of split-complex numbers, whose coordinates are equal to 1, in an 8-dimensional space.

7. GENETIC MATRICES AS SUMS OF KRONECKER PRODUCTS OF OBLIQUE (2*2)-PROJECTORS. EXTENSIONS OF GENETIC MATRICES INTO (2^N*2^N)-MATRICES

The Rademacher matrices R_4 and R_8 and also Hadamard matrices H_4 and H_8 (Figure 1) are interconnected by means of the following expressions:

$$R_4 \otimes \begin{bmatrix} 1 & 1 \\ 1 & 1 \end{bmatrix} = R_8, \quad H_4 \otimes \begin{bmatrix} 1 & -1 \\ 1 & 1 \end{bmatrix} = H_8 \quad (1)$$

where \otimes means Kronecker multiplication; the matrix $\begin{bmatrix} 1 & 1 \\ 1 & 1 \end{bmatrix}$ is a traditional (2*2)-matrix representation of split-complex number with unit coordinates; the matrix $\begin{bmatrix} 1 & -1 \\ 1 & 1 \end{bmatrix}$ is a traditional (2*2)-matrix representation of complex number with unit coordinates.

The following extensions of the expressions (1) lead to (2ⁿ*2ⁿ)-matrices R_K and H_K (where $K=2^n$, $n = 4, 5, 6, \dots$; (n-2) means a Kronecker power):

$$R_4 \otimes \begin{bmatrix} 1 & 1 \\ 1 & 1 \end{bmatrix}^{(n-2)} = R_K, \quad H_4 \otimes \begin{bmatrix} 1 & -1 \\ 1 & 1 \end{bmatrix}^{(n-2)} = H_K \quad (2)$$

In this algorithmic way we get a great set of (2ⁿ*2ⁿ)-matrices R_K and H_K , each of which can be represented as a sum of 2ⁿ «column projectors» (or 2ⁿ «row projectors») by analogy with cases described above. Summations of these new «column projectors» (and also «row projectors») in different combinations (in pairs, in fours, in eights, etc.) give many new operators, exponentiation of which generates a great number of cyclic groups and other kind of operators. They also give many new representations of complex numbers, split-complex numbers, Hamilton's quaternion, split-quaternions and their extensions in a form of (2ⁿ*2ⁿ)-matrices that correspond to 2ⁿ-dimensional spaces. These new operators possess many similar properties, including a selective control (or coding) of different subspaces in 2ⁿ-dimensional space, in analogy with operators described in previous sections.

Why one can declare that each of matrices in the «column decomposition» (or in the «row decomposition») of any of matrices R_K and H_K in the expressions (2) is a projection operator? It can be declared on basis of the following simple theorem, taking into account that main diagonals of all matrices R_K and H_K contains only entries +1.

Theorem: any sparse square matrix P , which contains only a single non-zero column or a single non-zero row and which has its entry +1 on the main diagonal, is a projection operator (it satisfies the criterion $P^2=P$).

Proof. When multiplying two matrices $|A_{ik}|$ and $|B_{kj}|$, the elements of the rows in the first matrix are multiplied with corresponding columns in the second matrix to receive the resulting matrix $(AB)_{ij} = \sum_{k=1}^m A_{ik} * B_{kj}$ (http://en.wikipedia.org/wiki/Matrix_multiplication). Let us consider a case of a square matrix $|P_{ij}|$ (here $i, j = 1, 2, \dots, m$) with only a single non-zero column $P_{is} \neq 0$, which is numerated by an index "s" and which contains +1 in its cell on the main diagonal of this matrix: $P_{ss} = 1$. It means that all entries $P_{ik} = 0$ if $k \neq s$. The second degree of this matrix gives a square matrix:

$$\sum_{k=1}^m P_{ik} * P_{kj} = \sum_{k=1}^m P_{ik} * P_{ks} \quad (3)$$

But among all P_{ik} only one column differs from zero: $P_{is} \neq 0$. In the equation (3), P_{is} corresponds to the second factor $P_{ss} = 1$. By these reasons we have $P_{is} * P_{ss} = P_{is}$ for the equation (3). So the sparse square matrix $|P_{ij}|^2$ contains only the same single non-zero column P_{is} like as the matrix $|P_{ij}|$. Consequently $|P_{ij}|^2 = |P_{ij}|$; in other words, this matrix $|P_{ij}|$ is a projection operator, Q.E.D. The case of similar representations of such $2^n * 2^n$ -matrices on basis of a sum of "row projectors" has its proof by analogy.

This theorem allows making the following conclusion about any variant of matrix presentations of complex numbers, split-complex numbers and their extensions into 2^n -dimensional numerical systems (including Hamilton's quaternions and biquaternions, split-quaternions and bisplit-quaternions by Cockle, etc.): if the real part of such 2^n -dimensional number is equal to +1, then its matrix presentation is a sum of 2^n «column projectors» (and «row projectors»). It is provided by the fact that real parts of such multidimensional numerical systems are represented by matrix diagonal that contains only entries +1. Figure 30 shows an example of one of matrix presentations of Hamilton quaternions in a case when their real parts are equal to +1.

1	b	c	d		1 0 0 0		0 b 0 0		0 0 c 0		0 0 0 d
-b	1	-d	c	=	-b 0 0 0	+	0 1 0 0	+	0 0 -d 0	+	0 0 0 c
-c	d	1	-b		-c 0 0 0		0 d 0 0		0 0 1 0		0 0 0 -b
-d	-c	b	1		-d 0 0 0		0 -c 0 0		0 0 b 0		0 0 0 1

Figure 30. The "column decomposition" of the classical (4*4)-matrix representation of Hamilton's quaternions (http://en.wikipedia.org/wiki/Quaternion#Matrix_representations) in cases when their real parts are equal to +1. Each of 4 matrices (on the right) is a projection operator in accordance with the described theorem. Here b, c, d are real numbers.

So, many kinds of hypercomplex numbers are based on sums of projectors. In this sense the notion "projectors" can be considered as more fundamental than the notion "hypercomplex numbers" of the mentioned types. Many of these hypercomplex numbers are applied widely in different fields of science: physics, chemistry, informatics, etc. Awareness of the fact that these systems of hypercomplex numbers are based on sums of projectors may help in a rethinking of existing theories and in developing new theories in the field of mathematical natural science. In particularly, it concerns Hamilton's quaternions. For example, Maxwell has used them in creation of his equations of electro-magnetic field. Could one develop an alternative description and development of the theory of electro-magnetic field on basis of sums of appropriate projectors? It is one of many open questions in theoretical applications of projectors.

Now we show that each of genetic Rademacher and Hadamard matrices (including R_2 , R_8 , H_4 , H_8 from Figure 1 and their extensions into $2^n \times 2^n$ -matrices R_K and H_K in expressions (2)) can be expressed as sums and Kronecker multiplications of four (2×2) -matrices of «column projectors» (or of analogical «row projectors»). Figure 31 shows these 4 basic (2×2) -projectors, which are marked by 4 different colours for visibility, and some examples of expressions of a few Rademacher and Hadamard matrices by means of their using.

$$\begin{array}{c}
 \begin{array}{|c|c|} \hline 1 & 0 \\ \hline 1 & 0 \\ \hline \end{array} ; \begin{array}{|c|c|} \hline 1 & 0 \\ \hline -1 & 0 \\ \hline \end{array} ; \begin{array}{|c|c|} \hline 0 & -1 \\ \hline 0 & 1 \\ \hline \end{array} ; \begin{array}{|c|c|} \hline 0 & 1 \\ \hline 0 & 1 \\ \hline \end{array} \\
 \\
 \begin{array}{|c|c|} \hline 1 & 1 \\ \hline 1 & 1 \\ \hline \end{array} = \begin{array}{|c|c|} \hline 1 & 0 \\ \hline 1 & 0 \\ \hline \end{array} + \begin{array}{|c|c|} \hline 0 & 1 \\ \hline 0 & 1 \\ \hline \end{array} ; \quad \begin{array}{|c|c|} \hline 1 & -1 \\ \hline 1 & 1 \\ \hline \end{array} = \begin{array}{|c|c|} \hline 1 & 0 \\ \hline 1 & 0 \\ \hline \end{array} + \begin{array}{|c|c|} \hline 0 & -1 \\ \hline 0 & 1 \\ \hline \end{array} \\
 \\
 R_4 = \begin{array}{|c|c|} \hline 1 & 0 \\ \hline 1 & 0 \\ \hline \end{array} \otimes \begin{array}{|c|c|} \hline 1 & 0 \\ \hline -1 & 0 \\ \hline \end{array} + \begin{array}{|c|c|} \hline 0 & 1 \\ \hline 0 & 1 \\ \hline \end{array} \otimes \begin{array}{|c|c|} \hline 1 & 0 \\ \hline -1 & 0 \\ \hline \end{array} + \begin{array}{|c|c|} \hline 1 & 0 \\ \hline -1 & 0 \\ \hline \end{array} \otimes \begin{array}{|c|c|} \hline 0 & 1 \\ \hline 0 & 1 \\ \hline \end{array} + \begin{array}{|c|c|} \hline 0 & -1 \\ \hline 0 & 1 \\ \hline \end{array} \otimes \begin{array}{|c|c|} \hline 0 & 1 \\ \hline 0 & 1 \\ \hline \end{array} \\
 \\
 H_4 = \begin{array}{|c|c|} \hline 1 & 0 \\ \hline 1 & 0 \\ \hline \end{array} \otimes \begin{array}{|c|c|} \hline 1 & 0 \\ \hline -1 & 0 \\ \hline \end{array} + \begin{array}{|c|c|} \hline 0 & -1 \\ \hline 0 & 1 \\ \hline \end{array} \otimes \begin{array}{|c|c|} \hline 1 & 0 \\ \hline -1 & 0 \\ \hline \end{array} + \begin{array}{|c|c|} \hline 1 & 0 \\ \hline -1 & 0 \\ \hline \end{array} \otimes \begin{array}{|c|c|} \hline 0 & 1 \\ \hline 0 & 1 \\ \hline \end{array} + \begin{array}{|c|c|} \hline 0 & 1 \\ \hline 0 & 1 \\ \hline \end{array} \otimes \begin{array}{|c|c|} \hline 0 & -1 \\ \hline 0 & 1 \\ \hline \end{array} + \begin{array}{|c|c|} \hline 0 & 1 \\ \hline 0 & 1 \\ \hline \end{array} \otimes \begin{array}{|c|c|} \hline 0 & 1 \\ \hline 0 & 1 \\ \hline \end{array}
 \end{array}$$

Figure 31. Examples of using the 4 basic (2×2) -projectors (upper level) to express (2×2) -matrix representations of split-complex number and of complex number with unit coordinates (the second level) and to express the Rademacher (4×4) -matrix R_4 and the Hadamard (4×4) -matrix H_4 from Figure 1 (two lower levels)

One can also note that every of the genetic “column $(2^n \times 2^n)$ -projectors” and the “row $(2^n \times 2^n)$ -projectors” can be expressed by means of Kronecker multiplications of appropriate (2×2) -projectors from their basic set of the 4 projectors (Figure 31, upper level). It means that cases of 2-dimensional spaces can be considered as basic in this model approach. It is interesting because of the known fact that namely 2-dimensional sub-spaces play a fundamental role in morphological organization and development of living bodies (see for example about a fundamental role of primary tissue layers or primary germ layers in http://en.wikipedia.org/wiki/Germ_layer; in accordance with germ layer theory, for example, all different organs of human bodies develop from one of the 3 germ layers).

8. AN APPLICATION OF OBLIQUE PROJECTORS TO SIMULATE ENSEMBLES OF PHYLLOTAXIS PATTERNS IN LIVING BODIES

In the field of mathematical biology, phyllotaxis phenomena are one of the most known [Adler, Barabe, Jean, 1997; Jean, 1995; http://www.goldenmuseum.com/0604Phyllotaxis_engl.html]. Usually phyllotaxis laws are described as those inherited spiral-like dislocations of leaves and some other parts of plants, which are connected with Fibonacci numbers. But the similar phyllotaxis laws dictate also inherited configurations of some biological molecules, parts of animal bodies, etc. (see, for example, a review in [Jean, 1995]). In other words, phyllotaxis laws appear in inherited morphological structures at very different levels and branches of biological evolution. Figure 32 shows a few examples of phyllotaxis spirals.

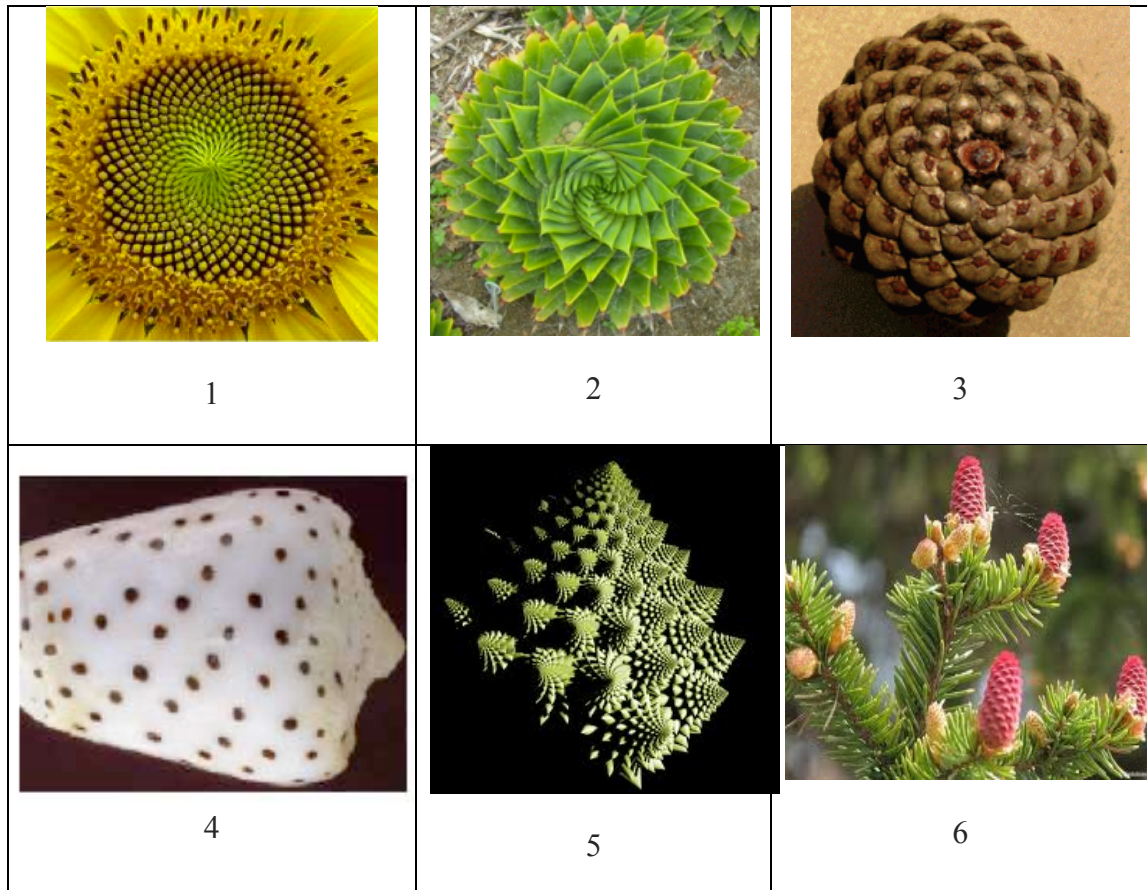


Figure 32. Examples of phyllotaxis patterns: 1) sunflower; 2) alloe (from <http://radiolus.com/index.php/nepoznannoe/255-paradoksy-posledovatelnosti-chisel-fibonachchi>); 3) a pine cone (from <http://www.maths.surrey.ac.uk/hosted-sites/R.Knott/Fibonacci/fibnat.html>); 4) a seashell (from <http://www.eb.tuebingen.mpg.de/?id=476>); 5) a fractal vegetable Romanesco Broccoli (*Brassica oleracea*) (from <http://egregores.blogspot.ru/2010/12/extremely-cool-natural-fractals.html>); 6) a spruce with cones (from <http://foto.rambler.ru/users/nadezhda-rodnejaja/albums/53780408/photo/4e9c302c-1a1a-3e9d-c61e-db70c258d714/>)

On Figure 32, images 5 and 6 illustrate that a whole organism can contain many parts with similar phyllotaxis patterns in each (like as a spruce with many phyllotaxis cones). For physicist or mathematician is natural to think that such organism can be modelled as a multidimensional phase space (or a configuration space) with an appropriate number of similar subspaces, each of which receives the same phyllotaxis pattern due to a selective control of subspaces or their selective genetic coding. Such selective control or coding in this phase space should be based on an appropriate system of operators (about a phase space see http://en.wikipedia.org/wiki/Phase_space).

Our model approach allows such modelling due to a discovered system of operators based on described sums of oblique projectors (including $2^n \times 2^n$ -dimensional matrices R_k and H_k in expressions (2)), which have such properties of a selective control (or coding) of subspaces of 2^n -dimensional space. In other words, we propose an approach to model ensembles of phyllotaxis patterns (or other patterns and processes) inside a multidimensional phase space that represents a whole organism. The described system of operators for a

selective control or coding can be conditionally named briefly as a «genetic system of operators» (or more briefly, «G-system of operators»). As we can judge, in the field of phyllotaxis study, other authors didn't simulate such ensembles of phyllotaxis patterns though many different models of separate patterns (without their ensembles in a joint phase space) exist. In addition, known models of inherited phyllotaxis patterns don't associate them with structural properties of the genetic coding system in contrast to our genetic approach. Let us explain our model approach to phyllotaxis phenomena in more details.

It is known that classical phyllotaxis patterns arise in the result of iterative rotations of initial object approximately on an angle 137° with a simultaneous increase of its distance from the center of the phyllotaxis pattern. On a complex plane such iterative operations can be simulated by means of iterative multiplication of an initial vector (or a point) with appropriate complex number $z = x + iy$, which provides such angle of rotation (due to its appropriate argument) and increase (due to its appropriate modulus) in accordance with known properties of complex numbers. The described G-system of operators, which contains many variants of sparse $2^n \times 2^n$ -matrix presentations of complex numbers on basis of sums of some genetic projectors (from "column decompositions" of $2^n \times 2^n$ -matrices R_K and H_K in expressions (2)), allows generating many phyllotaxis patterns, each of which belong to its own 2-dimensional plane inside a whole phase space. In these cases, each of phyllotaxis patterns in a separate phase plane can have its own degree of maturation (or development) and its own type of a phyllotaxis picture; it depends on a kind of complex numbers, which is chosen for its iterative generating.

This model approach does not pretend to a new explanation for existence of Fibonacci numbers in phyllotaxis patterns. But this model approach give abilities to simulate bunches of phyllotaxis patterns in separate organisms. Concerning to Fibonacci or Luca numbers in phyllotaxis laws, one should remind here that *"the phyllotaxis rules ... cannot be taken as applying to all circumstances, like a law of nature. Rather, in the words of the famous Canadian mathematician Coxeter, they are 'only a fascinatingly prevalent tendency'"* (<http://goldenratiomyth.weebly.com/phyllotaxis-the-fibonacci-sequence-in-nature.html>). One can think that the role of iterative operations in living nature is much more important than particular realizations of Fibonacci or Luca numbers.

To simulate an ensemble of phyllotaxis 3d-patterns (an ensemble of many cones of a spruce, etc.), each of which belongs to a separate subspace of a whole $2^n \times 2^n$ -dimensional phase space, an iterative application of Hamilton's quaternions can be used in their $2^n \times 2^n$ -matrix forms of presentation in the described G-system of operators.

In addition the author reminds here about cyclic groups on basis of Hamilton's quaternion and biquaternion with unit coordinates: these cyclic groups allow simulating some heritable biological phenomena including color perception, properties of which correspond to the Newton's color circle (see [Petoukhov, 2011b] and Section 17 in [Petoukhov, 2012a]). Using Hamilton's quaternions and biquaternions as $2^n \times 2^n$ -operators from the described G-system allows simulating some inherited ensembles of biological patterns including some inherited ensembles of color patterns and color changes of biological bodies.

9. THE SYMBOLIC MATRICES OF GENETIC DUPLETS AND TRIPLETS

In Section 1 the author promised to explain a relation of numeric matrices R_4 , R_8 , H_4 , H_8 (Figure 1), which were the initial matrices in this article, with a phenomenology of the genetic coding system in matrix forms of its representation. This Section is devoted to the

explanation. Theory of noise-immunity coding is based on matrix methods. For example, matrix methods allow transferring high-quality photos of Mar's surface via millions of kilometers of strong interference. In particular, Kronecker families of Hadamard matrices are used for this aim. Kronecker multiplication of matrices is the well-known operation in fields of signals processing technology, theoretical physics, etc. It is used for transition from spaces with a smaller dimension to associated spaces of higher dimension.

By analogy with theory of noise-immunity coding, the 4-letter alphabet of RNA (adenine A, cytosine C, guanine G and uracil U) can be represented in a form of the symbolic (2*2)-matrix [C U; A G] (Figure 33) as a kernel of the Kronecker family of symbolic matrices $[C U; A G]^{(n)}$, where (n) means a Kronecker power (Figure 33). Inside this family, this 4-letter alphabet of monoplets is connected with the alphabet of 16 duplets and 64 triplets by means of the second and third Kronecker powers of the kernel matrix: $[C U; A G]^{(2)}$ and $[C U; A G]^{(3)}$, where all duplets and triplets are disposed in a strict order (Figure 33). We begin with the alphabet A, C, G, U of RNA here because of mRNA-sequences of triplets define protein sequences of amino acids in a course of its reading in ribosomes.

Figure 33 contains not only 64 triplets but also amino acids and stop-codons encoded by the triplets in the case of the Vertebrate mitochondrial genetic code that is the most symmetrical among known variants of the genetic code (<http://www.ncbi.nlm.nih.gov/Taxonomy/Utils/wprintgc.cgi>). Let us explain the black-and-white mosaics of $[C U; A G]^{(2)}$ and $[C U; A G]^{(3)}$ (Figure 33) which reflect important features of the genetic code. These features are connected with a specificity of reading of mRNA-sequences in ribosomes to define protein sequences of amino acids (this is the reason, why we use the alphabet A, C, G, U of RNA in matrices on Figure 33; below we will consider the case of DNA-sequences separately).

C	U
A	G

CC	CU	UC	UU
CA	CG	UA	UG
AC	AU	GC	GU
AA	AG	GA	GG

CCC Pro	CCU Pro	CUC Leu	CUU Leu	UCC Ser	UCU Ser	UUC Phe	UUU Phe
CCA Pro	CCG Pro	CUA Leu	CUG Leu	UCA Ser	UCG Ser	UUA Leu	UUG Leu
CAC His	CAU His	CGC Arg	CGU Arg	UAC Tyr	UAU Tyr	UGC Cys	UGU Cys
CAA Gln	CAG Gln	CGA Arg	CGG Arg	UAA Stop	UAG Stop	UGA Trp	UGG trp
ACC Thr	ACU Thr	AUC Ile	AUU Ile	GCC Ala	GCU Ala	GUC Val	GUU Val
ACA Thr	ACG Thr	AUA Met	AUG Met	GCA Ala	GCG Ala	GUA Val	GUG Val
AAC Asn	AAU Asn	AGC Ser	AGU Ser	GAC Asp	GAU Asp	GGC Gly	GGU Gly
AAA Lys	AAG Lys	AGA Stop	AGG Stop	GAA Glu	GAG Glu	GGA Gly	GGG Gly

Figure 33. The first three representatives of the Kronecker family of RNA-alphabetic matrices $[C U; A G]^{(n)}$. Black color marks 8 strong duplets in the matrix $[C U; A G]^{(2)}$ (at the top) and 32 triplets with strong roots in the matrix $[C U; A G]^{(3)}$ (bottom). 20 amino acids and stop-codons, which correspond to the triplets, are also shown in the matrix $[C U; A G]^{(3)}$ for the case of the Vertebrate mitochondrial genetic code

A combination of letters on the two first positions of each triplet is usually termed as a “root” of this triplet [Konopelchenko, Rumer, 1975a,b; Rumer, 1968]. Modern science recognizes many variants (or dialects) of the genetic code, data about which are shown on the NCBI’s website <http://www.ncbi.nlm.nih.gov/Taxonomy/Utils/wprintgc.cgi>. 19 variants (or dialects) of the genetic code exist that differ one from another by some details of correspondences between triplets and objects encoded by them (these dialects are known at July 10, 2013, but perhaps later their list be increased). Most of these dialects (including the so called Standard Code and the Vertebrate Mitochondrial Code) have the symmetric general scheme of these correspondences, where 32 “black” triplets with “strong roots” and 32 “white” triplets with “weak” roots exist (the next Section shows all of these 19 dialects in details). In this basic scheme, the set of 64 triplets contains 16 subfamilies of triplets, every one of which contains 4 triplets with the same two letters on the first positions (an example of such subsets is the case of four triplets CAC, CAA, CAT, CAG with the same two letters CA on their first positions). In the described basic scheme, the set of these 16 subfamilies of *NN*-triplets is divided into two equal subsets. The first subset contains 8 subfamilies of so called “two-position” *NN*-triplets, a coding value of which is independent on a letter on their third position: (CCC, CCT, CCA, CCG), (CTC, CTT, CTA, CTG), (CGC, CGT, CGA, CGG), (TCC, TCT, TCA, TCG), (ACC, ACT, ACA, ACG), (GCC, GCT, GCA, GCG), (GTC, GTT, GTA, GTG), (GGC, GGT, GGA, GGG). An example of such subfamilies is the four triplets CGC, CGA, CGT, CGC, all of which encode the same amino acid Arg, though they have different letters on their third position. The 32 triplets of the first subset are termed as “triplets with strong roots” [Konopelchenko, Rumer, 1975a,b; Rumer, 1968]. The following duplets are appropriate 8 strong roots for them: CC, CT, CG, AC, TC, GC, GT, GG (strong duplets). All members of these 32 *NN*-triplets and 8 strong duplets are marked by black color in the matrices $[C\ U; A\ G]^{(3)}$ and $[C\ U; A\ G]^{(2)}$ on Figure 33.

The second subset contains 8 subfamilies of “three-position” *NN*-triplets, the coding value of which depends on a letter on their third position: (CAC, CAT, CAA, CAG), (TTC, TTT, TTA, TTG), (TAC, TAT, TAA, TAG), (TGC, TGT, TGA, TGG), (AAC, AAT, AAA, AAG), (ATC, ATT, ATA, ATG), (AGC, AGT, AGA, AGG), (GAA, GAT, GAA, GAG). An example of such subfamilies is the four triplets CAC, CAA, CAT, CAC, two of which (CAC, CAT) encode the amino acid His and the other two (CAA, CAG) encode another amino acid Gln. The 32 triplets of the second subset are termed as “triplets with weak roots” [Konopelchenko, Rumer, 1975a,b; Rumer, 1968]. The following duplets are appropriate 8 weak roots for them: CA, AA, AT, AG, TA, TT, TG, GA (weak duplets). All members of these 32 *NN*-triplets and 8 weak duplets are marked by white color in the matrices $[C\ U; A\ G]^{(3)}$ and $[C\ U; A\ G]^{(2)}$ on Figure 33.

From the point of view of its black-and-white mosaic, each of columns of genetic matrices $[C\ U; A\ G]^{(2)}$ and $[C\ U; A\ G]^{(3)}$ has a meander-like character and coincides with one of Rademacher functions that form orthogonal systems and well known in discrete signals processing. These functions contain elements “+1” and “-1” only. Due to this fact, one can construct Rademacher representations of the symbolic genomatrices $[C\ U; A\ G]^{(2)}$ and $[C\ U; A\ G]^{(3)}$ (Figure 33) by means of the following operation: each of black duplets and of black triplets is replaced by number “+1” and each of white duplets and white triplets is replaced by number “-1”. This operation leads immediately to the matrices R_4 and R_8 from Figure 1, that are the Rademacher representations of the phenomenological genomatrices $[C\ U; A\ G]^{(2)}$ and $[C\ U; A\ G]^{(3)}$.

If columns of the matrix $[C\ U; A\ G]^{(3)}$ on Figure 33 are numerated from left to right by indexes 0, 1, 2, ..., 7, one can see that 4 columns with even indexes 0, 2, 4, 6 contain 32 triplets, each of which has nitrogenous bases C or A on its third position, that is in its suffix (these C and A are usually termed “amino bases”). Other 4 columns with odd indexes 1, 3, 5, 7 contain other 32 triplets, each of which has nitrogenous bases T or G on its third position (these T and G are usually termed “keto bases”). The following important phenomenon is connected with this separation of the matrix $[C\ U; A\ G]^{(3)}$ in columns with even and odd indexes: adjacent columns with indexes “0 and 1”, “2 and 3”, “4 and 5” and “6 and 7” contain identical list of amino acids and stop-codons (these adjacent columns are twins from this point of view). Consequently the symbolic matrix $[C\ U; A\ G]^{(3)}$ can be represented as a sum of two sparse matrices with identical lists of amino acids and stop-codons: the first of these two matrices coincides with the matrix $[C\ U; A\ G]^{(3)}$ in columns with even indexes and has zero columns with odd indexes; the second one coincides with the matrix $[C\ U; A\ G]^{(3)}$ in columns with odd indexes and has zero columns with even indexes.

By analogy the Rademacher representation R_8 of this symbolic matrix $[C\ U; A\ G]^{(3)}$ can be also decomposed into two sparse matrices RL_8 and RR_8 (Figure 26), the first of which has all non-zero columns with even indexes and the second one has all non-zero columns with odd indexes. As it was shown above, each of these numeric (8×8) -matrices RL_8 and RR_8 represents split-quaternion by Cockle, whose coordinates are equal to 1, in an 8-dimensional space. It means that the system of correspondences between the set of 64 triplets (with their internal separation into subsets of triplets with strong and weak roots) and the set of 20 amino acids and stop-codon is created by the nature in accordance with the layout of these two split-quaternions RL_8 and RR_8 in an 8-dimensional space. In some extend this double numeric construction resembles double helix of DNA.

But each of these (8×8) -matrices RL_8 and RR_8 consists of two split-complex numbers (Figure 29): $RL_8 = (e_0 + e_4) + (e_2 + e_6)$ and $RR_8 = (e_1 + e_5) + (e_3 + e_7)$. In other words the system of correspondences between the set of triplets and the set of amino acids and stop-codons is based on the mentioned 4 split-complex numbers in an 8-dimensional space. One can mention that here we are meeting again with a set of 4 elements in some analogy with the sets of 4 elements in the genetic alphabets of nitrogenous bases in DNA and RNA - A, C, G, T/U (and also with the Ancient set of Pythagorean Tetraktys - <http://en.wikipedia.org/wiki/Tetraktys>). Whether any symmetry exists between structures of these 4 split-complex numbers and the phenomenological disposition of amino acids and stop-codons in the genomatrix $[C\ U; A\ G]^{(3)}$ on Figure 33? To receive an answer on this question, let us compare a content of corresponding cells of the symbolic genomatrix $[C\ U; A\ G]^{(3)}$ (Figure 33) with non-zero cells of matrices $(e_0 + e_4)$, $(e_2 + e_6)$, $(e_1 + e_5)$ and $(e_3 + e_7)$, which represent these 4 split-complex numbers (Figure 29). Figure 34 shows results of such comparison for the split-complex numbers $(e_0 + e_4)$ and $(e_2 + e_6)$ with even indexes of their column projectors; results of such comparison for the split-complex numbers $(e_1 + e_5)$ and $(e_3 + e_7)$ with odd indexes are identical because in the matrix $[C\ U; A\ G]^{(3)}$ (Figure 33) adjacent columns with indexes “0 and 1”, “2 and 3”, “4 and 5” and “6 and 7” contain identical lists of amino acids and stop-codons. Those amino acids, which belong to matrix cells with triplets of strong roots, are marked by bold letters on Figure 34. One can see here the following symmetrical feature: each of real and imagine parts of these split-complex numbers $(e_0 + e_4)$ and $(e_2 + e_6)$ contains an equal quantity of amino acids marked by bold letters and also an equal quantity of amino acids of another type. By such way we receive a special separation of the set of 20 amino acids into a few groups, which belong to real parts or to

imagine parts of these split-complex numbers and which should be analyzed in future more attentively.

$$\begin{aligned}
 e_0 + e_4 = & \begin{bmatrix} 1 & 0 & 0 & 0 & 0 & 0 & 0 & 0 \\ 1 & 0 & 0 & 0 & 0 & 0 & 0 & 0 \\ -1 & 0 & 0 & 0 & 0 & 0 & 0 & 0 \\ -1 & 0 & 0 & 0 & 0 & 0 & 0 & 0 \\ 0 & 0 & 0 & 0 & 1 & 0 & 0 & 0 \\ 0 & 0 & 0 & 0 & 1 & 0 & 0 & 0 \\ 0 & 0 & 0 & 0 & -1 & 0 & 0 & 0 \\ 0 & 0 & 0 & 0 & -1 & 0 & 0 & 0 \end{bmatrix} + \begin{bmatrix} 0 & 0 & 0 & 0 & 1 & 0 & 0 & 0 \\ 0 & 0 & 0 & 0 & 1 & 0 & 0 & 0 \\ 0 & 0 & 0 & 0 & -1 & 0 & 0 & 0 \\ 0 & 0 & 0 & 0 & -1 & 0 & 0 & 0 \\ 1 & 0 & 0 & 0 & 0 & 0 & 0 & 0 \\ 1 & 0 & 0 & 0 & 0 & 0 & 0 & 0 \\ -1 & 0 & 0 & 0 & 0 & 0 & 0 & 0 \\ -1 & 0 & 0 & 0 & 0 & 0 & 0 & 0 \end{bmatrix} \rightarrow \begin{bmatrix} \text{Pro} & 0 & 0 & 0 & 0 & 0 & 0 & 0 \\ \text{Pro} & 0 & 0 & 0 & 0 & 0 & 0 & 0 \\ \text{His} & 0 & 0 & 0 & 0 & 0 & 0 & 0 \\ \text{Gln} & 0 & 0 & 0 & 0 & 0 & 0 & 0 \\ 0 & 0 & 0 & 0 & \text{Ala} & 0 & 0 & 0 \\ 0 & 0 & 0 & 0 & \text{Ala} & 0 & 0 & 0 \\ 0 & 0 & 0 & 0 & \text{Asp} & 0 & 0 & 0 \\ 0 & 0 & 0 & 0 & \text{Glu} & 0 & 0 & 0 \end{bmatrix} + \begin{bmatrix} 0 & 0 & 0 & 0 & \text{Ser} & 0 & 0 & 0 \\ 0 & 0 & 0 & 0 & \text{Ser} & 0 & 0 & 0 \\ 0 & 0 & 0 & 0 & \text{Tyr} & 0 & 0 & 0 \\ 0 & 0 & 0 & 0 & \text{Stop} & 0 & 0 & 0 \\ \text{Thr} & 0 & 0 & 0 & 0 & 0 & 0 & 0 \\ \text{Thr} & 0 & 0 & 0 & 0 & 0 & 0 & 0 \\ \text{Asn} & 0 & 0 & 0 & 0 & 0 & 0 & 0 \\ \text{Lys} & 0 & 0 & 0 & 0 & 0 & 0 & 0 \end{bmatrix} \\
e_2 + e_6 = & \begin{bmatrix} 0 & 0 & 1 & 0 & 0 & 0 & 0 & 0 \\ 0 & 0 & 1 & 0 & 0 & 0 & 0 & 0 \\ 0 & 0 & 1 & 0 & 0 & 0 & 0 & 0 \\ 0 & 0 & 1 & 0 & 0 & 0 & 0 & 0 \\ 0 & 0 & 0 & 0 & 0 & 0 & 1 & 0 \\ 0 & 0 & 0 & 0 & 0 & 0 & 1 & 0 \\ 0 & 0 & 0 & 0 & 0 & 0 & 1 & 0 \\ 0 & 0 & 0 & 0 & 0 & 0 & 1 & 0 \end{bmatrix} + \begin{bmatrix} 0 & 0 & 0 & 0 & 0 & 0 & -1 & 0 \\ 0 & 0 & 0 & 0 & 0 & 0 & -1 & 0 \\ 0 & 0 & 0 & 0 & 0 & 0 & -1 & 0 \\ 0 & 0 & 0 & 0 & 0 & 0 & -1 & 0 \\ 0 & 0 & -1 & 0 & 0 & 0 & 0 & 0 \\ 0 & 0 & -1 & 0 & 0 & 0 & 0 & 0 \\ 0 & 0 & -1 & 0 & 0 & 0 & 0 & 0 \\ 0 & 0 & -1 & 0 & 0 & 0 & 0 & 0 \end{bmatrix} \rightarrow \begin{bmatrix} 0 & 0 & \text{Leu} & 0 & 0 & 0 & 0 & 0 \\ 0 & 0 & \text{Leu} & 0 & 0 & 0 & 0 & 0 \\ 0 & 0 & \text{Arg} & 0 & 0 & 0 & 0 & 0 \\ 0 & 0 & \text{Arg} & 0 & 0 & 0 & 0 & 0 \\ 0 & 0 & 0 & 0 & 0 & 0 & \text{Val} & 0 \\ 0 & 0 & 0 & 0 & 0 & 0 & \text{Val} & 0 \\ 0 & 0 & 0 & 0 & 0 & 0 & \text{Gly} & 0 \\ 0 & 0 & 0 & 0 & 0 & 0 & \text{Gly} & 0 \end{bmatrix} + \begin{bmatrix} 0 & 0 & 0 & 0 & 0 & 0 & 0 & \text{Phe} & 0 \\ 0 & 0 & 0 & 0 & 0 & 0 & 0 & \text{Leu} & 0 \\ 0 & 0 & 0 & 0 & 0 & 0 & 0 & \text{Cys} & 0 \\ 0 & 0 & 0 & 0 & 0 & 0 & 0 & \text{Trp} & 0 \\ 0 & 0 & \text{Ile} & 0 & 0 & 0 & 0 & 0 & 0 \\ 0 & 0 & \text{Met} & 0 & 0 & 0 & 0 & 0 & 0 \\ 0 & 0 & \text{Ser} & 0 & 0 & 0 & 0 & 0 & 0 \\ 0 & 0 & \text{Stop} & 0 & 0 & 0 & 0 & 0 & 0 \end{bmatrix}
 \end{aligned}$$

Figure 34. The separation of 20 amino acids and stop-codons in accordance with real and imagine parts of split-complex numbers of $e_0 + e_4$ and $e_0 + e_4$. Those amino acids, which belong to matrix cells with triplets of strong roots, are marked by bold letters.

				CCC Pro	CCU Pro	CUC Leu	CUU Leu	UCC Ser	UCU Ser	UUC Phe	UUU Phe
				CCA Pro	CCG Pro	CUA Leu	CUG Leu	UCA Ser	UCG Ser	UUA Leu	UUG Leu
				CAC His	CAU His	CGC Arg	CGU Arg	UAC Tyr	UAU Tyr	UGC Cys	UGU Cys
				CAA Gln	CAG Gln	CGA Arg	CGG Arg	UAA Stop	UAG Stop	UGA Trp	UGG Trp
				ACC Thr	ACU Thr	AUC Ile	AUU Ile	GCC Ala	GCU Ala	GUC Val	GUU Val
				ACA Thr	ACG Thr	AUA Met	AUG Met	GCA Ala	GCG Ala	GUA Val	GUG Val
				AAC Asn	AAU Asn	AGC Ser	AGU Ser	GAC Asp	GAU Asp	GGC Gly	GGU Gly
				AAA Lys	AAG Lys	AGA Stop	AGG Stop	GAA Glu	GAG Glu	GGA Gly	GGG Gly

Figure 35. The first three representatives $[C\ T; A\ G]$, $[C\ T; A\ G]^{(2)}$ and $[C\ T; A\ G]^{(3)}$ of the Kronecker family of DNA-alphabetic matrices $[C\ T; A\ G]^{(n)}$. These symbolic matrices $[C\ T; A\ G]^{(2)}$ and $[C\ T; A\ G]^{(3)}$ have mosaics, which coincide with the mosaics of their Hadamard representations H_4 and H_8 on Figure 1. All amino acids and stop-codons are shown for the case of the Vertebrate mitochondrial genetic code by analogy with Figure 33.

Now let us pay attention to Figure 35, where beginnings of appropriate Kronecker family of matrices $[C\ T; A\ G]^{(n)}$ for the case of the DNA alphabet (adenine A, cytosine C, guanine G and thymine T) are shown. What kind of black-and-white mosaics (or a

disposition of elements “+1” and “-1” in numeric representations of these symbolic matrices) can be appropriate in the case of the DNA alphabet for the basic matrix [C T; A G] and [C T; A G]⁽²⁾? The important phenomenological fact is that the thymine T is a single nitrogenous base in DNA which is replaced in RNA by another nitrogenous base U (uracil) for unknown reason (this is one of the mysteries of the genetic system). In other words, in this system the letter T is the opposition in relation to the letter U, and so the letter T can be symbolized by number “-1” (instead of number “+1” for U). Taking this into account, a simple algorithm exists, which transforms the black-and-white mosaics of matrices [C U; A G]⁽²⁾ and [C U; A G]⁽³⁾ into other mosaics of matrices [C T; A G]⁽²⁾ and [C T; A G]⁽³⁾ that are shown on Figure 35. Concerning to their mosaics, the matrices [C T; A G]⁽²⁾ and [C T; A G]⁽³⁾ coincide with mosaics of the Hadamard matrices H₄ and H₈ (Figure 1), which are their Hadamard representations (here one should remind that Hadamard matrices contain only entries +1 and -1). The mentioned algorithm was described in a few author's works (see for example [Petoukhov, 2012a,b]).

10. GENETIC PROJECTORS AND THE EXCLUSION PRINCIPLE FOR EVOLUTIONARY CHANGES OF DIALECTS OF THE GENETIC CODE

This Section describes an exclusion principle of evolution of dialects of the genetic code. This principle, which was discovered by the author, shows that evolutionary changes of dialects of the genetic code are related with the genetic projectors. One should note that discovering of exclusion principles of nature is a significant task of mathematical natural science (the exclusion principle by Pauli in quantum mechanics is one of examples).

The following list contains all known 19 dialects of the genetic code presented at July 10, 2013 on the NCBI's website <http://www.ncbi.nlm.nih.gov/Taxonomy/Utils/wprintgc.cgi>:

- 1 The Standard Code
- 2 The Vertebrate Mitochondrial Code
- 3 The Yeast Mitochondrial Code
- 4 The Mold, Protozoan, and Coelenterate Mitochondrial Code and the Mycoplasma/Spiroplasma Code
- 5 The Invertebrate Mitochondrial Code
- 6 The Ciliate, Dasycladacean and Hexamita Nuclear Code
- 7 The Echinoderm and Flatworm Mitochondrial Code
- 8 The Euplotid Nuclear Code
- 9 The Bacterial, Archaeal and Plant Plastid Code
- 10 The Alternative Yeast Nuclear Code
- 11 The Ascidian Mitochondrial Code
- 12 The Alternative Flatworm Mitochondrial Code
- 13 Blepharisma Nuclear Code
- 14 Chlorophycean Mitochondrial Code
- 15 Trematode Mitochondrial Code
- 16 Scenedesmus Obliquus Mitochondrial Code
- 17 Thraustochytrium Mitochondrial Code
- 18 Pterobranchia Mitochondrial Code
- 19 Candidate Division SR1 and Gracilibacteria Code

Figure 36 shows these dialects in typical forms of black-and-white genetic matrices [C U; A G]⁽³⁾, where black cells correspond to triplets with strong roots and white cells correspond to triplets with weak roots in cases of each individual dialect. One can see that the

vast majority of dialects (13 dialect from the set of 19 dialects) possesses the identical black-and-white mosaics though some triplets have different code meanings in different dialects (they encode different amino acid or stop-signal in different dialects) in comparison with their meanings in the vertebrate mitochondria genetic code (the author takes the case of the vertebrate mitochondria genetic code as the basic case because this dialect is the most symmetrical). All such triplets, which change their code meaning, are marked by red letters on Figure 36. From the list of 19 dialects only the following 6 dialects have their matrix $[C\ U; A\ G]^{(3)}$ with atypical black-and-white mosaics (see Figure 36): 5) The Invertebrate Mitochondrial Code; 7) The Echinoderm and Flatworm Mitochondrial Code; 10) The Alternative Yeast Nuclear Code; 12) The Alternative Flatworm Mitochondrial Code; 15) Trematode Mitochondrial Code; 16) Scenedesmus Obliquus Mitochondrial Code.

By analogy with the Rademacher presentation R_8 (see above Figures 1, 33, and Section 10), one can again replace black triplets by elements «+1» and white triplets by elements «-1» to receive numeric representations of these genetic matrices $[C\ U; A\ G]^{(3)}$ of all dialects. Such numeric representations of genetic matrices can be conditionally called as « ± 1 -representations». The result is the following: this numeric ± 1 -representation of matrices $[C\ U; A\ G]^{(3)}$ of every of 19 dialects is decomposed into a sum of 8 sparse (8*8)-matrices of «column projectors» (or «row projectors») (see Figure 36). It is connected with the fact that all cells on main diagonals of these numeric matrices contain only «+1» (see the theorem in Section 7). This general feature of all dialects is a consequence of the following phenomenologic fact: biological evolution never changes code meaning of 16 black triplets, which occupies (2*2)-sub-quadrants along the main diagonal of these matrices (CCC, CCU, CCA, CCG, CGC, CGU, CGA, CGG, GCC, GCU, GCA, GCG, GGC, GGU, GGA, GGG).

From the point of view of algebra of projection operators, the described facts mean that biologic evolution of dialects of the genetic code is connected with a condition of conservation of the numeric ± 1 -representation of the genetic matrix $[C\ U; A\ G]^{(3)}$ as a sum of 8 column projectors (or 8 row projectors). In other words, algebra of projectors shows an existence of an algebraic invariant of biological evolution.

One can formulate here the phenomenologic **exclusion principle for evolutionary changes of dialects of the genetic code**: it is forbidden for biological evolution to violate a separation of the set of 64 triplets into two subsets of triplets with strong and weak roots (black and white triplets) in a such way that a black-and-white mosaic of the genetic matrix $[C\ U; A\ G]^{(3)}$ in its « ± 1 -representation» ceases to be a sum of 8 column projectors (or 8 row projectors).

The Vertebrate Mitochondrial Code:

CCC Pro	CCU Pro	CUC Leu	CUU Leu	UCC Ser	UCU Ser	UUC Phe	UUU Phe
CCA Pro	CCG Pro	CUA Leu	CUG Leu	UCA Ser	UCG Ser	UUA Leu	UUG Leu
CAC His	CAU His	CGC Arg	CGU Arg	UAC Tyr	UAU Tyr	UGC Cys	UGU Cys
CAA Gln	CAG Gln	CGA Arg	CGG Arg	UAA Stop	UAG Stop	UGA Trp	UGG trp
ACC Thr	ACU Thr	AUC Ile	AUU Ile	GCC Ala	GCU Ala	GUC Val	GUU Val
ACA Thr	ACG Thr	AUA Met	AUG Met	GCA Ala	GCG Ala	GUA Val	GUG Val
AAC Asn	AAU Asn	AGC Ser	AGU Ser	GAC Asp	GAU Asp	GGC Gly	GGU Gly
AAA Lys	AAG Lys	AGA Stop	AGG Stop	GAA Glu	GAG Glu	GGA Gly	GGG Gly

The Standard Code:

CCC Pro	CCU Pro	CUC Leu	CUU Leu	UCC Ser	UCU Ser	UUC Phe	UUU Phe
CCA Pro	CCG Pro	CUA Leu	CUG Leu	UCA Ser	UCG Ser	UUA Leu	UUG Leu
CAC His	CAU His	CGC Arg	CGU Arg	UAC Tyr	UAU Tyr	UGC Cys	UGU Cys
CAA Gln	CAG Gln	CGA Arg	CGG Arg	UAA Stop	UAG Stop	UGA Stop	UGG trp
ACC Thr	ACU Thr	AUC Ile	AUU Ile	GCC Ala	GCU Ala	GUC Val	GUU Val
ACA Thr	ACG Thr	AUA Ile	AUG Met	GCA Ala	GCG Ala	GUA Val	GUG Val
AAC Asn	AAU Asn	AGC Ser	AGU Ser	GAC Asp	GAU Asp	GGC Gly	GGU Gly
AAA Lys	AAG Lys	AGA Arg	AGG Arg	GAA Glu	GAG Glu	GGA Gly	GGG Gly

The Yeast Mitochondrial Code:

CCC Pro	CCU Pro	CUC Thr	CUA Thr	UCC Ser	UCU Ser	UUC Phe	UUU Phe
CCA Pro	CCG Pro	CUU Thr	CUG Thr	UCA Ser	UCG Ser	UUA Leu	UUG Leu
CAC His	CAU His	CGC Arg	CGU Arg	UAC Tyr	UAU Tyr	UGC Cys	UGU Cys
CAA Gln	CAG Gln	CGA Arg	CGG Arg	UAA Stop	UAG Stop	UGA Trp	UGG trp
ACC Thr	ACU Thr	AUC Ile	AUU Ile	GCC Ala	GCU Ala	GUC Val	GUU Val
ACA Thr	ACG Thr	AUA Met	AUG Met	GCA Ala	GCG Ala	GUA Val	GUG Val
AAC Asn	AAU Asn	AGC Ser	AGU Ser	GAC Asp	GAU Asp	GGC Gly	GGU Gly
AAA Lys	AAG Lys	AGA Arg	AGG Arg	GAA Glu	GAG Glu	GGA Gly	GGG Gly

The Mold, Protozoan, and Coelenterate Mitochondrial Code and the Mycoplasma/Spiroplasma Code:

CCC Pro	CCU Pro	CUC Leu	CUU Leu	UCC Ser	UCU Ser	UUC Phe	UUU Phe
CCA Pro	CCG Pro	CUA Leu	CUG Leu	UCA Ser	UCG Ser	UUA Leu	UUG Leu
CAC His	CAU His	CGC Arg	CGU Arg	UAC Tyr	UAU Tyr	UGC Cys	UGU Cys
CAA Gln	CAG Gln	CGA Arg	CGG Arg	UAA Stop	UAG Stop	UGA Trp	UGG trp
ACC Thr	ACU Thr	AUC Ile	AUU Ile	GCC Ala	GCU Ala	GUC Val	GUU Val
ACA Thr	ACG Thr	AUA Ile	AUG Met	GCA Ala	GCG Ala	GUA Val	GUG Val
AAC Asn	AAU Asn	AGC Ser	AGU Ser	GAC Asp	GAU Asp	GGC Gly	GGU Gly
AAA Lys	AAG Lys	AGA Arg	AGG Arg	GAA Glu	GAG Glu	GGA Gly	GGG Gly

The Invertebrate Mitochondrial Code:

CCC Pro	CCU Pro	CUC Leu	CUU Leu	UCC Ser	UCU Ser	UUC Phe	UUU Phe
CCA Pro	CCG Pro	CUA Leu	CUG Leu	UCA Ser	UCG Ser	UUA Leu	UUG Leu
CAC His	CAU His	CGC Arg	CGU Arg	UAC Tyr	UAU Tyr	UGC Cys	UGU Cys
CAA Gln	CAG Gln	CGA Arg	CGG Arg	UAA Stop	UAG Stop	UGA Trp	UGG trp
ACC Thr	ACU Thr	AUC Ile	AUU Ile	GCC Ala	GCU Ala	GUC Val	GUU Val
ACA Thr	ACG Thr	AUA Met	AUG Met	GCA Ala	GCG Ala	GUA Val	GUG Val
AAC Asn	AAU Asn	AGC Ser	AGU Ser	GAC Asp	GAU Asp	GGC Gly	GGU Gly
AAA Lys	AAG Lys	AGA Ser	AGG Ser	GAA Glu	GAG Glu	GGA Gly	GGG Gly

The Ciliate, Dasycladacean and Hexamita Nuclear Code:

CCC Pro	CCU Pro	CUC Leu	CUU Leu	UCC Ser	UCU Ser	UUC Phe	UUU Phe
CCA Pro	CCG Pro	CUA Leu	CUG Leu	UCA Ser	UCG Ser	UUA Leu	UUG Leu
CAC His	CAU His	CGC Arg	CGU Arg	UAC Tyr	UAU Tyr	UGC Cys	UGU Cys
CAA Gln	CAG Gln	CGA Arg	CGG Arg	UAA Gln	UAG Gln	UGA Stop	UGG trp
ACC Thr	ACU Thr	AUC Ile	AUU Ile	GCC Ala	GCU Ala	GUC Val	GUU Val
ACA Thr	ACG Thr	AUA Ile	AUG Met	GCA Ala	GCG Ala	GUA Val	GUG Val
AAC Asn	AAU Asn	AGC Ser	AGU Ser	GAC Asp	GAU Asp	GGC Gly	GGU Gly
AAA Lys	AAG Lys	AGA Arg	AGG Arg	GAA Glu	GAG Glu	GGA Gly	GGG Gly

The Echinoderm and Flatworm Mitochondrial Code:

CCC Pro	CCU Pro	CUC Leu	CUU Leu	UCC Ser	UCU Ser	UUC Phe	UUU Phe
CCA Pro	CCG Pro	CUA Leu	CUG Leu	UCA Ser	UCG Ser	UUA Leu	UUG Leu
CAC His	CAU His	CGC Arg	CGU Arg	UAC Tyr	UAU Tyr	UGC Cys	UGU Cys
CAA Gln	CAG Gln	CGA Arg	CGG Arg	UAA Stop	UAG Stop	UGA Trp	UGG trp
ACC Thr	ACU Thr	AUC Ile	AUU Ile	GCC Ala	GCU Ala	GUC Val	GUU Val
ACA Thr	ACG Thr	AUA Ile	AUG Met	GCA Ala	GCG Ala	GUA Val	GUG Val
AAC Asn	AAU Asn	AGC Ser	AGU Ser	GAC Asp	GAU Asp	GGC Gly	GGU Gly
AAA Asn	AAG Lys	AGA Ser	AGG Ser	GAA Glu	GAG Glu	GGA Gly	GGG Gly

The Euplotid Nuclear Code:

CCC Pro	CCU Pro	CUC Leu	CUU Leu	UCC Ser	UCU Ser	UUC Phe	UUU Phe
CCA Pro	CCG Pro	CUA Leu	CUG Leu	UCA Ser	UCG Ser	UUA Leu	UUG Leu
CAC His	CAU His	CGC Arg	CGU Arg	UAC Tyr	UAU Tyr	UGC Cys	UGU Cys
CAA Gln	CAG Gln	CGA Arg	CGG Arg	UAA Stop	UAG Stop	UGA Cys	UGG trp
ACC Thr	ACU Thr	AUC Ile	AUU Ile	GCC Ala	GCU Ala	GUC Val	GUU Val
ACA Thr	ACG Thr	AUA Ile	AUG Met	GCA Ala	GCG Ala	GUA Val	GUG Val
AAC Asn	AAU Asn	AGC Ser	AGU Ser	GAC Asp	GAU Asp	GGC Gly	GGU Gly
AAA Lys	AAG Lys	AGA Arg	AGG Arg	GAA Glu	GAG Glu	GGA Gly	GGG Gly

The Bacterial, Archaeal and Plant Plastid Code:

CCC Pro	CCU Pro	CUC Leu	CUU Leu	UCC Ser	UCU Ser	UUC Phe	UUU Phe
CCA Pro	CCG Pro	CUA Leu	CUG Leu	UCA Ser	UCG Ser	UUA Leu	UUG Leu
CAC His	CAU His	CGC Arg	CGU Arg	UAC Tyr	UAU Tyr	UGC Cys	UGU Cys
CAA Gln	CAG Gln	CGA Arg	CGG Arg	UAA Stop	UAG Stop	UGA Stop	UGG trp
ACC Thr	ACU Thr	AUC Ile	AUU Ile	GCC Ala	GCU Ala	GUC Val	GUU Val
ACA Thr	ACG Thr	AUA Ile	AUG Met	GCA Ala	GCG Ala	GUA Val	GUG Val
AAC Asn	AAU Asn	AGC Ser	AGU Ser	GAC Asp	GAU Asp	GGC Gly	GGU Gly
AAA Lys	AAG Lys	AGA Arg	AGG Arg	GAA Glu	GAG Glu	GGA Gly	GGG Gly

The Alternative Yeast Nuclear Code:

CCC Pro	CCU Pro	CUC Leu	CUU Leu	UCC Ser	UCU Ser	UUC Phe	UUU Phe
CCA Pro	CCG Pro	CUA Leu	CUG Ser	UCA Ser	UCG Ser	UUA Leu	UUG Leu
CAC His	CAU His	CGC Arg	CGU Arg	UAC Tyr	UAU Tyr	UGC Cys	UGU Cys
CAA Gln	CAG Gln	CGA Arg	CGG Arg	UAA Stop	UAG Stop	UGA Stop	UGG trp
ACC Thr	ACU Thr	AUC Ile	AUU Ile	GCC Ala	GCU Ala	GUC Val	GUU Val
ACA Thr	ACG Thr	AUA Ile	AUG Met	GCA Ala	GCG Ala	GUA Val	GUG Val
AAC Asn	AAU Asn	AGC Ser	AGU Ser	GAC Asp	GAU Asp	GGC Gly	GGU Gly
AAA Lys	AAG Lys	AGA Arg	AGG Arg	GAA Glu	GAG Glu	GGA Gly	GGG Gly

The Ascidian Mitochondrial Code:

CCC Pro	CCU Pro	CUC Leu	CUU Leu	UCC Ser	UCU Ser	UUC Phe	UUU Phe
CCA Pro	CCG Pro	CUA Leu	CUG Leu	UCA Ser	UCG Ser	UUA Leu	UUG Leu
CAC His	CAU His	CGC Arg	CGU Arg	UAC Tyr	UAU Tyr	UGC Cys	UGU Cys
CAA Gln	CAG Gln	CGA Arg	CGG Arg	UAA Stop	UAG Stop	UGA Trp	UGG trp
ACC Thr	ACU Thr	AUC Ile	AUU Ile	GCC Ala	GCU Ala	GUC Val	GUU Val
ACA Thr	ACG Thr	AUA Met	AUG Met	GCA Ala	GCG Ala	GUA Val	GUG Val
AAC Asn	AAU Asn	AGC Ser	AGU Ser	GAC Asp	GAU Asp	GGC Gly	GGU Gly
AAA Lys	AAG Lys	AGA Gly	AGG Gly	GAA Glu	GAG Glu	GGA Gly	GGG Gly

The Alternative Flatworm Mitochondrial Code:

CCC Pro	CCU Pro	CUC Leu	CUU Leu	UCC Ser	UCU Ser	UUC Phe	UUU Phe
CCA Pro	CCG Pro	CUA Leu	CUG Leu	UCA Ser	UCG Ser	UUA Leu	UUG Leu
CAC His	CAU His	CGC Arg	CGU Arg	UAC Tyr	UAU Tyr	UGC Cys	UGU Cys
CAA Gln	CAG Gln	CGA Arg	CGG Arg	UAA Stop	UAG Stop	UGA Trp	UGG trp
ACC Thr	ACU Thr	AUC Ile	AUU Ile	GCC Ala	GCU Ala	GUC Val	GUU Val
ACA Thr	ACG Thr	AUA Ile	AUG Met	GCA Ala	GCG Ala	GUA Val	GUG Val
AAC Asn	AAU Asn	AGC Ser	AGU Ser	GAC Asp	GAU Asp	GGC Gly	GGU Gly
AAA Asn	AAG Lys	AGA Ser	AGG Ser	GAA Glu	GAG Glu	GGA Gly	GGG Gly

Blepharisma Nuclear Code:

CCC Pro	CCU Pro	CUC Leu	CUU Leu	UCC Ser	UCU Ser	UUC Phe	UUU Phe
CCA Pro	CCG Pro	CUA Leu	CUG Leu	UCA Ser	UCG Ser	UUA Leu	UUG Leu
CAC His	CAU His	CGC Arg	CGU Arg	UAC Tyr	UAU Tyr	UGC Cys	UGU Cys
CAA Gln	CAG Gln	CGA Arg	CGG Arg	UAA Stop	UAG Gln	UGA Stop	UGG trp
ACC Thr	ACU Thr	AUC Ile	AUU Ile	GCC Ala	GCU Ala	GUC Val	GUU Val
ACA Thr	ACG Thr	AUA Ile	AUG Met	GCA Ala	GCG Ala	GUA Val	GUG Val
AAC Asn	AAU Asn	AGC Ser	AGU Ser	GAC Asp	GAU Asp	GGC Gly	GGU Gly
AAA Lys	AAG Lys	AGA Arg	AGG Arg	GAA Glu	GAG Glu	GGA Gly	GGG Gly

Chlorophycean Mitochondrial Code:

CCC Pro	CCU Pro	CUC Leu	CUU Leu	UCC Ser	UCU Ser	UUC Phe	UUU Phe
CCA Pro	CCG Pro	CUA Leu	CUG Leu	UCA Ser	UCG Ser	UUA Leu	UUG Leu
CAC His	CAU His	CGC Arg	CGU Arg	UAC Tyr	UAU Tyr	UGC Cys	UGU Cys
CAA Gln	CAG Gln	CGA Arg	CGG Arg	UAA Stop	UAG Leu	UGA Stop	UGG trp
ACC Thr	ACU Thr	AUC Ile	AUU Ile	GCC Ala	GCU Ala	GUC Val	GUU Val
ACA Thr	ACG Thr	AUA Ile	AUG Met	GCA Ala	GCG Ala	GUA Val	GUG Val
AAC Asn	AAU Asn	AGC Ser	AGU Ser	GAC Asp	GAU Asp	GGC Gly	GGU Gly
AAA Lys	AAG Lys	AGA Arg	AGG Arg	GAA Glu	GAG Glu	GGA Gly	GGG Gly

Trematode Mitochondrial Code:

CCC Pro	CCU Pro	CUC Leu	CUU Leu	UCC Ser	UCU Ser	UUC Phe	UUU Phe
CCA Pro	CCG Pro	CUA Leu	CUG Leu	UCA Ser	UCG Ser	UUA Leu	UUG Leu
CAC His	CAU His	CGC Arg	CGU Arg	UAC Tyr	UAU Tyr	UGC Cys	UGU Cys
CAA Gln	CAG Gln	CGA Arg	CGG Arg	UAA Stop	UAG Stop	UGA Trp	UGG trp
ACC Thr	ACU Thr	AUC Ile	AUU Ile	GCC Ala	GCU Ala	GUC Val	GUU Val
ACA Thr	ACG Thr	AUA Met	AUG Met	GCA Ala	GCG Ala	GUA Val	GUG Val
AAC Asn	AAU Asn	AGC Ser	AGU Ser	GAC Asp	GAU Asp	GGC Gly	GGU Gly
AAA Asn	AAG Lys	AGA Ser	AGG Ser	GAA Glu	GAG Glu	GGA Gly	GGG Gly

Scenedesmus Obliquus Mitochondrial Code:

CCC Pro	CCU Pro	CUC Leu	CUU Leu	UCC Ser	UCU Ser	UUC Phe	UUU Phe
CCA Pro	CCG Pro	CUA Leu	CUG Leu	UCA Stop	UCG Ser	UUA Leu	UUG Leu
CAC His	CAU His	CGC Arg	CGU Arg	UAC Tyr	UAU Tyr	UGC Cys	UGU Cys
CAA Gln	CAG Gln	CGA Arg	CGG Arg	UAA Stop	UAG Leu	UGA Stop	UGG trp
ACC Thr	ACU Thr	AUC Ile	AUU Ile	GCC Ala	GCU Ala	GUC Val	GUU Val
ACA Thr	ACG Thr	AUA Ile	AUG Met	GCA Ala	GCG Ala	GUA Val	GUG Val
AAC Asn	AAU Asn	AGC Ser	AGU Ser	GAC Asp	GAU Asp	GGC Gly	GGU Gly
AAA Lys	AAG Lys	AGA Arg	AGG Arg	GAA Glu	GAG Glu	GGA Gly	GGG Gly

Thraustochytrium Mitochondrial Code:

CCC Pro	CCU Pro	CUC Leu	CUU Leu	UCC Ser	UCU Ser	UUC Phe	UUU Phe
CCA Pro	CCG Pro	CUA Leu	CUG Leu	UCA Ser	UCG Ser	UUA Stop	UUG Leu
CAC His	CAU His	CGC Arg	CGU Arg	UAC Tyr	UAU Tyr	UGC Cys	UGU Cys
CAA Gln	CAG Gln	CGA Arg	CGG Arg	UAA Stop	UAG Stop	UGA Stop	UGG trp
ACC Thr	ACU Thr	AUC Ile	AUU Ile	GCC Ala	GCU Ala	GUC Val	GUU Val
ACA Thr	ACG Thr	AUA Ile	AUG Met	GCA Ala	GCG Ala	GUA Val	GUG Val
AAC Asn	AAU Asn	AGC Ser	AGU Ser	GAC Asp	GAU Asp	GGC Gly	GGU Gly
AAA Lys	AAG Lys	AGA Arg	AGG Arg	GAA Glu	GAG Glu	GGA Gly	GGG Gly

Pterobranchia Mitochondrial Code:

CCC Pro	CCU Pro	CUC Leu	CUU Leu	UCC Ser	UCU Ser	UUC Phe	UUU Phe
CCA Pro	CCG Pro	CUA Leu	CUG Leu	UCA Ser	UCG Ser	UUA Leu	UUG Leu
CAC His	CAU His	CGC Arg	CGU Arg	UAC Tyr	UAU Tyr	UGC Cys	UGU Cys
CAA Gln	CAG Gln	CGA Arg	CGG Arg	UAA Stop	UAG Stop	UGA Trp	UGG trp
ACC Thr	ACU Thr	AUC Ile	AUU Ile	GCC Ala	GCU Ala	GUC Val	GUU Val
ACA Thr	ACG Thr	AUA Ile	AUG Met	GCA Ala	GCG Ala	GUA Val	GUG Val
AAC Asn	AAU Asn	AGC Ser	AGU Ser	GAC Asp	GAU Asp	GGC Gly	GGU Gly
AAA Lys	AAG Lys	AGA Ser	AGG Lys	GAA Glu	GAG Glu	GGA Gly	GGG Gly

Candidate Division SR1 and Gracilibacteria Code:

CCC Pro	CCU Pro	CUC Leu	CUU Leu	UCC Ser	UCU Ser	UUC Phe	UUU Phe
CCA Pro	CCG Pro	CUA Leu	CUG Leu	UCA Ser	UCG Ser	UUA Leu	UUG Leu
CAC His	CAU His	CGC Arg	CGU Arg	UAC Tyr	UAU Tyr	UGC Cys	UGU Cys
CAA Gln	CAG Gln	CGA Arg	CGG Arg	UAA Stop	UAG Stop	UGA Gly	UGG trp
ACC Thr	ACU Thr	AUC Ile	AUU Ile	GCC Ala	GCU Ala	GUC Val	GUU Val
ACA Thr	ACG Thr	AUA Ile	AUG Met	GCA Ala	GCG Ala	GUA Val	GUG Val
AAC Asn	AAU Asn	AGC Ser	AGU Ser	GAC Asp	GAU Asp	GGC Gly	GGU Gly
AAA Lys	AAG Lys	AGA Arg	AGG Arg	GAA Glu	GAG Glu	GGA Gly	GGG Gly

Figure 36. The matrices [C U; A G]⁽³⁾ show 19 known dialects of the genetic code. Black (white) cells contain triplets with strong (weak) roots. Red color shows triplets, which

have different code meanings in a considered dialect in comparison with their code meanings in the Vertebrate Mitochondrial Code, which is the most symmetrical among all dialects.

11 ABOUT «TENSORCOMPLEX» NUMBERS

This Section describes a system of multidimensional numbers, which seem to be a new one for mathematical natural sciences and which are constructed on the basis of sums of genetic projectors described above. Here the author will take some data from his work [Petoukhov, 2012b].

First of all, let us return to two sums of genetic projectors h_0+h_2 and h_1+h_3 (from Figure 10), which were received from the Hadamard matrix H_4 (Figure 1). The first sum h_0+h_2 is decomposed into two basic matrices $e_0 = [1 \ 0 \ 0 \ 0; -1 \ 0 \ 0 \ 0; 0 \ 0 \ 1 \ 0; 0 \ 0 \ -1 \ 0]$ and $e_2 = [0 \ 0 \ -1 \ 0; 0 \ 0 \ 1 \ 0; 1 \ 0 \ 0 \ 0; -1 \ 0 \ 0 \ 0]$, the set of which is closed relative to multiplication and defines the multiplication table of complex numbers. The second sum h_1+h_3 is decomposed into other basic matrices $e_1 = [0 \ 1 \ 0 \ 0; 0 \ 1 \ 0 \ 0; 0 \ 0 \ 0 \ 1; 0 \ 0 \ 0 \ 1]$ and $e_3 = [0 \ 0 \ 0 \ 1; 0 \ 0 \ 0 \ 1; 0 \ -1 \ 0 \ 0; 0 \ -1 \ 0 \ 0]$, the set of which is closed relative to multiplication and also defines the multiplication table of complex numbers (see Figure 10). Now one can consider linear compositions C_L and G_R on basis of these basic matrices (Figure 37, upper level). The work [Petoukhov, 2012b] shows that each of C_L and C_R is a (4*4)-matrix representation of 2-parametric complex numbers over field of real numbers but these representations concern different 2-dimensional planes (x_0, x_2) and (x_1, x_3) of a 4-dimensional vector space.

Everyone got used to that in the case of two complex numbers, their sum gives a new complex number, and their product is commutative. This is true when these complex numbers belong to the same complex plane. But the sum of these (4x4)-representations of two complex numbers C_L and C_R , which belong to different planes of 4-dimensional space, is not equal to a new complex number, and their product is not commutative: $C_L * C_R \neq C_R * C_L$. Each of these products $C_L * C_R$ and $C_R * C_L$ gives a new complex number. Figure 37 (two middle levels) show expressions $C_L * C_R$ and $C_R * C_L$ with their decompositions into sets of two matrices, which correspond to the multiplication table of complex numbers. Figure 37 (bottom level) also shows an expression of a corresponding commutator. One should note here that the expression of the commutator $C_L * C_R - C_R * C_L$ on Figure 37 belongs to so called “tensorcomplex numbers”, which will be introduced below (Figures 38 and 39) with marks of their quadrants by means of yellow and green colors to emphasise a special cross-like structure of this type of numbers.

$$C_L = a_0 * e_0 + a_2 * e_2 = \begin{bmatrix} a_0 & 0 & -a_2 & 0 \\ -a_0 & 0 & a_2 & 0 \\ a_2 & 0 & a_0 & 0 \\ -a_2 & 0 & -a_0 & 0 \end{bmatrix}; \quad C_R = a_1 * e_1 + a_3 * e_3 = \begin{bmatrix} 0 & a_1 & 0 & a_3 \\ 0 & a_1 & 0 & a_3 \\ 0 & -a_3 & 0 & a_1 \\ 0 & -a_3 & 0 & a_1 \end{bmatrix}$$

$C_L * C_R =$	$\begin{bmatrix} 0, & a_0 * a_1 + a_2 * a_3, & 0, & a_0 * a_3 - a_1 * a_2 \\ 0, & -a_0 * a_1 - a_2 * a_3, & 0, & a_1 * a_2 - a_0 * a_3 \\ 0, & a_1 * a_2 - a_0 * a_3, & 0, & a_0 * a_1 + a_2 * a_3 \\ 0, & a_0 * a_3 - a_1 * a_2, & 0, & -a_0 * a_1 - a_2 * a_3 \end{bmatrix}$	$= -(a_0 * a_1 + a_2 * a_3) *$	$\begin{bmatrix} 0 & -1 & 0 & 0 \\ 0 & 1 & 0 & 0 \\ 0 & 0 & 0 & -1 \\ 0 & 0 & 0 & 1 \end{bmatrix}$	$+ (a_1 * a_2 - a_0 * a_3) *$	$\begin{bmatrix} 0 & 0 & 0 & -1 \\ 0 & 0 & 0 & 1 \\ 0 & 1 & 0 & 0 \\ 0 & -1 & 0 & 0 \end{bmatrix}$
---------------	--	--------------------------------	--	-------------------------------	--

$C_R * C_L =$	$\begin{bmatrix} -a_0 * a_1 - a_2 * a_3, & 0, & a_1 * a_2 - a_0 * a_3, & 0 \\ -a_0 * a_1 - a_2 * a_3, & 0, & a_1 * a_2 - a_0 * a_3, & 0 \\ a_0 * a_3 - a_1 * a_2, & 0, & -a_0 * a_1 - a_2 * a_3, & 0 \\ a_0 * a_3 - a_1 * a_2, & 0, & -a_0 * a_1 - a_2 * a_3, & 0 \end{bmatrix}$	$= -(a_0 * a_1 + a_2 * a_3) *$	$\begin{bmatrix} 1 & 0 & 0 & 0 \\ 1 & 0 & 0 & 0 \\ 0 & 0 & 1 & 0 \\ 0 & 0 & 1 & 0 \end{bmatrix}$	$- (a_1 * a_2 - a_0 * a_3) *$	$\begin{bmatrix} 0 & 0 & -1 & 0 \\ 0 & 0 & -1 & 0 \\ 1 & 0 & 0 & 0 \\ 1 & 0 & 0 & 0 \end{bmatrix}$
---------------	--	--------------------------------	--	-------------------------------	--

$C_L \cdot C_R - C_R \cdot C_L =$	$a_0 \cdot a_1 + a_2 \cdot a_3$	$a_0 \cdot a_1 + a_2 \cdot a_3$	$a_0 \cdot a_3 - a_1 \cdot a_2$	$a_0 \cdot a_3 - a_1 \cdot a_2$
	$a_0 \cdot a_1 + a_2 \cdot a_3$	$-a_0 \cdot a_1 - a_2 \cdot a_3$	$a_0 \cdot a_3 - a_1 \cdot a_2$	$a_1 \cdot a_2 - a_0 \cdot a_3$
	$a_1 \cdot a_2 - a_0 \cdot a_3$	$a_1 \cdot a_2 - a_0 \cdot a_3$	$a_0 \cdot a_1 + a_2 \cdot a_3$	$a_0 \cdot a_1 + a_2 \cdot a_3$
	$a_1 \cdot a_2 - a_0 \cdot a_3$	$a_0 \cdot a_3 - a_1 \cdot a_2$	$a_0 \cdot a_1 + a_2 \cdot a_3$	$-a_0 \cdot a_1 - a_2 \cdot a_3$

Figure 37. Upper level: C_L is a (4*4)-matrix representation of complex numbers $z = a_0 + a_2 \cdot i$ on a 2-dimensional plane (x_0, x_2) in a 4-dimensional space (x_0, x_1, x_2, x_3); here i is imaginary unit of complex numbers ($i^2 = -1$). C_R is a (4*4)-matrix representation of complex numbers $z = a_1 + a_3 \cdot i$ on another 2-dimensional plane (x_1, x_3) in the same 4-dimensional space (x_0, x_1, x_2, x_3). Here a_0, a_1, a_2 and a_3 are real numbers. Two middle levels: expressions of products $C_L \cdot C_R$ and $C_R \cdot C_L$; in both cases two basic matrices define the multiplication table of complex numbers. Bottom level: the expression of the commutator $C_L \cdot C_R - C_R \cdot C_L$.

Now let us take a sum $V = C_L + C_R$ of these (4*4)-matrix representations of complex numbers, which are related with different planes of the 4-dimensional space (Figure 38).

$$V = C_L + C_R = \begin{bmatrix} a_0 & a_1 & -a_2 & a_3 \\ -a_0 & a_1 & a_2 & a_3 \\ a_2 & -a_3 & a_0 & a_1 \\ -a_2 & -a_3 & -a_0 & a_1 \end{bmatrix} = [1 \ 0; 0 \ 1] \otimes M + [0 \ 1; -1 \ 0] \otimes P$$

$$V^{-1} = (2 \cdot (a_0^2 + a_2^2))^{-1} \cdot \begin{bmatrix} a_0 & -a_0 & a_2 & -a_2 \\ 0 & 0 & 0 & 0 \\ -a_2 & a_2 & a_0 & -a_0 \\ 0 & 0 & 0 & 0 \end{bmatrix} + (2 \cdot (a_1^2 + a_3^2))^{-1} \cdot \begin{bmatrix} 0 & 0 & 0 & 0 \\ a_1 & a_1 & -a_3 & -a_3 \\ 0 & 0 & 0 & 0 \\ a_3 & a_3 & a_1 & a_1 \end{bmatrix}$$

Figure 38. Upper level: the sum $V = C_L + C_R$ (see Figure 37). Here $M = [a_0 \ a_1; -a_0 \ a_1]$ and $P = [-a_2 \ a_3; a_2 \ a_3]$; \otimes is a symbol of tensor (or Kronecker) multiplication. Bottom level: the expression of the inverse matrix V^{-1} .

Figure 38 shows that $V = C_L + C_R$ is a (4*4)-matrix of a special type, where both quadrants (marked by yellow color) along the main diagonal are identical each other, and two other quadrants (marked by green color) differ each from other only by inversion of sign in their entries. This matrix can be written in a form $V = [1 \ 0; 0 \ 1] \otimes M + [0 \ 1; -1 \ 0] \otimes P$, where $M = [a_0 \ a_1; -a_0 \ a_1]$ and $P = [-a_2 \ a_3; a_2 \ a_3]$; \otimes is a symbol of tensor (or Kronecker) multiplication; $[1 \ 0; 0 \ 1]$ – a matrix representation of real unit; $[0 \ 1; -1 \ 0]$ – a matrix representation of imaginary unit; a_0, a_1, a_2 and a_3 are real numbers. Such form of denotation resembles a well-known matrix representation of usual complex numbers: $z = [1 \ 0; 0 \ 1] \cdot a + [0 \ 1; -1 \ 0] \cdot b$, where a and b are real numbers. But it differs in the following aspects:

- 1) the expression $V = [1 \ 0; 0 \ 1] \otimes M + [0 \ 1; -1 \ 0] \otimes P$ includes tensor multiplication \otimes instead of usual multiplication in the matrix representation of complex numbers;
- 2) in the case of V , multipliers of the basic elements are square matrices M and P instead of real numbers « a » and « b » in the case of complex numbers.
- 3) The order of the factors inside V is essential since tensor multiplication is not commutative.

What one can say about algebraic properties of matrices of such type V (Figure 38)? Matrices of this type can be added and subtracted. The matrix V has its inverse matrix V^{-1} (Figure 39), which is defined on the basis of the condition $V \cdot V^{-1} = V^{-1} \cdot V = E_4$, where E_4 is unit matrix $[1\ 0\ 0\ 0; 0\ 1\ 0\ 0; 0\ 0\ 1\ 0; 0\ 0\ 0\ 1]$. Product of two different matrices G and S generates a new (4*4)-matrix $W = G \cdot S$ (Figure 39), where both (2*2)-quadrants (marked by yellow color) along the main diagonal are identical each other, and two other (2*2)-quadrants (marked by green color) differ each from other only by inversion of sign in their entries. This matrix can be written in a form $W = [1\ 0; 0\ 1] \otimes Q + [0\ 1; -1\ 0] \otimes K$, where $Q = [a \cdot k - c \cdot k - b \cdot n - d \cdot n, a \cdot m + c \cdot m + b \cdot p - d \cdot p; b \cdot n - c \cdot k - a \cdot k - d \cdot n, c \cdot m - a \cdot m - b \cdot p - d \cdot p]$ and $K = [c \cdot n - a \cdot n - d \cdot k - b \cdot k, a \cdot p - b \cdot m + d \cdot m + c \cdot p; b \cdot k + a \cdot n - d \cdot k + c \cdot n, b \cdot m - a \cdot p + d \cdot m + c \cdot p]$; \otimes is a symbol of tensor (or Kronecker) multiplication; $[1\ 0; 0\ 1]$ – a matrix representation of real unit; $[0\ 1; -1\ 0]$ – a matrix representation of imaginary unit; a, b, c, d, k, m, n and p are real numbers. Such form of denotation resembles the known matrix representation of usual complex numbers: $z = [1\ 0; 0\ 1] \cdot a + [0\ 1; -1\ 0] \cdot b$, where a and b are real numbers. But it differs again in the following aspects:

- 1) the expression $W = [1\ 0; 0\ 1] \otimes Q + [0\ 1; -1\ 0] \otimes K$ includes tensor multiplication \otimes instead of usual multiplication in the matrix representation of complex numbers;
- 2) in the case of W, multipliers of the basic elements are square matrices Q and K instead of real numbers «a» and «b» in the case of complex numbers.
- 3) The order of the factors inside W is essential since tensor multiplication is not commutative.

Taking into account a significant role of tensor multiplication \otimes in W, the author names algebraic constructions in a form W as “tensorcomplex numbers” because such matrices W have the following algebraic properties in relation to usual operations of addition, subtraction, multiplication and division:

- Addition and subtraction of two different matrices of this type W create a new matrix of the same type. Multiplication of different matrices of this type with each other is noncommutative and it gives a new matrix of the same type (Figure 39).
- Each non-zero matrix $W = G \cdot S$ has an inverse matrix $W^{-1} = G^{-1} \cdot S^{-1}$ (expressions for G^{-1} and S^{-1} were shown on Figure 38). It allows a definition of operation of division of two matrices of this type as a multiplication with an inverse matrix.

Such properties of tensorcomplex numbers resemble algebraic properties of quaternions by Hamilton, which represent noncommutative division algebra (<http://en.wikipedia.org/wiki/Quaternion>). Here one should emphasize that tensorcomplex numbers cardinally differ from hypercomplex numbers $x_0 + x_1 \cdot i_1 + \dots + x_n \cdot i_n$, where x_0, x_1, \dots, x_n are real numbers, because, in the case of tensorcomplex numbers, multipliers of the basic elements are square matrices but not real numbers. By this reason, the famous Frobenius theorem ([http://en.wikipedia.org/wiki/Frobenius_theorem_\(real_division_algebras\)](http://en.wikipedia.org/wiki/Frobenius_theorem_(real_division_algebras))) for hypercomplex numbers is not related to tensorcomplex numbers. This theorem says that any finite-dimensional associative division algebra is isomorphic to one of the following algebras: the real numbers, the complex numbers, the quaternions by Hamilton.

$$G = \begin{bmatrix} a & c & -b & d \\ -a & c & b & d \\ b & -d & a & c \\ -b & -d & -a & c \end{bmatrix}; \quad S = \begin{bmatrix} k & m & -n & p \\ -k & m & n & p \\ n & -p & k & m \\ -n & -p & -k & m \end{bmatrix}$$

$$G*S = \begin{array}{|c|c|c|c|} \hline a*k-c*k-b*n-d*n & a*m+c*m+b*p-d*p & c*n-a*n-d*k-b*k & a*p-b*m+d*m+c*p \\ \hline b*n-c*k-a*k-d*n & c*m-a*m-b*p-d*p & b*k+a*n-d*k+c*n & b*m-a*p+d*m+c*p \\ \hline b*k+a*n+d*k-c*n & b*m-a*p-d*m-c*p & a*k-c*k-b*n-d*n & a*m+c*m+b*p-d*p \\ \hline d*k-a*n-b*k-c*n & a*p-b*m-d*m-c*p & b*n-c*k-a*k-d*n & c*m-a*m-b*p-d*p \\ \hline \end{array}$$

Figure 39. Multiplication of two matrices G and S gives a new matrix $W = G*S$, which belong to so called «tensorcomplex numbers». Here a, b, c, d, k, m, n and p are real numbers.

This set of tensorcomplex numbers is one of examples of numeric systems, where real numbers exist only inside matrices in a form of whole ensembles but not as individual multipliers (or as individual personages) inside such numeric systems. It is one of differences of tensorcomplex numbers from hypercomplex systems. One can mention that the commutator $C_L*C_R - C_R*C_L$ (Figure 37) belongs to tensorcomplex numbers.

Till now in this Section we considered the case of tensorcomplex numbers, which were represented by means of the expression $W = [1 \ 0; 0 \ 1] \otimes Q + [0 \ 1; -1 \ 0] \otimes K$, where Q and K are $(2*2)$ -matrices. But our work [Petoukhov, 2012b,...] describes that complex numbers can be also represented by means of sparse (2^N*2^N) -matrices on the basis of sums of projectors (here $N = 2, 3, 4, \dots$). One can take sum of two complex numbers, which belong to different planes of the same 2^N -dimensional space and which are represented by means of appropriate (2^N*2^N) -matrices. In this case new types of tensorcomplex numbers arise. Theory and expressions for such tensorcomplex numbers in spaces of higher dimensions are developed now for a publication in the nearest future.

The author hopes that tensorcomplex numbers, which seem to be a new type of multidimensional numbers for mathematical natural sciences, will be useful not only in bioinformatics, but also in physics, theory of communication, logic and other fields.

12 ABOUT «TENSORDOUBLE» NUMBERS

Now let us return to the Rademacher $(4*4)$ -matrix R_4 , which is a sum of 4 column projectors c_0, c_1, c_2, c_3 : $R_4 = c_0 + c_1 + c_2 + c_3$ (Figures 1 and 2). Our work [Petoukhov, 2012b, Figures 11-13] shows that sum $c_0 + c_2$ is decomposed into basic matrices $e_0 = [1 \ 0 \ 0 \ 0; -1 \ 0 \ 0 \ 0; 0 \ 0 \ 1 \ 0; 0 \ 0 \ -1 \ 0]$ and $e_2 = [0 \ 0 \ 1 \ 0; 0 \ 0 \ -1 \ 0; 1 \ 0 \ 0 \ 0; -1 \ 0 \ 0 \ 0]$, the set of which is closed relative to multiplication and defines the multiplication table of split-complex numbers; their known synonyms are “double numbers” or “Lorentz numbers” (http://en.wikipedia.org/wiki/Split-complex_number). In this Section we will prefer using the name «double numbers» for such type of 2-dimensional numbers. Another sum $c_1 + c_3$ is decomposed into basic matrices $e_1 = [0 \ 1 \ 0 \ 0; 0 \ 1 \ 0 \ 0; 0 \ 0 \ 0 \ 1; 0 \ 0 \ 0 \ 1]$ and $e_3 = [0 \ 0 \ 0 \ -1; 0 \ 0 \ 0 \ -1; 0 \ -1 \ 0 \ 0; 0 \ -1 \ 0 \ 0]$. Now one can consider linear compositions D_L and D_R on basis of these basic matrices (Figure 40). The work [Petoukhov, 2012b, Figures 12, 13] shows that each of D_L and D_R is a $(4*4)$ -matrix representation of 2-parametric double numbers over field of real numbers but these representations concern different 2-dimensional planes (x_0, x_2) and (x_1, x_3) of a 4-dimensional vector space.

$$D_L = a_0 * e_0 + a_2 * e_2 = \begin{array}{|c|c|c|c|} \hline a_0 & 0 & a_2 & 0 \\ \hline -a_0 & 0 & -a_2 & 0 \\ \hline a_2 & 0 & a_0 & 0 \\ \hline -a_2 & 0 & -a_0 & 0 \\ \hline \end{array} ; \quad D_R = a_1 * e_1 + a_3 * e_3 = \begin{array}{|c|c|c|c|} \hline 0 & a_1 & 0 & -a_3 \\ \hline 0 & a_1 & 0 & -a_3 \\ \hline 0 & -a_3 & 0 & a_1 \\ \hline 0 & -a_3 & 0 & a_1 \\ \hline \end{array}$$

Figure 40. Left side: D_L is a $(4*4)$ -matrix representation of double (or split-complex) numbers $z = a_0 + a_2*j$ on a 2-dimensional plane (x_0, x_2) in a 4-dimensional space (x_0, x_1, x_2, x_3) ; here j is imaginary unit of double numbers ($j^2=1$). Right side: D_R is a $(4*4)$ -matrix representation of double numbers $z = a_1 + a_3*j$ on another 2-dimensional plane (x_1, x_3) in the same 4-dimensional space (x_0, x_1, x_2, x_3) . Here a_0, a_1, a_2 and a_3 are real numbers.

Now let us take a sum $D_L + D_R$ of these $(4*4)$ -matrix representations of double numbers, which are related with different planes of the 4-dimensional space (Figure 41).

$$D = D_L + D_R = \begin{bmatrix} a_0 & a_1 & a_2 & -a_3 \\ -a_0 & a_1 & -a_2 & -a_3 \\ a_2 & -a_3 & a_0 & a_1 \\ -a_2 & -a_3 & -a_0 & a_1 \end{bmatrix} = [1 \ 0; 0 \ 1] \otimes M + [0 \ 1; 1 \ 0] \otimes K$$

$$\begin{bmatrix} a & 0 & a & 0 \\ -a & 0 & a & 0 \\ a & 0 & a & 0 \\ -a & 0 & -a & 0 \end{bmatrix} * \begin{bmatrix} 0 & c & 0 & -c \\ 0 & c & 0 & -c \\ 0 & -c & 0 & c \\ 0 & -c & 0 & c \end{bmatrix} = \begin{bmatrix} 0 & 0 & 0 & 0 \\ 0 & 0 & 0 & 0 \\ 0 & 0 & 0 & 0 \\ 0 & 0 & 0 & 0 \end{bmatrix}$$

$$D^{-1} = (2*(a_0^2 - a_2^2))^{-1} * \begin{bmatrix} a_0 & -a_0 & -a_2 & a_2 \\ 0 & 0 & 0 & 0 \\ -a_2 & a_2 & a_0 & -a_0 \\ 0 & 0 & 0 & 0 \end{bmatrix} + (2*(a_1^2 - a_3^2))^{-1} * \begin{bmatrix} 0 & 0 & 0 & 0 \\ a_1 & a_1 & -a_3 & -a_3 \\ 0 & 0 & 0 & 0 \\ -a_3 & -a_3 & a_1 & a_1 \end{bmatrix}$$

Figure 41. Upper level: the sum $D = D_L + D_R$ (see Figure 40). Here $M = [a_0 \ a_1; -a_0 \ a_1]$ and $K = [a_2 \ -a_3; -a_2 \ -a_3]$; \otimes is a symbol of tensor multiplication. Middle level: the example of zero divisors in this type of matrices. Bottom level: the inverse matrix D^{-1} for the matrix D .

Figure 41 shows that $D = D_L + D_R$ is a $(4*4)$ -matrix of a special type, where both quadrants along each of diagonals are identical (they are marked by yellow and blue colors). This matrix can be written in a form $D = [1 \ 0; 0 \ 1] \otimes M + [0 \ 1; 1 \ 0] \otimes K$, where $M = [a_0 \ a_1; -a_0 \ a_1]$ and $K = [a_2 \ -a_3; -a_2 \ -a_3]$, where $[1 \ 0; 0 \ 1]$ – a matrix representation of real unit; $[0 \ 1; 1 \ 0]$ – a matrix representation of imaginary unit j of double numbers ($j^2=1$); a_0, a_1, a_2 and a_3 are real numbers. Such form of denotation resembles a well-known matrix representation of usual double numbers: $y = [1 \ 0; 0 \ 1]*a + [0 \ 1; 1 \ 0]*b$, where « a » and « b » are real numbers. But it differs again in the following aspects:

- 1) the expression $D = [1 \ 0; 0 \ 1] \otimes M + [0 \ 1; 1 \ 0] \otimes K$ includes tensor multiplication \otimes instead of usual multiplication in the matrix representation of double numbers;
- 2) in the case of D , multipliers of the basic elements are square matrices M and K instead of real numbers « a » and « b » in the case of double numbers;
- 3) The order of factors inside D is essential since tensor multiplication is not commutative.

The set of matrix D has zero divisors, examples of which are shown on Figure 41. Figure 41 also shows a general expression of the inverse matrix D^{-1} for the matrix D .

Multiplication of two matrices D_0 and D_1 of this type gives a new matrix L (Figure 42), where both quadrants along each of diagonals are identical (they are marked by yellow and blue colors). This matrix can be represented in the following form: $L = [1 \ 0; 0 \ 1] \otimes Q + [0 \ 1; 1 \ 0] \otimes K$, where $Q = [a*k-c*k+b*n+d*n, \ a*m+c*m-b*p+d*p; \ d*n-c*k-b*n-a*k, \ c*m-a*m+b*p+d*p]$, $K = [a*n+b*k-c*n+d*k, \ b*m-a*p-c*p-d*m; \ d*k-b*k-c*n-a*n, \ a*p-b*m-c*p-d*m]$.

Taking into account a significant role of tensor multiplication \otimes in L , the author names algebraic constructions in a form L (Figure 42) as “tensordouble numbers” because such matrices L have the following algebraic properties in relation to usual operations of addition, subtraction, multiplication and division:

- Addition, subtraction and multiplication of two different matrices of this type create a new matrix of the same type. Multiplication of different matrices of this type with each other is noncommutative. The set of matrices L has zero divisors.
- Each non-zero matrix $L=D_0*D_1$, if it is not a zero divisor, has an inverse matrix $L^{-1} = D_0^{-1}*D_1^{-1}$ (expressions for D^{-1} was shown on Figure 41). It allows a definition of operation of division of two matrices of this type as a multiplication with an inverse matrix.

$$D_0 = \begin{bmatrix} a & c & b & -d \\ -a & c & -b & -d \\ b & -d & a & c \\ -b & -d & -a & c \end{bmatrix}; \quad D_1 = \begin{bmatrix} k & m & n & -p \\ -k & m & -n & -p \\ n & -p & k & m \\ -n & -p & -k & m \end{bmatrix}$$

$$L=D_0*D_1 = \begin{bmatrix} a*k-c*k+b*n+d*n, & a*m+c*m-b*p+d*p & a*n+b*k-c*n+d*k, & b*m-a*p-c*p-d*m \\ d*n-c*k-b*n-a*k, & c*m-a*m+b*p+d*p & d*k-b*k-c*n-a*n, & a*p-b*m-c*p-d*m \\ a*n+b*k-c*n+d*k, & b*m-a*p-c*p-d*m & a*k-c*k+b*n+d*n, & a*m+c*m-b*p+d*p \\ d*k-b*k-c*n-a*n, & a*p-b*m-c*p-d*m & d*n-c*k-b*n-a*k, & c*m-a*m+b*p+d*p \end{bmatrix}$$

Figure 42. Multiplication of two matrices D_0 and D_1 (of the type D from Figure 41) gives a new matrix $L = D_0*D_1$, which belongs to so called «tensordouble numbers». Here a, b, c, d, k, m, n and p are real numbers.

This Section has described the case of tensordouble numbers in the form of $(4*4)$ -matrices for 4-dimensional spaces. But tensordouble numbers and their generalization can be expressed in forms of (2^N*2^N) -matrices for 2^N -dimensional spaces. These materials will be published later together with data about «tensordual» numbers, «tensorquaternions», etc.

Different types of such multidimensional numbers can be combined under a brief name «tensornumbers». Tensornumbers $[1] \otimes M_0 + [i_1] \otimes M_1 + \dots + [i_n] \otimes M_n$ (here M_n are square matrices) are a generalization of hypercomplex numbers in the case when the following changes are made in the usual denotation of hypercomplex numbers $1*x_0 + i_1*x_1 + \dots + i_n*x_n$:

- Real multipliers x_0, x_1, \dots, x_n are replaced by square matrices M_0, M_1, \dots, M_n ;
- Usual multiplication is replaced by tensor multiplication.

It is obvious that hypercomplex numbers $1*x_0 + i_1*x_1 + \dots + i_n*x_n$ are a degenerate case of tensornumbers when their matrices M_n have the first order: 1) $(1*1)$ -matrices $M_n = [x_n]$ are real numbers x_n ; 2) tensor multiplication $[i_n] \otimes [x_n]$ of $(1*1)$ -matrix $[x_n]$ with the matrix representation $[i_n]$ of any of the basic elements is commutative and it coincides with usual multiplication. By these reasons the following equation is true:

$$[1] \otimes [x_0] + [i_1] \otimes [x_1] + \dots + [i_n] \otimes [x_n] = [1] * x_0 + [i_1] * x_1 + \dots + [i_n] * x_n.$$

What one can say at this initial stage about a future of tensor numbers in mathematical natural sciences and technologies? Two extreme points of view are possible here: 1) tensor complex numbers will have no applications; 2) tensor complex numbers will have a great significance for mathematical natural sciences including a creation of new theories of physical fields and their generalization, new laws of conservation, generalization of many physical and other rules and knowledge, new approaches in engineering and biological informatics, mathematical logics, etc. The author believes that the second point of view will coincide with a real future in a higher extent.

SOME CONCLUDING REMARKS

As it was noted in the beginning of the article, living organism is a machine for coding and processing of information. For example, visual information about external objects is transmitted through the nerves from the eye retina to the brain already in a logarithmically encoded form. This article shows some evidences that oblique projection operators and their combinations, which are connected with matrix representations of the genetic coding system, can be a basis of adequate approaches to simulate ensembles of inherited biological phenomena. Only some of such phenomena were considered in this article. Some other phenomena will be described from the proposed point of view later. In addition, the author reminds about fractal genetic nets (FGN), which can be represented as a construction on a base of orthogonal projectors and which lead to new genetic rules in structures of long nucleotide sequences [Petoukhov, 2012; Petoukhov, Svirin, 2012].

The revealed genetic system of operators connected with oblique projectors allows modeling multi-dimensional phase spaces with many subspaces, processes in which can be selectively determined and controled. One can think that the nature «likes» projectors, which allow modelling of many natural phenomena in non-living systems. For example, a vector of the electromagnetic field by means of orthogonal projections is represented as a sum of electric and magnetic vectors, which are orthogonal each other. Now projectors and their combinations become interesting instruments to study and simulate genetic phenomena and inherited structures and processes in living matter. A new conceptual notion with appropriate mathematical formalisms are proposed about a «multi-dimensional control space (or coding space) with subspaces of a selective control in each on basis of a participation of projection operators in such control». Here one can remember the statement: “*Profound study of nature is the most fertile source of mathematical discoveries*” (Fourier, 2006, Chapter 1, p. 7).

Using this ideology of projection operators, one can get many unexpected results and approaches. In author's opinion, one of many promising applications of projectors in mathematical biology and bioinformatics is the study of connections between genetic projectors and Boolean algebra. It is known that every family of commutative projectors generates a Boolean algebra of projectors. The Boolean algebra plays a great role in the modern science because of its connections with many scientific branches: mathematical logic, the problem of artificial intelligence, computer technologies, bases of theory of probability, etc. G.Boole was creating such algebra of logics (or logical operators), which would reflect inherited laws of human thought. One should note here that some of genetic projectors form commutative pairs; this fact provokes thoughts about Boolean algebras in genetics and bioinformatics and also about genetic basis of logics of human thought.

Materials of this article reinforce the author's point of view that living matter in its informational fundamentals is an algebraic essence. The author believes that a development of algebraic biology, elements of which are contained in this and other author's articles, is possible. By analogy with the known fact that molecular foundations of molecular genetics turned up unexpectedly very simple, perhaps algebraic foundations of living matter are also relative simple.

Concerning the new theme of tensor numbers, which were revealed in our study of genetic projectors, one can remind that the idea of multi-dimensional numbers and multi-dimensional spaces works intensively for a long time in the theoretical physics and other fields of science for modeling the phenomena of our physical world. Our results add mathematical formalisms, first of all, into the fields of molecular genetics and bioinformatics. After the discovery of non-Euclidean geometries and of Hamilton quaternions, it is known that different natural systems can possess their own geometry and their own algebra (see about this [Kline, 1980]). The genetic code is connected with its own multi-dimensional numerical systems or the multi-dimensional algebras. These algebras allow revealing hidden peculiarities of the structure of the genetic code and its evolution. It seems that many difficulties of modern bioinformatics and mathematical biology are connected with utilizing for their natural structures inadequate algebras, which were developed for completely other natural systems. Hamilton had similar difficulties in his attempts to describe 3D-space transformations by means of 3-dimensional numbers while this description needs quaternions. The author hopes that proposed tensor numbers will help to make progress not only in bioinformatics and mathematical biology, where algebraization of biology seems to be possible, but also in many fields of sciences and technologies.

"Complexity of a civilization is reflected in complexity of numbers used by this civilization" [Davis, 1967]. Whether modern civilization will use tensor numbers or not? It is the open question. Pythagoras has formulated the idea: *"all things in the world are numbers"* or *"number rules the world"*. B. Russell noted that that he did not know other person who would exert such influence on thinking of people as Pythagoras. From this viewpoint, there is no more fundamental scientific idea in the world, than this idea about a basic meaning of numbers. Our researches of oblique projectors in the field of matrix genetics have led to new systems of multidimensional numbers and have given new materials to the great idea by Pythagoras in its modernized formulating: *"All things are multi-dimensional numbers"*.

This article proposes a new mathematical approach to study *"a partnership between genes and mathematics"* (see Section 1 above). In the author's opinion, this kind of mathematics is beautiful and it can be used for further developing of algebraic biology and theoretical physics in accordance with the famous statement by P. Dirac, who taught that a creation of a physical theory must begin with the beautiful mathematical theory: *"If this theory is really beautiful, then it necessarily will appear as a fine model of important physical phenomena. It is necessary to search for these phenomena to develop applications of the beautiful mathematical theory and to interpret them as predictions of new laws of physics"* (this quotation is taken from [Arnold, 2007]). According to Dirac, all new physics, including relativistic and quantum, are developing in this way. One can suppose that this statement is also true for mathematical biology.

REFERENCES

- Adler I., Barabe D., Jean R. V.** (1997) A History of the Study of Phyllotaxis. *Annals of Botany* 80: 231–244, <http://aob.oxfordjournals.org/content/80/3/231.full.pdf>
- Ahmed N., Rao K.** (1975) *Orthogonal transforms for digital signal processing*. N-Y, Springer-Verlag Inc.
- Arnold, V.** (2007) A complexity of the finite sequences of zeros and units and geometry of the finite functional spaces. *Lecture at the session of the Moscow Mathematical Society*, May 13, <http://elementy.ru/lib/430178/430281>.
- Cook, T.A.** (1914). *The curves of life*. London: Constable and Company Ltd, 524 p.
- Davis P.J.** (1964). Arithmetics. – In: “*Mathematics in the modern world*”, N. Y., Scientific American, p. 29-45.
- Eigen, M.** (1979) *The hypercycle - a principle of natural self-organization*. Berlin: Springer-Verlag.
- Fourier J.** (1878). *The analytical theory of heat*. – Cambridge: Deighton, Bell and Co.
- Halmos P.R.** (1974) *Finite-dimensional vector spaces*. London: Springer, 212 p.
- He M., Petoukhov S.V.** (2011) *Mathematics of bioinformatics: theory, practice, and applications*. USA: John Wiley & Sons, Inc., 295 p.
- Jean, R.V.** (1995) *Phyllotaxis: A Systemic Study in Plant Morphogenesis*. Cambridge University Press, 1995. (Russian edition, 2005, Scientific Editor – S.Petoukhov)
- Kline, M.** (1980) *Mathematics. The loss of certainty*. New York: Oxford University Press.
- Konopelchenko, B. G., Rumer, Yu. B.** (1975a) Classification of the codons of the genetic code. I & II. *Preprints 75-11 and 75-12 of the Institute of Nuclear Physics of the Siberian department of the USSR Academy of Sciences*. Novosibirsk: Institute of Nuclear Physics.
- Konopelchenko, B. G., Rumer, Yu. B.** (1975b). Classification of the codons in the genetic code. *Doklady Akademii Nauk SSSR*, 223(2), 145-153 (in Russian).
- Messiah A.** (1999) *Quantum mechanics*. New York: Dover Publications, 1152 p.
- Meyer C. D.** (2000), *Matrix Analysis and Applied Linear Algebra*, Society for Industrial and Applied Mathematics, 2000. ISBN 978-0-89871-454-8.
- Petoukhov S.V.** (1981). *Biomechanics, bionics and symmetry*. – Moscow, Nauka, 239 p. (in Russian).
- Petoukhov S.V.** (2001a) Genetic codes I: binary sub-alphabets, bi-symmetric matrices and the golden section; Genetic codes II: numeric rules of degeneracy and the chronocyclic theory. *Symmetry: Culture and Science*, vol. 12, #3-4, p. 255-306.
- Petoukhov S.V.** (2005) The rules of degeneracy and segregations in genetic codes. The chronocyclic conception and parallels with Mendel’s laws. - In: *Advances in Bioinformatics and its Applications, Series in Mathematical Biology and Medicine*, 8, p. 512-532, World Scientific.
- Petoukhov S.V.** (2006a) Bioinformatics: matrix genetics, algebras of the genetic code and biological harmony. *Symmetry: Culture and Science*, 17, #1-4, p. 251-290.
- Petoukhov S.V.** (2008a) The degeneracy of the genetic code and Hadamard matrices. arXiv:0802.3366 [q-bio.QM].
- Petoukhov S.V.** (2008b) *Matrix genetics, algebras of the genetic code, noise immunity*. M., RCD, 316 p. (in Russian).
- Petoukhov S.V.** (2010) Matrix genetics, part 5: genetic projection operators and direct sums. <http://arxiv.org/abs/1005.5101>.
- Petoukhov S.V.** (2011a). Matrix genetics and algebraic properties of the multi-level system of genetic alphabets. - *Neuroquantology*, 2011, Vol 9, No 4, p. 60-81, <http://www.neuroquantology.com/index.php/journal/article/view/501>

- Petoukhov S.V.** (2011b). Hypercomplex numbers and the algebraic system of genetic alphabets. Elements of algebraic biology. – *Hypercomplex numbers in geometry and physics*, v.8, No2(16), p. 118-139 (in Russian).
- Petoukhov S.V.** (2012a) The genetic code, 8-dimensional hypercomplex numbers and dyadic shifts. (7th version from January, 30, 2012), <http://arxiv.org/abs/1102.3596>
- Petoukhov S.V.** (2012b) Symmetries of the genetic code, hypercomplex numbers and genetic matrices with internal complementarities. - “*Symmetries in genetic information and algebraic biology*”, special issue of journal “*Symmetry: Culture and Science*” (Guest editor: S. Petoukhov), vol. 23, № 3-4, p. 275-301. http://symmetry.hu/scs_online/SCS_23_3-4.pdf
- Petoukhov S.V., He M.** (2009) *Symmetrical Analysis Techniques for Genetic Systems and Bioinformatics: Advanced Patterns and Applications*. Hershey, USA: IGI Global. 271 p.
- Poincare H.** (1913). The foundations of science. Science and hypothesis. The value of science. Science and method. – N. Y., The Science Press New York and Garrison. http://www.gutenberg.org/files/39713/39713-h/39713-h.htm#Page_264
- Rumer Yu. B.** (1968). Systematization of the codons of the genetic code. - *Doklady Akademii Nauk SSSR*, vol. 183(1), p. 225-226 (in Russian).
- Russel B.A.W.** An essay on the foundations of geometry. N-Y: Dover, 1956, 201 p.
- Stewart I.** (1999). *Life's other secret: The new mathematics of the living world*. New-York: Penguin.
- Vetter R.J., Weinstein S.** (1967). The history of the phantom in congenitally absent limbs. – *Neuropsychologia*, № 5, p.335-338
- Vladimirov Y.S.** (2008). *Foundations of Physics*. – Moscow, Binom, 456 p. (in Russian)
- Weinstein S., Sersen E.A.** (1961). Phantoms in cases of congenital absence of limbs. – *Neurology*, №11, p.905-911.